A NUMERICAL AND EXPERIMENTAL INVESTIGATION OF VIBRATORY BOWL FEEDERS

by

Denise Morrey

MA(Cantab), CEng, MIMechE, CDipAF

A thesis submitted in partial fulfilment of the requirements of the Council for National Academic Awards for the award of Doctor of Philosophy

School of Engineering

Oxford Polytechnic

September 1989

Any maps, pages, tables, figures graphs,or photographs, missing from this digital copy, have been excluded at the request of the university.

A NUMERICAL AND EXPERIMENTAL INVESTIGATION OF VIBRATORY BOWL FEEDERS

by Denise Morrey

ABSTRACT

Vibratory bowl feeders are widely used in automation processes for the storage, feeding and orientation of identical components for presentation to workstations or other mechanical handling devices.

The investigation described here has been directed at modelling the dynamic behaviour of vibratory bowl feeders, both to improve understanding of their behaviour, and to facilitate improvements in their design. The work undertaken has involved the following stages:

i) A numerical model for the prediction of the eigenvalues and eigenvectors of the bowl feeder was developed, modelling the structure as a lumped parameter eight degree-of-freedom system;

ii) The natural frequencies and mode shapes predicted by the model were compared with those obtained from experimental modal analysis. There was good agreement for the first three natural frequencies. Differences in the higher frequency modes indicated an overconstrained model which could be accounted for by the flexural vibration of the bowl;

iii) A numerical model of the forced response of a bowl feeder when driven by a harmonic excitation was developed using a spreadsheet package, and verified experimentally;

iv) The spreadsheet package was developed further, varying the geometric parameters of the bowl and springs over specified ranges. Changes in spring angles were investigated experimentally to verify the predicted values;

v) A customised design tool was developed using the spreadsheet package to enable engineers to investigate the behaviour of different configuration feeders;

vi) An investigation of the causes of dead-spots was undertaken. These were shown to be due to the asymmetrical arrangement of the springs and electromagnetic coil relative to each other; and

vii) Solutions proposed to the problem of dead-spots were the use of four spring banks instead of three, and the specification of an annular shaped pole piece for the electromagnetic coil.

Acknowledgements

The author wishes to acknowledge the help received from Dr.J.E.Mottershead of Liverpool University, her Director of Studies, throughout this project.

Thanks are also due to those fellow members of staff and technicians who provided assistance during the period of research; in particular D.Flanagan for his technical support in all the experimental work undertaken.

The author is particularly grateful to Paula Williams, for her careful proof reading of the text, and the support given, both practical and moral, during the latter stages of the project.

Finally, the author would like to thank her parents for their continued support and encouragement.

Nomenclature

Note: vectors and matrices are denoted by enclosure in brackets, not by bold characters.

A	cross-sectional area of a spring bank
A_n	normal track amplitude
A_p	parallel track amplitude
${}_rA_{jk}$	modal constant (or residue)
[A]	coefficient matrix of constraint equations
[B]	coefficient matrix of constraint equations
[C]	connection matrix
$[C_p]$	proportional damping matrix
E	Young's modulus of Elasticity
{F}	forcing vector
G	Shear modulus
$H(j\omega)$	transfer function
I_u	second moment of area of spring bank about the u axis
I_v	second moment of area of spring bank about the v axis
I_x	moment of inertia of the bowl about the x axis
I_y	moment of inertia of the bowl about the y axis

I_z	moment of inertia of the bowl about its vertical axis
J	torsional constant of a spring bank
K_v	non-dimensional component of acceleration normal to a vibrating table
[K]	stiffness matrix
$[K_u]$	stiffness matrix in terms of localised coordinates
[M]	mass matrix
{N}	vector of normalised or principal forces
$P_{ff}(\omega)$	auto or power spectral density (PSD)
$P_{xf}(\omega)$	cross spectral density (CSD)
[P]	modal matrix
Q_r	rth element in the normalised forcing vector
U	strain energy
Y_{jk}	mobility at point j due to an input at k
a	peak-to-peak displacement of the forcing waveform
b	plate radius
f	frequency of vibration of the track
f_n	natural frequency
g	acceleration due to gravity (9.81 m/s^2)
h	thickness of circular plate
k_e	equivalent spring constant

l	spring length
m	mass of the bowl
m_e	equivalent inertia mass of the bowl
n	number of leaf springs
$\{n\}$	vector of normal or principal coordinates
n_r	rth element in the vector of principal coordinates
r	radius of base circle
r_1	radius of spring attachment points on the bowl
r_2	radius of spring attachment points on the base
$r_{ff}(\tau)$	autocorrelation function (ACF)
$r_{xf}(\tau)$	cross correlation function (CCF)
t	spring thickness
t_s	Spacing between leaf springs
u-v-w	local coordinate set in the plane of a leaf spring
$\{u\}$	vector of localised coordinates
v	conveying velocity
v_m	mean conveying velocity
w	spring width
$\{x\}$	vector of generalised coordinates
Δ	vertical coordinate of motion of the bowl and base
$[\Lambda]$	spectral matrix

Ω	forcing frequency
α	proportional damping constant
β	proportional damping constant
δ	deflection of the upper end of the leaf spring
ϕ	offset angle
$\{\phi\}_r$	rth eigenvector
${}_r\phi_k$	kth term of the rth eigenvector or mode shape vector
γ	angle of inclination of spring to the horizontal
γ'	vibration angle in a bowl feeder
$\gamma(j\omega)^2$	coherence function
κ	offset factor
λ_i	eigenvalue
μ_d	coefficient of dynamic friction between component and track
μ_e	effective coefficient of friction between component and track
μ_s	coefficient of static friction between component and track
ψ	vibration angle

ρ	mass per unit area of circular plate
$\tau_{a\text{-}d}$	points where changes in slope occur in the forcing waveform
τ_o	crossing point of the forcing waveform
θ	track angle
θ_z	rotation about the vertical z-axis for both bowl and base
θ_x, θ_y	tipping about x- and y-axes for both bowl and base
υ	Poisson's ratio
ω	angular frequency of vibration of the track
ω_r	natural frequency or pole
ξ	timing factor
ζ	viscous damping ratio

CONTENTS

Appendix 5 - Auto-exec macro, 'Bowl Feeder', for the control of the execution of the customised design software

Appendix 6 - User manual for operation of the design software

1. INTRODUCTION

Mechanical parts handling systems are used in a wide range of automated industrial processes where identical parts and components are oriented and presented at workstations for assembly, machining or processing. One of the most flexible components of these systems is the vibratory bowl feeder. A photograph of this is shown as Plate 1.1. Parts for feeding are placed inside the bowl, and these move along the internal spiral track in response to the driving force provided by the electromagnetic coil, which is mounted between the bowl and base. Orientation of parts is carried out by the careful design and positioning of tooling along the track. This allows correctly oriented parts to pass through, but rejects others, returning them to the bottom of the bowl. A full description of bowl feeder tooling and other mechanical parts handling machinery is given in the text by Boothroyd, Poli and Murch (1).

In addition to requiring parts which are correctly oriented, workstations in automation processes, which often operate on inflexible, fixed cycle times, require a steady, continuous feed of parts. The requirements of the bowl feeder as an element in such a system are therefore as follows:

i) to carry out the suitable orientation of all

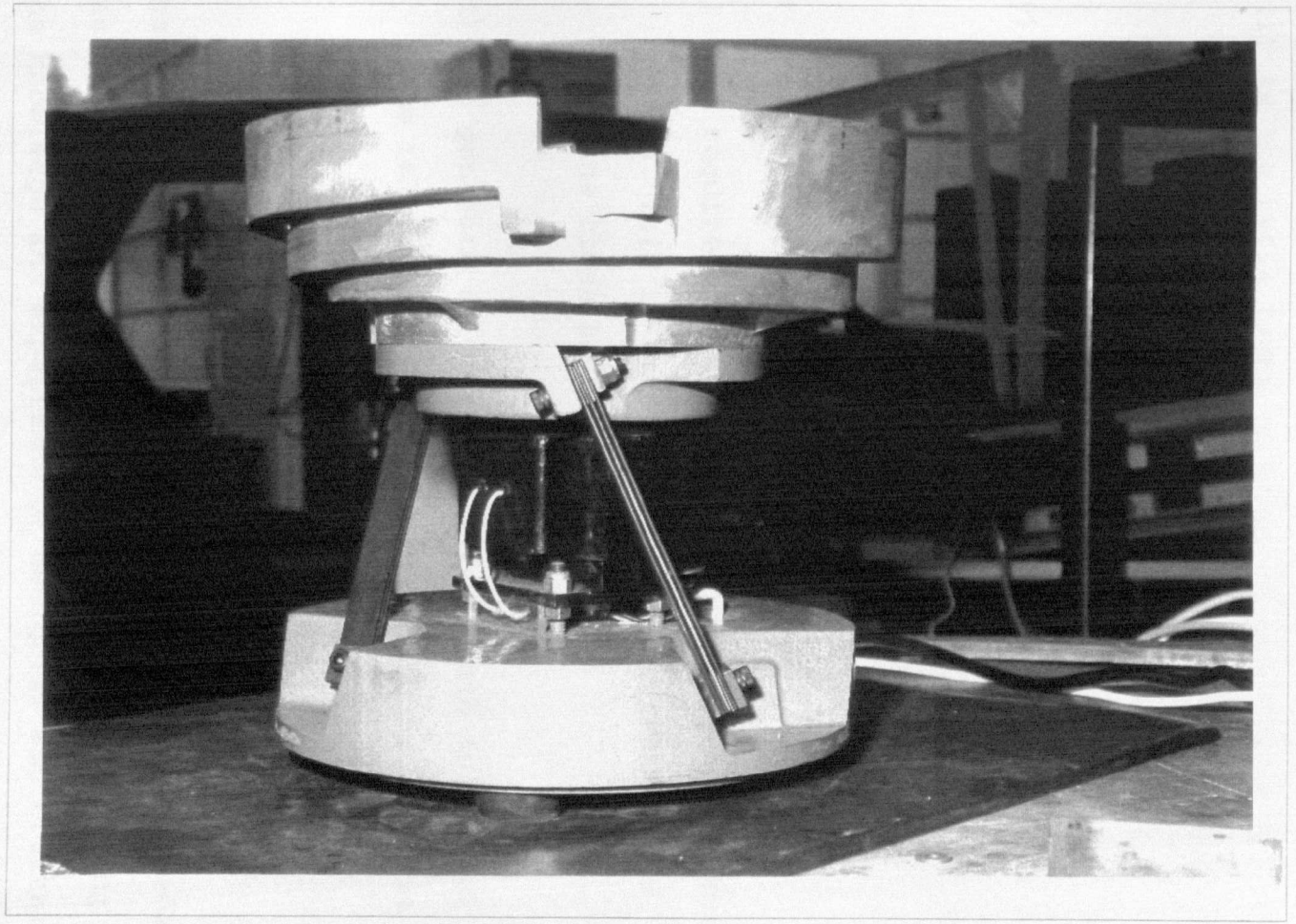

Plate 1.1 Bowl Feeder

components;

ii) to provide a uniform and continuous feed rate of components, with sufficient adjustment to this to be able to accommodate the associated cycle times;

iii) as the cycle times of other automation machinery decrease, there is a corresponding requirement for higher feed rates from vibratory bowl feeders;

iv) to provide free, untroubled operation without the requirement for frequent supervision. Tooling and unpredictable feeding may cause jamming of components;

v) to require a low power input and therefore running costs. This is usually achieved by running the machine close to resonance; and

vi) to generate a low noise output; both to fall within the relevant noise regulations, and to minimise any power losses and therefore improve efficiency.

Most of the development work undertaken on bowl feeders has been carried out on an empirical basis, building on the knowledge and experience of designers and craftsmen working within the field of vibratory feeding equipment.

In addition, because each bowl feeder system is manufactured to feed specific components, it consists of the basic structure of bowl, base and springs, along with individually designed tooling for component orientation. This specific requirement for each customer has meant that the majority of skill and expertise which has grown up within the industry has been directed at the production and development of tooling and orienting devices.

Despite widespread use, the manufacture and operation of bowl feeders is not without problems which affect both manufacturers and customers. These are as follows:

i) Feeders can often be difficult to 'tune' (the matching of springs to bowl and base in order to give a smooth continuous feed rate). This manifests itself by the occurrence of 'dead spots' where components either remain stationary or feed backwards. This can either happen during manufacture, or on delivery, or resiting in the field;

ii) Feeders can be prone to unpredictable feeding or even jamming of components;

iii) The 'load sensitivity' of bowl feeders, whereby a machine's behaviour changes in response to the loading of the components held in the bowl, can result in poor or unpredictable feeding at certain times;

iv) Feeders can be very noisy. When operating at high feed rates the noise levels produced are usually very close to the permissible legal limits; and

v) A combination of the high vibration and resulting stress levels experienced by the springs, and tuning arrangements which result in uneven loading of the spring banks, can result in fatigue failures of the leaf springs.

In addition, both manufacturers and customers have development requirements which need to be addressed:

i) increased feed rates, though this is limited, since at high feed rates components tend to jam; and

ii) a reduction in power input and running costs.

Earlier work which has been carried out in this area has concentrated on the simulation of component dynamics under feed conditions (2,3,4,5). Okabe and Yokoyama (6) modelled the structure of the feeder as a single

degree-of-freedom system allowing a single natural frequency to be computed. It was felt, however, that this neglected certain aspects of the dynamic behaviour of the structure. Thus, if further work were to be undertaken to make improvements to performance and to solve problems which occur during both manufacture and operation, a numerical model which gave a more faithful representation of the dynamic behaviour was required. This could be used to further current understanding of the actual operation of the bowl feeder and enable the effects of any modifications to be predicted.

2. REVIEW OF PREVIOUS WORK

Within this summary of the experimental and numerical investigations previously carried out on vibratory bowl feeders, the work undertaken falls into three main areas:

i) consideration of the mechanics of conveying of individual components(2);

ii) consideration of the dynamic behaviour of the structure i.e. the bowl, springs and base(6); and

iii) bowl feeder design using a step-by-step procedure which considers the interdependence of the functions of conveying and orienting and the individual parts of the bowl feeder structure(7).

A review of the developments in bowl feeder design has also been presented(8).

In addition to these investigations carried out on vibratory bowl feeders, a larger volume of work has been directed at the analysis of vibratory conveyors. These devices usually consist of a single horizontal deck or trough mounted on inclined springs and driven by an electromagnetic coil. The motion is similar to that which

occurs in vibratory bowl feeders, consisting of a combination of 'hop' and 'slides'.

Because of the similar nature of the motion, some of the work which deals with aspects not covered by the studies on vibratory bowl feeders is relevant background to this particular investigation. These areas include the use of non-sinusoidal waveforms(9), and the characteristics of loaded conveyors(10).

Other work in the area of vibratory conveying has been a survey of methods of material handling by vibrating equipment by Paz and Morris(11), and a review of the work undertaken in the analysis of vibratory conveying by Parameswaran and Ganapathy(12).

Published work which was considered to be of particular relevance to this study will be described in more detail.

2.1 Mechanics of Vibratory Conveying

An analysis of the mechanics of vibratory conveying has been carried out by Redford and Boothroyd(2).

Unlike most of the earlier work undertaken, this study analyses motion where a component periodically leaves the track, sometimes called 'free-flight' or the 'hopping'

mode. The impact velocity on landing is also taken into account.

The theoretical analysis carried out enables the mean conveying velocity of a component to be calculated in terms of the following variables:

i) track angle, θ;

ii) track amplitude, both parallel and normal to the track, A_p and A_n;

iii) angular frequency of vibration of the track, ω;

iv) coefficient of static friction between the track and component, μ_s;

v) coefficient of dynamic friction, μ_d; and

vi) vibration angle, ψ.

The model considers the motion along a very short length of track which is assumed to move as a rigid body with simple harmonic motion at a fixed frequency and amplitude. During the single cycle of vibration of the track the possible modes of motion of the component relative to the track are:

i) Forward sliding:

ii) Backward sliding:

iii) Hopping or free flight; and

iv) Periods where the component is stationary relative to the track.

The relationship between these modes is given in Fig.2.1. Coding has been written which determines the times when the various modes of component motion start and finish, for given input parameters. This enables integration to be carried out to calculate the distance travelled during each mode. By summing the individual distances, the total distance travelled, S, is determined, and hence the mean conveying velocity, v_m, is given by:

$$v_m = \frac{S\omega}{2\pi} \qquad (2.1)$$

By making substitutions in equation (2.1) in terms of the track variables, it was shown that the product $v_m f$ is constant for given values of θ, A_n/g, A_p/A_n, μ_s, μ_d and ψ, where f is the frequency of vibration. This statement neglects the fact that, in practice, any variation in f will affect variables such as A_n and A_p; in the case of simple harmonic motion in proportion to f^2.

Fig.2.1 Flow diagram showing the various component motions when the component periodically leaves the track (Redford and Boothroyd)

Experimental work has been carried out to verify the numerical results. This involved the excitation of a straight piece of track by two electromagnetic vibrators mounted in the parallel and normal directions and mounted independently. The track was machined with a 90° vee, and several different bowl-component combinations were used to give a range of values of the effective coefficient of friction, μ_e. For values of $A_n/g > 0.5$, it was assumed that $\mu_e = \mu_s = \mu_d$. The coefficient of friction was measured for the case when $\theta = 0°$, $A_n/g = 1.0$ and $\psi = 20°$, and it was assumed that these values would hold for the full range of variables.

Graphs comparing theoretical and experimental results are given as Fig.2.2 and 2.3. Fig.2.2 shows the variation of the product $v_m f$ with A_n/g for a range of vibration frequencies from 15 Hz to 45 Hz in 5 Hz steps. This shows good correlation between predicted and experimental results, except for large values of A_n/g, when there was thought to be a large impact velocity between the component and the track. The graph demonstrates the following:

Fig.2.2 Theoretical and experimental results showing the effect of vibration angle on mean conveying velocity (Redford and Boothroyd)

Fig.2.3 Theoretical and experimental results showing the effects of track and vibration angles on the mean conveying velocity (Redford and Boothroyd)

i) An increase in A_n/g causes a corresponding increase in $v_m f$. This increase is greater for smaller vibration angles.

ii) At fixed values of A_n/g, a variation in the vibration frequency gives constant values of the product $v_m f$ as predicted.

Fig.2.3 shows the variation of $v_m f$ with the vibration angle ψ for different values of the track angle θ. It shows that for a low value of μ_e (which is often the case in practice), forward conveying can only be achieved with very small track angles or very large vibration angles.

The other results obtained can be summarised as follows:

i) For high values of μ_e, forward conveying is always achieved over a wide range of track angles;

ii) Smaller values of the track angle θ give larger values of $v_m f$;

iii) The mean conveying velocity is very dependent on μ_e for all but very large vibration angles. For small values of μ_e only very small conveying speeds can be obtained; and

iv) An optimum vibration angle ψ_{opt} exists for given values of μ_e and θ, giving a maximum conveying velocity. However, an increase in the track angle and an increase in the coefficient of friction cause an increase in the maximum obtainable conveying velocity.

The authors also identified the undesirable features of conventional vibratory feeders:

i) Feeding is usually obtained by the pushing action of components travelling around the flat bowl bottom where the conveying velocity is greatest. This can cause jamming of orienting devices;

ii) Unstable motion of components may result in these being returned to the bottom of the bowl reducing the operating efficiency;

iii) Bowl feeders are often excessively noisy in operation;

iv) In some applications it is difficult to achieve desired feed rates. Although an increase in conveying velocity is possible, this is often accompanied by undesirable unstable motion; and

v) Changes in bowl loading often cause an undesirable change in the performance of bowl feeders.

In addition, the following points were identified for efficient feeding under ideal conditions:

i) Component conveying velocity should be independent of the nature of the components being conveyed;

ii) Component motion should not be erratic or unstable; and

iii) Components should be conveyed separately along the bowl track.

As a solution to the problems caused by the erratic feeding of components and the difficulty in obtaining a positive conveying velocity for small coefficients of friction, the concept of out-of-phase vibratory

conveying, which allows independent control of the normal and parallel components of acceleration, has been developed. Feed rates can be altered by adjusting the parallel motion only, and the normal motion can be set at a level which does not cause erratic movement of both track and components. In addition, by introducing a phase difference between the two components (parallel component leading the normal component), both theoretical and experimental results show that forward conveying can be achieved for all values of μ_e.

It is also shown that it is possible to design the bowl so that the conveying velocity of components around the track is greater than that of components travelling round the bottom of the bowl. Therefore the pushing action which occurs with in-phase conveying is eliminated.

The implementation of out-of-phase conveying on a three spring-bank feeder required at minimum four electromagnetic coils. A diagram of a possible arrangement is shown in Fig.2.4.

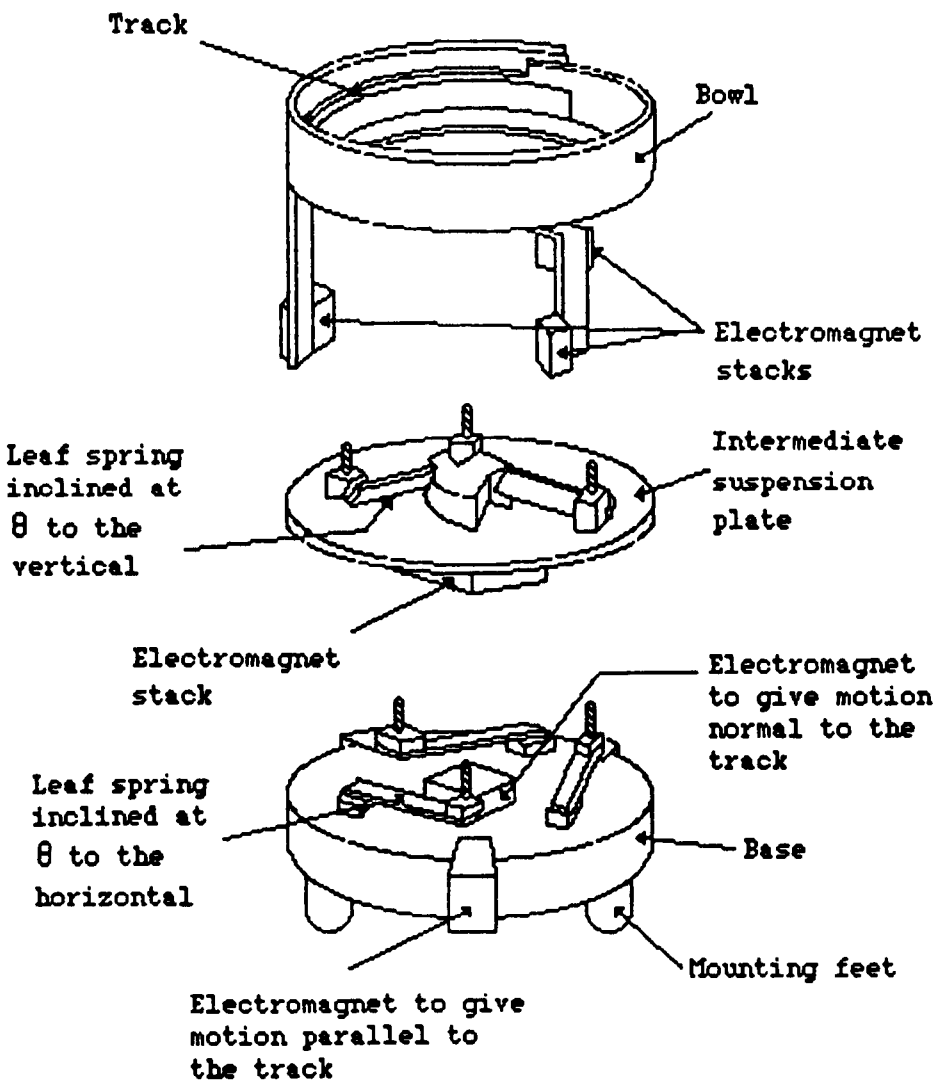

Fig. 2.4 Exploded view of an out-of-phase vibratory bowl feeder

2.2 Dynamics of the Bowl Feeder Structure

An analysis of the dynamic characteristics of the bowl feeder structure has been undertaken by Okabe and Yokoyama(6). This has yielded a formula for an equivalent spring constant, and a single natural frequency in terms of the following structural parameters:

i) Spring angle, γ;

ii) Spring length, l, width, w, and thickness, t;

iii) Radius of the base circle, r, which is defined as being tangential to the centre lines of the springs and in the horizontal plane of the bowl. This is shown in Fig.2.5;

iv) Offset factor, κ, which is an indication of the offset of the upper end of the spring, and is a function of the offset angle, ϕ, which is also shown in Fig.2.5. The defining equation is

$$\kappa = \frac{r \tan \phi}{l \cos \gamma} \qquad (2.2)$$

v) Number of leaf springs, n;

vi) Mass of the bowl, m; and

vii) Moment of inertia of the bowl about the vertical axis, I_z.

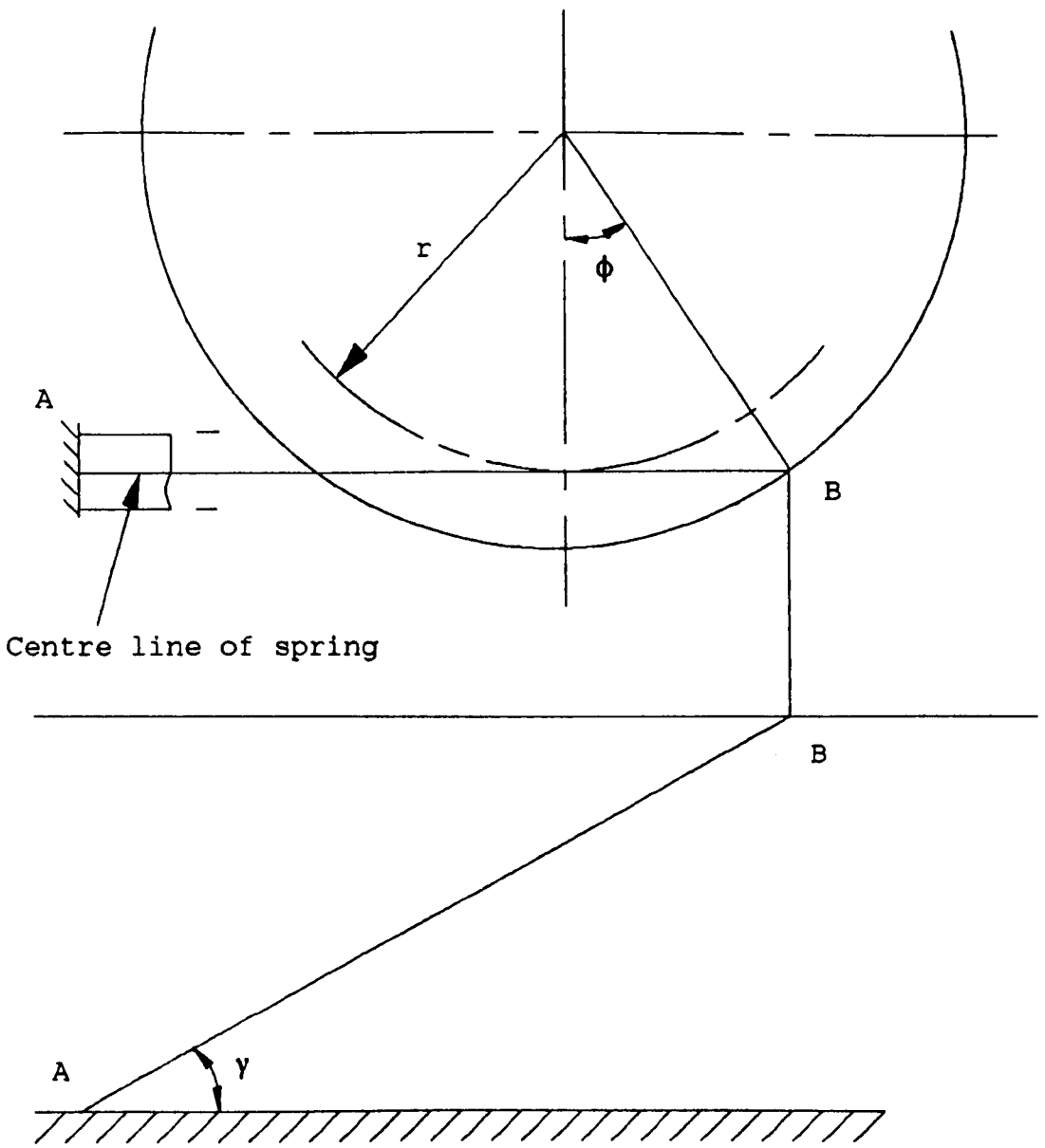

Fig.2.5 Plan and side view of a spring bank showing attachment points to the base and bowl (A and B)

The natural frequency is determined by considering the feeder as a single degree-of-freedom system with an equation of motion of the form

$$m_e\ddot{\delta} + k_e\delta = 0 \qquad (2.3)$$

where m_e is the equivalent inertia mass of the bowl, k_e is the equivalent spring constant, and δ is the actual deflection at the upper end of a leaf spring.

The equivalent spring stiffness is established by considering the deformations of a leaf spring:

i) in the thickness direction;
ii) in the width direction; and
iii) in torsion independently.

Expressions for strain energies in the three directions are established in terms of the principal coordinate δ. However, the effects due to the torsion of the spring itself are considered to be negligible compared with the bending effects.

The equivalent inertia term is derived by considering the

kinetic energy of the bowl resulting from its simultaneous vertical and rotational motion.

Assuming that the motion of the bowl is simple harmonic, and that the following structural relationships exist for an ordinary bowl feeder:

$$\frac{w}{t} \approx 10 - 20$$

$$\frac{l}{r} \approx 1.0$$

$$\kappa = 0$$

$$\gamma = 40^\circ - 70^\circ$$

the equation of motion (2.3) yields the following expression for the natural frequency

$$f_n = 0.046 \left[\frac{nEw^3t \sin^2(2\gamma)}{l(mr^2 \cos^2 \gamma + I_z \sin^2 \gamma)} \right] \quad (2.4)$$

The study also attempted to make comparisons between behaviour of a bowl feeder and a linear vibratory conveyor. To do this, a quantity termed the magnification factor was used. This was defined as the spring constant ratio of a bowl-type feeder to that of a linear-type feeder using the same leaf springs. Theoretical predictions made have shown the following:

i) The magnification factor increases as l/r and w/t increase, but is a minimum for an offset factor κ = 0.5, and a maximum for κ = 0 and 1.0.

ii) The magnification factor is unity for spring angles of 0° and 90°, and attains a maximum value when γ = 45°.

The equivalent spring constant in a bowl feeder can be between 2 and 40 times as large as in a linear vibratory conveyor using the same leaf springs.

The complex structure of the bowl feeder also affects the vibration direction and its relationship to the inclination angle of a leaf spring. From further analysis, the following points regarding the vibration angle in a bowl feeder, γ', were established:

i) For small values of γ, less than 50°, and values of κ close to unity there is a considerable difference between γ' and γ; and

ii) For κ = 0, γ' = γ.

This has implications for the setting position of the springs relative to the base circle.

Experimental work was undertaken using a three bank vibratory bowl feeder, and this showed good agreement with the theoretical results in the range of practical use. The investigations carried out were:

i) Load-displacement curves were plotted for different values of cramping torque of the leaf springs. These exhibited a hysteresis loop, and the softening tendency of the springs was large when the cramping torque was small. It was concluded that, for large displacements, micro-slip occurs at the cramping of the springs. However, the assumption that the spring constant is linear was held to be valid since the range of displacement is small;

ii) The spring constant was measured for a range of offset factors and three spring widths. This showed good correlation with the theoretical predictions, giving a minimum at $\kappa = 0.5$, and a maximum for $\kappa = 0$ and 1.0; and

iii) Both spring constant and natural frequency were measured for a range of spring widths. This showed good agreement with theoretical values for spring widths less than 25 mm, and demonstrated that as spring width increases, both the spring constant and the natural frequency increase.

2.3 Design of Vibratory Bowl Feeders

A step-by-step procedure for the design of bowl feeders, taking into account all its functions, has been proposed by Wiendahl and Ahrens(7). This also uses earlier work carried out in this area by Ahrens(13).

The study highlights the fact that all previous work has treated the separate functions of conveying and orienting independently, whereas in practice these are interlinked and must therefore be considered together. This interrelationship can be described in terms of a functions-component matrix.

In common with the work by Redford and Boothroyd(2), the mechanics of vibratory conveying is considered, identifying the four basic modes of motion. A factor called the throw coefficient is also defined. This is the ratio of the normal component of acceleration to the

component parallel to the acceleration due to gravity.

The hopping phases of the motion are referred to as 'micro-throws'. The impact between component and track directly after the 'micro-throw' is considered. Previous work has assumed that this is completely plastic, and that the component returns to one of the other modes of motion immediately after landing. This assumption is valid for bulk materials, where there is a high degree of damping, but not for individual components. Experimental work has been carried out to measure the normal and parallel acceleration components of a part by mounting two miniature accelerometers on it. The resulting acceleration-time curves show large peaks in the region of impact with acceleration levels many times the driving acceleration. This must cause stressing of the component and will affect the whole conveying process.

In order to take account of the impact in the modelling of the motion of the part, the impact is treated as being partly plastic, and is analysed as an impulse-excited mass-spring-damper system formed by the part, the track lining, and the track itself. The theoretical predictions of acceleration-time curves show reasonable agreement with the experimental results.

High-speed films were used to make a close examination of the conveying process. These show that even with a uniform cuboid, it is not possible to detect the uniform flight path or parabola predicted by theory. Instead, the resulting impacts act differently on the part, resulting in wobbling and hopping between the front and rear edges. Repeated impulses on one particular edge can cause the part to tilt, giving a total 'micro-throw' of the order of several millimetres. This behaviour needs to be taken into account, particularly when designing orienting devices.

Eleven stages are suggested for the effective design of bowl feeders. The first stage involves the collection of all relevant data from the customer. This is then used, along with catalogue examples, to provide a basic solution for the orientation of the part. An important criteria here is the smallest orienting dimension, which gives the maximum permissible throwing height of the component; this can be used to determine a permissible throw coefficient.

It is recommended that the effective throw angle, defined as the projection angle relative to the track surface or the vibration angle minus the track angle, is kept to a value below 8^{o}, since steeper angles may cause a reduction in the conveying speed. Special features may necessitate

a steeper angle. When both the throw coefficient and the throw angle have been chosen, the maximum achievable conveying speed can be determined from the graph given as Fig.2.6. An order of magnitude reduction of the feed rate because of the orienting tooling needs to be applied before it is possible to see whether the basic design will give the required output.

The next step suggested in the design process is the selection of the spring angle so that the effective throw angle relative to the track is obtained. This requires the coordination of track angle, track radius, effective throw angle, and spring radius. Folowing this, it may be necessary to change the value of the throw coefficient in order to achieve the minimum conveying velocity determined from the operating data.

A recommendation regarding the setting up of bowl and drive is also made. This involves ensuring that the two are parallel by the use of an insert fitted during assembly and by the specification of large tolerances in the fixing holes of springs.

The selection of a suitable operating frequency ratio is then required. This is defined as the ratio of the exciting frequency to the natural frequency of the feeder. The effect of a variable load in the bowl on the

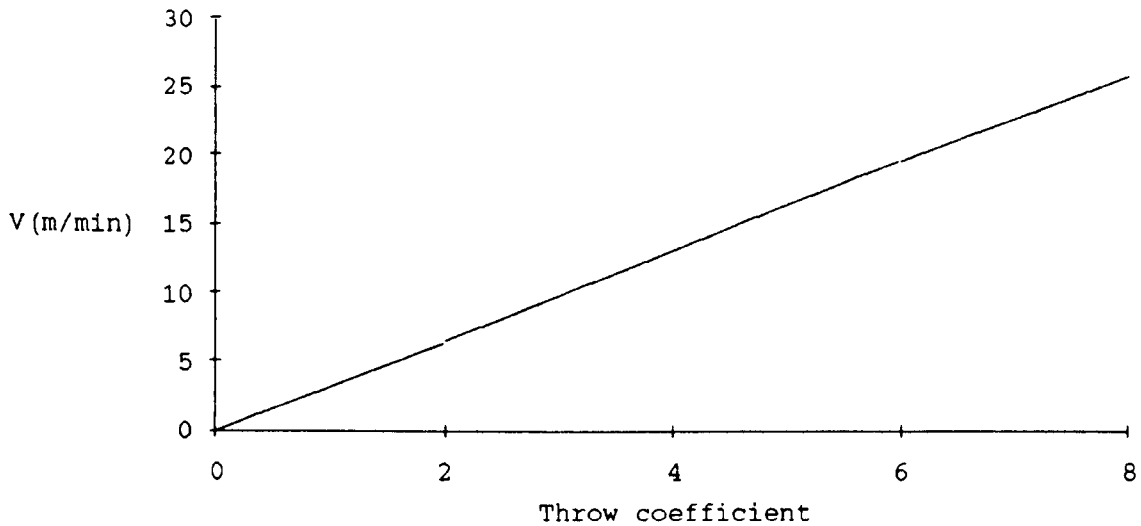

Fig.2.6 Plot of predicted values of the feed speed against throw coefficient for an effective track angle of 8° (Wiendahl and Ahrens)

throw coefficient and conveying speed can be kept to a minimum if a suitable value is chosen. The variation in load can also be minimised by using an additional hopper to top-up the feeder or by using a constant amplitude control.

At this stage, the orientation tooling can be fitted. The resulting reduction in feed rate should be documented in order to establish a catalogue of examples, and to aid in establishing more accurate values for use in determining conveying speeds during the design process.

2.4 Review of Developments in Bowl Feeder Design

A summary of the three generations of vibratory bowl feeders has been presented by Burgess(8). This describes the developments which have taken place with each generation, and the increased control which can be achieved with the third generation.

First generation non-resonant feeders used a fixed frequency electromagnet mounted centrally and pulling vertically with a driving frequency a few Hz above the natural frequency. The majority of feeders in use today are of this type.

The second generation non-resonant feeders had an electromagnet mounted on the periphery of the bowl pulling in a horizontal direction. The power requirement of these was six to twelve times greater than the first generation feeders. Tuning was often a problem, but the feeders were well suited to the feeding of intricate parts requiring precision tooling.

A third generation non-resonant feeder with many magnets mounted on the springs outperformed the earlier models, but had a prohibitive cost.

The first generation of resonant feeders used a new type of variable frequency free piston pneumatic motor which locked in on the natural frequency of the mechanical device. This gave a wide range of amplitudes of movement. The free piston was attached centrally and acted vertically. This gave an increase in speed of two to three times over non-resonant feeders and was less sensitive to changes in load. It was mainly used as a heavy duty feeder.

The second generation of resonant feeders had the piston mounted horizontally at the bottom of the bowl. There were large asymmetric effects, and, at low power levels, dead spots. However, there were increases in load

carrying capacity, six to twelve times over the first generation feeders.

In the third generation of resonant feeders, the axis of the free piston vibratory motor was permitted to rotate in a stepless manner throughout a large range of angles. The free piston unit was mounted at the side of the drive. Earlier assumptions about the need for a base with a large mass to balance any asymmetrical forces were found to be incorrect. By suitable choice of the angle for the motor the mass of the base could be reduced without affecting the feed rate. This was verified by carrying out experimental tests with a base which was 39 % lighter than the standard base used.

2.5 Vibratory Conveyors

2.5.1 Use of non-sinusoidal vibration

An investigation into the use of a non-sinusoidal waveform for vibration generation with linear vibratory conveyors has been carried out by Okabe, Kamiya, Tsujikado and Yokoyama(9). This uses the fact that periodic waveforms can either be modelled as a Fourier Series or as a series of connected straight lines. When there is only one zero crossing per cycle i.e. the

waveform has just one positive part and one negative part, the approximation can be made by the use of just six lines. This is the simplified approach which is adopted here.

The points during a cycle where the changes in slope occur are denoted as τ_a, τ_b, τ_c, and τ_d. The crossing point where the waveform changes sign is denoted by τ_o. Various distortion factors associated with these points are defined; these indicate the shifts along the time axis when compared with a standard sinewave.

The investigation shows that by suitable selection of these conditions:

i) The motion of the particle is made independent of the negative part of the waveform;

ii) The instantaneous velocity of the particle never takes a negative value; and

iii) A vibration component perpendicular to the surface is unnecessary to feed the particle.

The optimum conditions are as follows:

$$\frac{\tau_o}{2} > \tau_b > \tau_o \qquad (2.5)$$

$$0 < \tau_a < \frac{\tau_o}{2} \qquad (2.6)$$

$$\tau_b - \tau_a = \pi \qquad (2.7)$$

$$0.3 < \xi < 0.5 \qquad (2.8)$$

where the timing factor

$$\xi = \frac{\tau_o - \pi}{\pi} \qquad (2.9)$$

and these give a theoretical conveying velocity of

$$v = \frac{4af}{(2 + \xi)} \qquad (2.10)$$

where a is the peak to peak displacement of the waveform, and f is the frequency of vibration.

The theoretical predictions were compared with experimental results which were obtained by inputting waveforms with a range of distortion factors into a horizontal track mounted on vertical parallel leaf springs. The drive was provided by an electromagnetic

vibrator acting in the horizontal direction only. Waveforms of the output displacement, velocity and acceleration were examined, and the mean conveying velocity measured by timing the rate of travel of components. There was found to be good agreement between theoretical and experimental results.

2.5.2 Characteristics of a loaded vibratory feeder

An investigation into the effect of the load on the feeding characteristics of vibratory conveyors has been carried out by Sakaguchi(10). This involved both analytical and experimental work.

The theoretical approach isolates the vibrating table as a free body and considers the forces acting on this. These include both the input driving force and the reaction forces from the load. When the driving surface is an inclined plane, both frictional and inertia effects are considered.

An equation of motion in terms of the displacement of the table in the direction of the input force is then set up. This enables the critical points during the cycle, where the mode of motion changes between the following:

forward sliding;

backward sliding;

stationary motion; and

jumping motion;

to be determined. The reaction force of the load is expressed as a Fourier Series in order to take into account its cyclic variation. The Fourier coefficients are established by considering the inertia and friction forces during each separate mode of motion. Solution of the equation of motion then gives the response acceleration amplitude and phase relative to the input as a function of the driving frequency. The energy dissipation during impact is accounted for by including an equivalent inertia term in the equation of motion.

The resulting frequency response curves of the feeder are shown in Fig.2.7, where K_v is the non-dimensional component of acceleration normal to the vibrating table. The curves are clearly non-linear, and the inclination of the peaks to the right indicate that vibration is unstable to the right of the resonance frequency, but stable to the left. These also demonstrate the fact that the resonant frequency decreases as the load increases.

Fig.2.7 Frequency response curves of a loaded vibratory feeder (Sakaguchi)

2.5.3 Other work on vibratory feeders

Most of the work carried out in the field of mechanical handling by vibratory conveying has been directed at the linear vibratory conveyor. The hopping motion of components on a track driven by both triangular and sinusoidal waveforms has been analysed by Winkler(3), and a computer model for parts being fed with in-phase or out-of-phase excitation has been developed and verified experimentally by Ng, Ang and Chng(4). An analysis of the sliding, hopping and stationary modes of motion has also been undertaken by Taniguchi, Sakata, Suzuki and Osanai(5), and developed further by Sakaguchi and Taniguchi to consider the resulting conveying velocity and power(14): it is suggested that these concepts of velocity and energy can be used in the design of vibratory feeders.

3. DEVELOPMENT OF A NUMERICAL MODEL OF THE BOWL FEEDER STRUCTURE

As the review of earlier work shows, most of the work in the area of vibratory feeding had concentrated on the motion of individual components. A study carried out by Okabe and Yokoyama(6) had concentrated on modelling the bowl feeder structure, but had chosen to analyse it as a single degree of freedom system. It was felt that this neglected important aspects of the structure's behaviour, and there were two main reasons why a more accurate working model of the feeder was desirable:

i) This should give a better understanding of the behaviour of the feeder, enabling the solution of problems such as the occurrence of 'dead spots' and other unpredictable aspects which arise during both manufacture and operation to be approached in a more logical and reasoned manner.

ii) This would enable the effect of design modifications to be investigated without the necessity to build a prototype bowl feeder.

This chapter describes the stages involved in the development of the numerical model of the bowl feeder,

describing the decisions taken in attempting to faithfully represent its behaviour in a computer simulation.

Since this was the first phase of the project, the sole objective was to model the dynamic behaviour of the feeder, predicting its natural frequencies and mode shapes. Once this had been successfully completed, predictions of its actual operating performance i.e. the feed rate of components in response to a particular forcing input, could be tackled.

3.1 Description of the Bowl Feeder Structure

The main components of a vibratory bowl feeder are shown in the diagram in Fig.3.1. The bowl, which can be either cast or fabricated, is used as both a storage and a feeding and orienting device; components to be fed are placed inside the bowl and under the action of the vertical forcing function provided by the electromagnetic coil move up the spiral feed track around the inside of the bowl. The base is normally a cast, solid component with a much larger mass than that of the bowl. The two are separated by banks of inclined leaf springs (more commonly three banks, but occasionally four) which are arranged at regular intervals along the circumference of

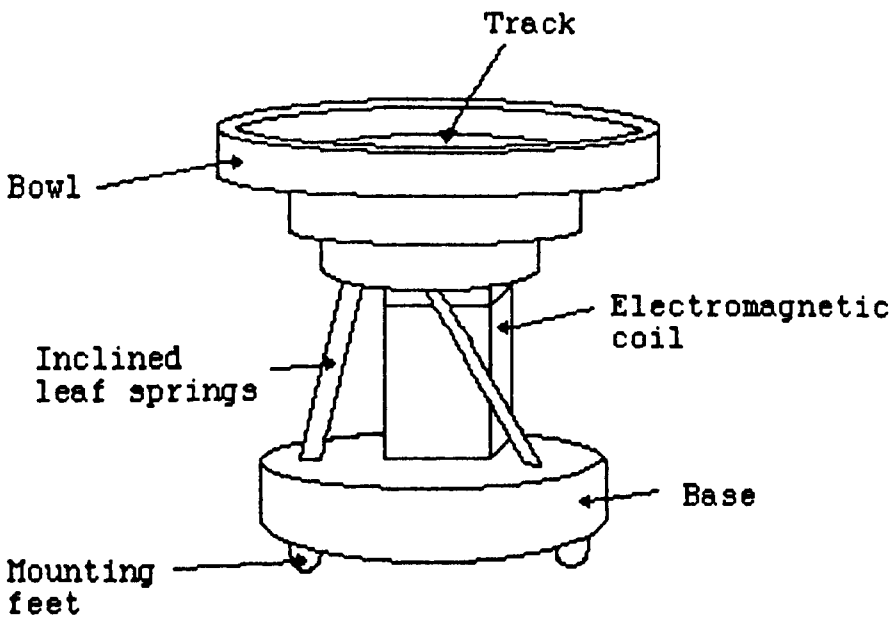

Fig.3.1 Vibratory Bowl Feeder

a circle in the plane of the bowl. The inclination of the springs, along with the vertical driving force provided by the electromagnet, gives rise to a combined twisting and vertical motion of the bowl which propels components along the track.

3.2 Development of a Numerical Model

In order to develop an accurate model of the structure, the following needed to be addressed:

i) What were the main modes of vibration of the structure? This was necessary in order to specify the number and type (rotational or translational) of degrees of freedom required.

ii) Do the main components of the feeder, such as the bowl and base, behave as rigid bodies within its operating frequency range, or is successful operation also dependent upon the flexural vibration of these parts?

Observation and simple tests have indicated that the main modes of vibration, which provide the actual motion of the components, are the vertical and rotational motion of the bowl relative to the base. In addition, however, it

was also decided that 'tipping' of the bowl in its own plane should be included. This was done for the following reasons:

i) The asymmetry of the bowl which results from its spiral track could excite this particular mode of vibration; and

ii) The supporting arrangement of the bowl where it is mounted on three banks of springs meant that small differences in spring constants could result in a 'tipping' motion.

It was felt that the 'tipping' motion might be counter-productive in obtaining the desired motion of the components in the bowl.

It was therefore decided to model the structure as an eight degree-of-freedom system. This included vertical motion, Δ, rotation, θ_z, and tipping about both x and y axes, θ_x and θ_y, of both the bowl and the base. These coordinates are shown related to the x-y-z coordinate system of the feeder in Fig.3.2.

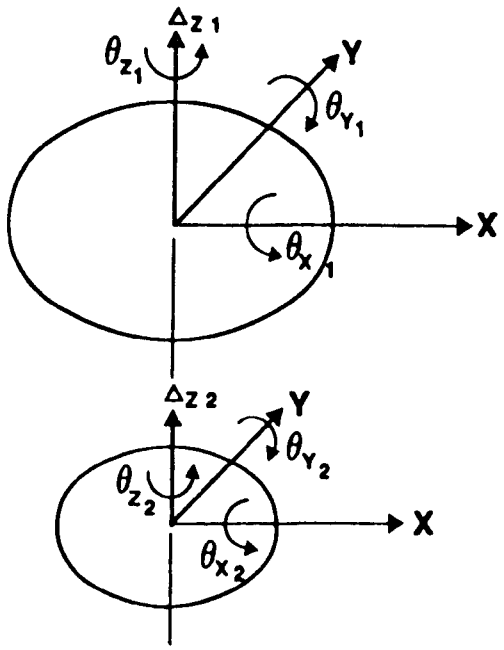

Fig.3.2 Eight degree-of-freedom bowl feeder model

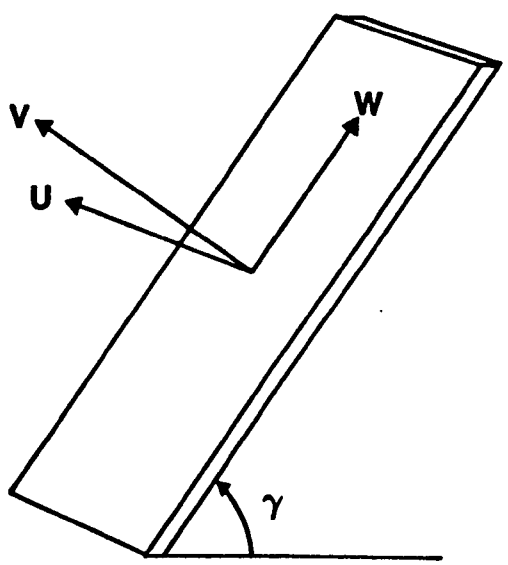

Fig.3.3 Local coordinate system for leaf springs

Observation also suggested that within its operating range the main components of the structure behaved as rigid bodies. It was necessary that the bowl should impart the same motion to all components, and this could only be the case if it were sufficiently rigid. It was therefore decided to model the bowl, base and springs using a lumped parameter approach. It was possible, however, that the higher modes of vibration of this model could fall within the frequency range of the modes of flexural vibration, and that this might affect the behaviour of the structure.

3.3 Formulation of Mass and Stiffness Matrices

The natural frequencies and mode shapes of the eight degree-of-freedom lumped parameter model of the bowl feeder were determined by solving the well known eigenproblem, the equation of motion for free vibration:

$$[M]\{\ddot{x}\} + [K]\{x\} = 0 \qquad (3.1)$$

where [M] is the mass matrix,

[K] is the stiffness matrix, and

{x} the vector of generalised coordinates or degrees of freedom in the x-y-z coordinates of the system.

The solutions would be the eigenvalues, λ_i (i=1,8), which are related to the natural frequencies by

$$\lambda_i = \omega_i^2 \qquad (3.2)$$

and the eigenvectors or mode shapes, $\{x\}_i$ (i=1,8).

The lumped parameter model of the bowl feeder was based on the assumption that all the stiffness of the structure was concentrated in the springs, and that all the mass or inertia was concentrated in the bowl and base. In order to formulate the stiffness matrix it was easiest to work in terms of the local orthogonal u-v-w coordinate set for each individual spring bank, and then relate this to the system of generalised coordinates using a set of connecting equations. The system of local spring coordinates is shown in Fig.3.3.

The three translations Δ_u, Δ_v, and Δ_w, and the three rotations θ_u, θ_v, and θ_w at both ends of each spring bank result in a set of 36 localised coordinates for the structure as a whole. These can then be related to the generalised coordinates by a set of 36 equations of kinematic constraints in terms of the geometry of the feeder. The attachment points of the springs and the

resulting geometry are shown in Fig.3.4 where the attachment points on the bowl are a,b and c, and those on the base are d,e and f. The leaf springs themselves are arranged at regular intervals on the circumference of a circle of radius r. The connection points on the bowl are at a radius r_1, where $r_1 = r/\cos \phi_1$ as shown in Fig.3.4. Similarly the radius of the attachment points on the base is given by $r_2 = r/\cos \phi_2$. The constraint equations can be written in matrix form:

$$[A]\{x\} = [B]\{u\} \qquad (3.3)$$

where {x} is an 8 x 1 vector of generalised coordinates;

{u} is a 36 x 1 vector of localised coordinates;

[A] is a 36 x 8 coefficient matrix; and

[B] is a 36 x 36 coefficient matrix.

The full set of constraint equations is included as Appendix 1.

If [B] is non-singular, we can now define a matrix [C], where

$$[C] = [B]^{-1}[A] \qquad (3.4)$$

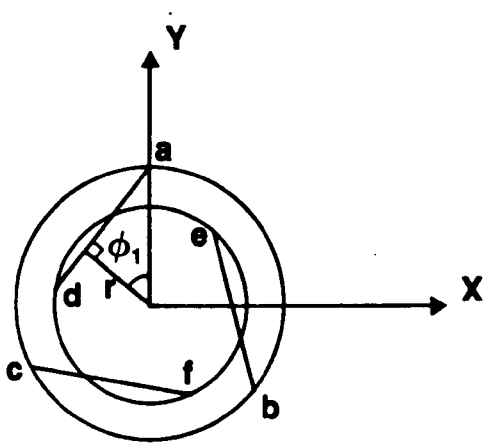

Fig.3.4 Connection points on the bowl and base

and (3.3) can be rewritten as

$$\{u\} = [C]\{x\} \tag{3.5}$$

where [C] is the 36 x 8 connection matrix. A more detailed description of the use of connection matrices is given in the texts by Kron(34) and Richards(36).

The connection matrix [C] is used to derive a global stiffness matrix from the stiffness matrices of each bank of leaf springs in terms of the u-v-w coordinates. The bending of the springs was modelled using the Euler-Bernoulli beam theory which neglects any effects due to shear deformation. This resulted in a 4 x 4 stiffness matrix in the u-w plane of the form:

$$\frac{EI_u}{l^3}\begin{bmatrix} 12 & -6l & 12 & -6l \\ & 4l^2 & 6l & 2l^2 \\ & & 12 & 6l \\ \text{symmetric} & & & 4l^2 \end{bmatrix} \tag{3.6}$$

where E is Young's modulus;

l the length of the spring; and

I_u the second moment of area about the u-axis.

Similarly in the v-w plane:

$$\frac{EI_v}{l^3}\begin{bmatrix} 12 & 6l & -12 & 6l \\ & 4l^2 & -6l & 2l^2 \\ & & 12 & -6l \\ \text{symmetric} & & & 4l^2 \end{bmatrix} \qquad (3.7)$$

where I_v is the second moment of area about the v-axis.

A section through a bank of springs showing the position and orientation of the u and v axes is given as Fig.3.5. Taking into account the spacing between springs, the equations used for I_u and I_v were:

$$I_u = \frac{3wt^3}{12} + 2wt(t+t_s)^2 \qquad (3.8)$$

$$I_v = \frac{3tw^3}{12} \qquad (3.9)$$

where w is the spring width;

t is the spring thickness; and

t_s the spacing between springs.

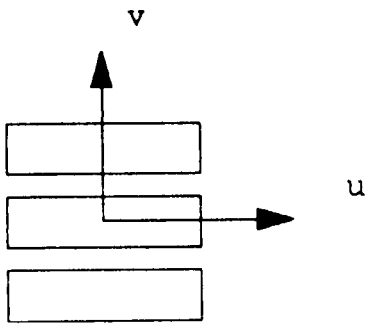

Fig.3.5 Section through a spring bank for calculation of second moment of area

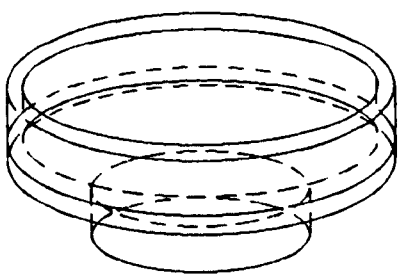

Fig.3.6 Arrangement of two solid and one hollow disc used as an idealisation of the bowl for the calculation of its moments of inertia

A linear displacement function was assumed in extension, resulting in a 2 x 2 matrix:

$$\frac{EA}{l}\begin{bmatrix} 1 & -1 \\ -1 & 1 \end{bmatrix} \qquad (3.10)$$

where A is the cross-sectional area of the spring bank.

Similarly a linear deformation model in torsion gave the following 2 x 2 matrix:

$$\frac{GJ}{l}\begin{bmatrix} 1 & -1 \\ -1 & 1 \end{bmatrix} \qquad (3.11)$$

where G is the shear modulus; and
J is a torsional constant for rectangular section bars with a cross-section of length 2a and width 2b given in Roark and Young(15) as:

$$J = ab^3\left(\frac{16}{3}\right) - \left[3.36\left(\frac{b}{a}\right)\left(1 - \frac{b^4}{12a^4}\right)\right] \qquad (3.12)$$

In this case the length of the rectangle used was w, and the width was 3t.

The stiffness matrices given in equations (3.6), (3.7), (3.10), and (3.11) can be combined to give a 36 x 36 stiffness matrix corresponding to the localised coordinates at each end of the spring banks.

The stiffness matrix for the system as a whole is determined by considering the expression for strain energy:

$$U = \frac{1}{2} \{u\}^T [K_u] \{u\} \qquad (3.13)$$

where $[K_u]$ is the 36 x 36 stiffness matrix obtained for the u-v-w coordinate set.

Combining this with equation (3.5) gives

$$U = \frac{1}{2} \{x\}^T [C]^T [K_u] [C] \{x\} \qquad (3.14)$$

or

$$U = \frac{1}{2} \{x\}^T [K] \{x\} \qquad (3.15)$$

Hence the stiffness matrix in terms of the generalised coordinates in the x-y-z plane, [K], is given by

$$[K] = [C]^T [K_u] [C] \qquad (3.16)$$

where [K] is a square symmetric 8 x 8 matrix.

The mass matrix of the system [M] was an 8 x 8 diagonal matrix and consisted of the following elements:

m the mass of the bowl;

I_x the moment of inertia of the bowl about the x axis;

I_y the moment of inertia of the bowl about the y axis;

and

I_z the polar moment of inertia of the bowl.

Similar quantities are used for the base.

The moments of inertia of the bowl are calculated by idealising this as two solid discs and a hollow cylinder arranged concentrically as shown in Fig.3.6. The base is idealised as a single solid disc. It was assumed that both the bowl and base were axi-symmetric with their centres of mass on the central axis of the feeder.

All the steps described in this section were coded using FORTRAN IV as the front end of the full program for the numerical modelling of the bowl feeder. A flow chart showing the stages involved and the inputs and outputs is given as Figs.3.7 and 3.8.

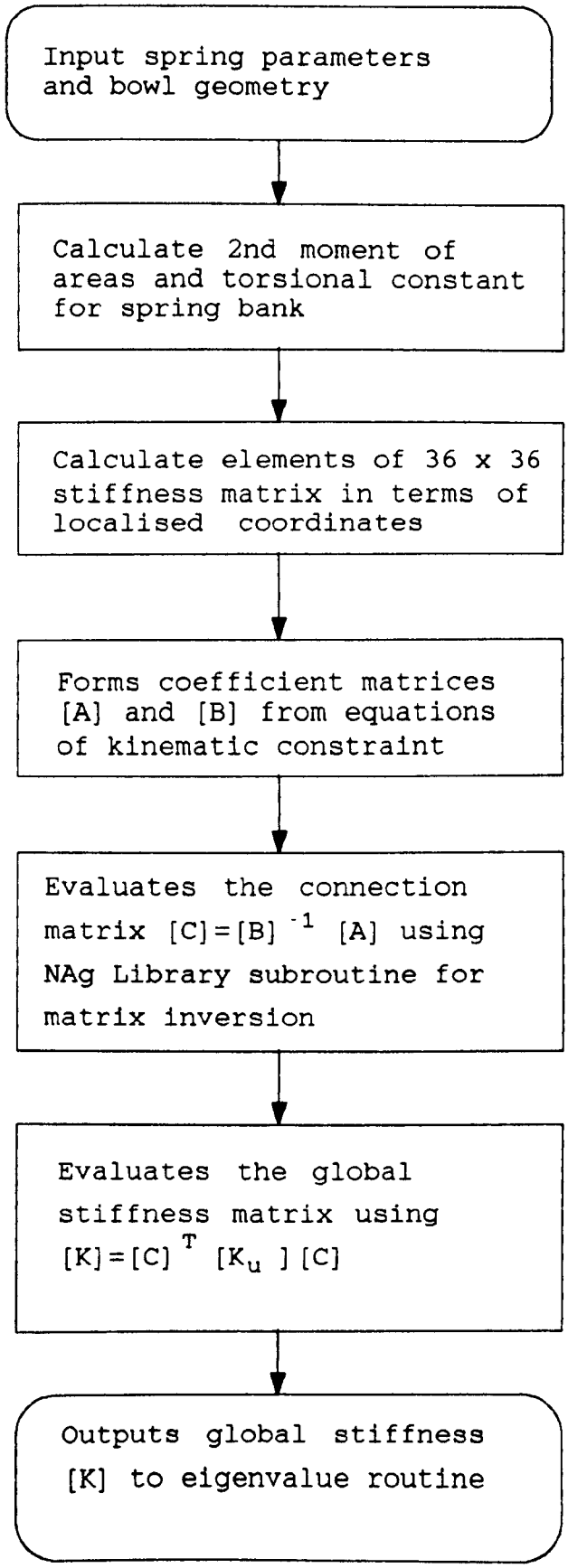

Fig.3.7 Flow chart of coding for evaluation of stiffness matrix

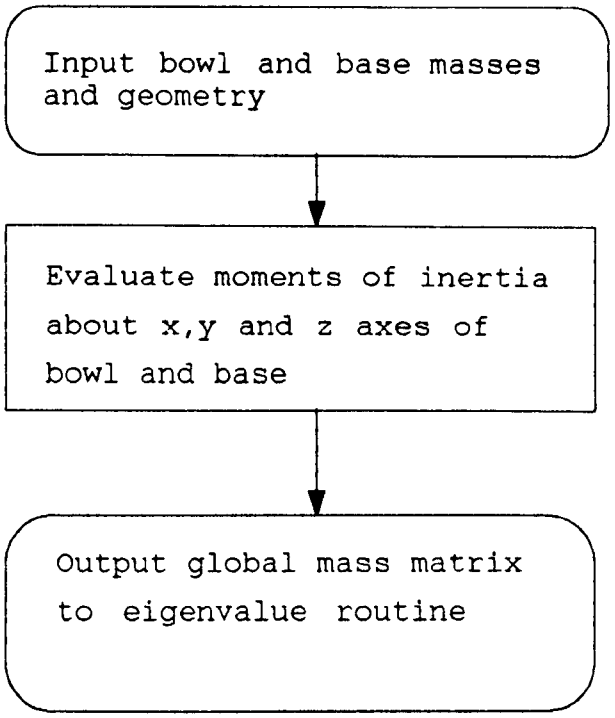

Fig.3.8 Flow chart of coding for evaluation of mass matrix

Inversion of the coefficient matrix [B] is carried out by the NAg Library subroutine(16) F04AEF for matrix inversion. A separate subroutine for matrix multiplication was written.

3.4 Solution of the Eigenproblem

As discussed in section 3.3, the natural frequencies and mode shapes of the bowl feeder can be found from the solution of the eigenvalue/eigenvector equation (3.1).

This was implemented using the following NAg Library subroutines (16) incorporated in FORTRAN IV coding:

F01AEF Cholesky decomposition of the eigenproblem $[A]\{x\} = \lambda[B]\{x\}$ to the standard symmetric eigenproblem $[P]\{z\} = \lambda\{z\}$, where [A] is a real symmetric matrix, and [B] is a real symmetric positive definite matrix.

The equation of motion of the system is of the form

$$[K]\{x\} = \lambda[M]\{x\} \qquad (3.17)$$

As [M] is real symmetric positive definite it can be factorised using Cholesky's method

so that

$$[M] = [L][L]^T \tag{3.18}$$

Rewriting equation (3.17) gives

$$[L]^{-1}[K]([L]^T)^{-1}([L]^T\{x\}) = \lambda([L]^T\{x\}) \tag{3.19}$$

which is the standard eigenproblem

$$[P]\{z\} = \lambda\{z\} \tag{3.20}$$

where

$$[P] = [L]^{-1}[K]([L]^T)^{-1} \tag{3.21}$$

$$\{z\} = [L]^T\{x\} \tag{3.22}$$

The subroutine F01AEF calculates [L] and $[L]^{-1}[K]([L]^T)^{-1}$.

F01AJF This gives the Householder reduction of a real symmetric matrix to tridiagonal form for use in F02AMF.

The symmetric matrix [P] is reduced to the symmetric tridiagonal matrix $[P]_{n-1}$ by n-2 orthogonal transformations. Each transformation gives a complete row of zeroes except in the triple diagonal positions without affecting

previous rows.

F02AMF This calculates all the eigenvalues and eigenvectors of a real symmetric tridiagonal matrix.

The eigenvalues and eigenvectors are derived using the QL algorithm which is an adaptation of the QR algorithm, as described in the text by Wilkinson and Reinsch(35). The eigenvectors are $\{z\} = [L]^T\{x\}$, and these are normalised so that the sum of the squares of the elements is equal to 1.

F01AFF This derives the eigenvectors $\{x\}$ from the corresponding eigenvectors $\{z\} = [L]^T\{x\}$ of the standard symmetric eigenproblem.

The routine solves $[L]^T\{x\} = \{z\}$ by backward substitution. If $\{z\}$ is normalised so that $\{z\}\{z\}^T = 1$, then $\{x\}$ is normalised such that $\{x\}[M]\{x\}^T = 1$.

Details of the arguments for these subroutines and any error indicators are given in the relevant NAg Library manual(16).

A listing of the coding for the full numerical model based on the flow chart in Figs.3.7 and 3.8 and the NAg Library subroutines is given as Appendix 2.

3.5 Graphical Display of the Mode Shapes

The output of the coding described in the previous two sections was the eigenvalues, λ_i (i=1,8), and their corresponding eigenvectors, $\{x\}_i$ (i=1,8). In order to visualise the actual motion which these represented and to compare with any experimental verification, a graphical display of the mode shapes was necessary.

A flow chart of the inputs and procedures used in carrying out the plotting of the mode shapes is given as Fig.3.9. From this coding was written in FORTRAN 77 using GHOST graphics routines(17). A listing of the program is given as Appendix 3.

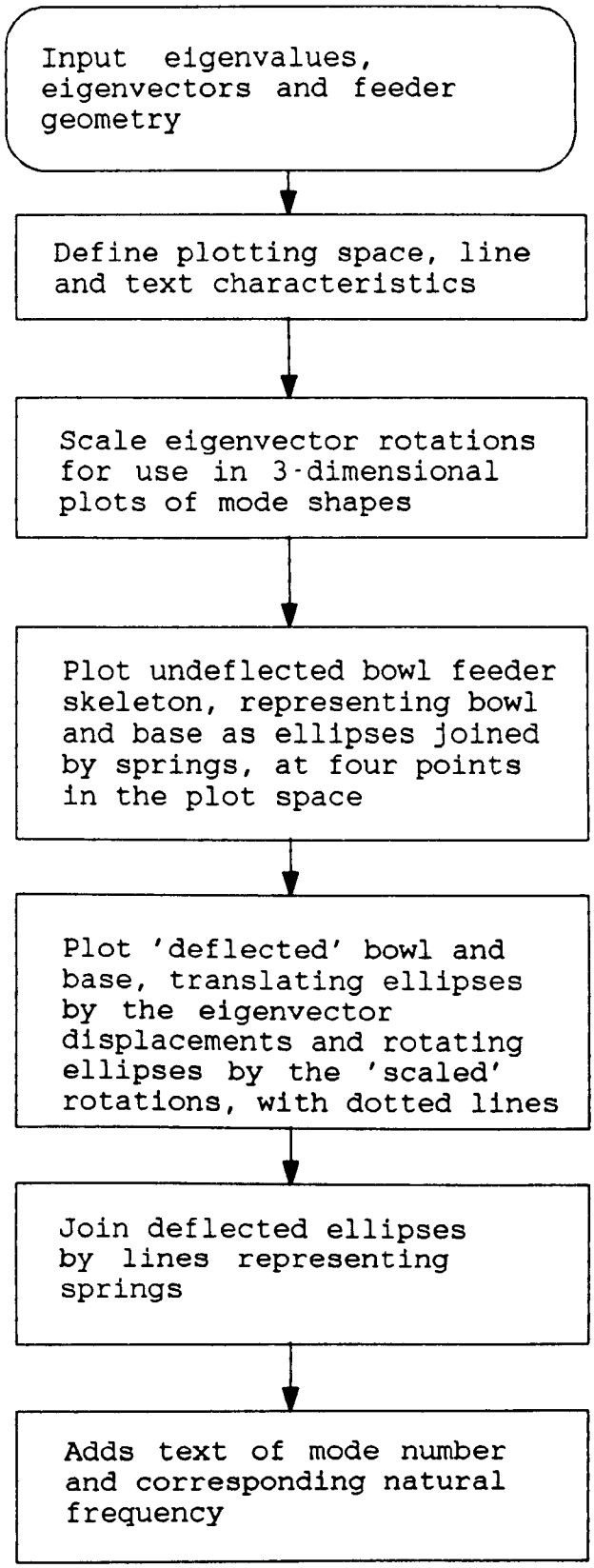

Fig.3.9 Flow chart of procedures used for the plotting of mode shapes using GHOST

4. MODAL TESTING OF A BOWL FEEDER

In order to test the validity of the numerical model of the bowl feeder in predicting its dynamic characteristics and behaviour, it was decided to undertake a programme of experimental work. This would enable measured values of natural resonant frequencies and the corresponding mode shapes to be compared with those calculated by the numerical model.

The most appropriate technique for the determination of natural frequencies and mode shapes experimentally was that of modal analysis. This was carried out using a microcomputer driven system, interfaced with a dual-channel FFT analyser.

4.1 Experimental Modal Analysis

Because of the quite significant hazard which structural vibration problems present to the operation of a wide range of structures, machines and mechanisms, engineers have expended a great deal of time and effort in the experimental study of structural vibration.

This has enabled them to understand and control the vibration phenomena which occur in practice. One of the most important advances was the work carried out by Kennedy and Pancu in 1947 (18).

Following this, major advances in transducers, electronics and digital analysers meant that by 1970 the technique of modal testing was well established. Further developments in computer technology have resulted in relatively cheap microcomputer-based systems becoming available in recent years.

The technique of modal testing enables frequency-response or mobility data i.e. the harmonic response at one of the coordinates, x_j, caused by a single input at a different coordinate, f_k, to be analysed in order to determine the modal properties of the structure, namely the natural resonant frequencies, damping factors and mode shapes. This relationship can be seen from the equation for the mobility at a forcing frequency ω

$$Y_{jk}(\omega) = \left(\frac{x_j}{f_k}\right) = j\omega \sum_{r=1}^{N} \left[\frac{({}_r\phi_j)\ ({}_r\phi_k)}{(\lambda_r - \omega^2)}\right] \qquad (4.1)$$

where λ_r is the eigenvalue of the rth mode (its natural frequency and damping factor combined);

$_r\phi_j$ is the jth element of the rth eigenvector $\{\phi\}_r$ (i.e. the relative displacement at that point during vibration in the rth mode);

N is the number of degrees-of-freedom.

This equation is the foundation of experimental modal analysis, providing a link between the modal properties of a system and its response characteristics. However, because the full technique involves other stages of measurement and analysis, a clear understanding of the theory and operation of these is necessary to ensure both high-quality data and accurate results. The test procedure itself consists of the following main stages:

i) measurement of transfer mobility functions at all points on a specified grid on the structure in response to an excitation force at one point (or excitation at all points on the grid and measurement of the responses at a single point);

ii) analysis of the resulting frequency response functions using curve-fitting routines; and

iii) combination of the results of the curve-fits to construct a model of the structure in terms of its modal properties.

These will now be considered in more detail, concentrating specifically on the testing of the bowl feeder structure. Any theoretical background which it has been necessary to cover in order to carry out the successful implementation of the experimental modal analysis will be introduced in the relevant section.

4.2 Experimental Apparatus

A block diagram including model numbers of the instrumentation used in the modal testing is given as Fig.4.1.

A detailed description of the function of individual components is given in the following sections.

The bowl feeder used in these tests was a model 15 Aylesbury Automation feeder. A full specification of this is given in Chapter 5.

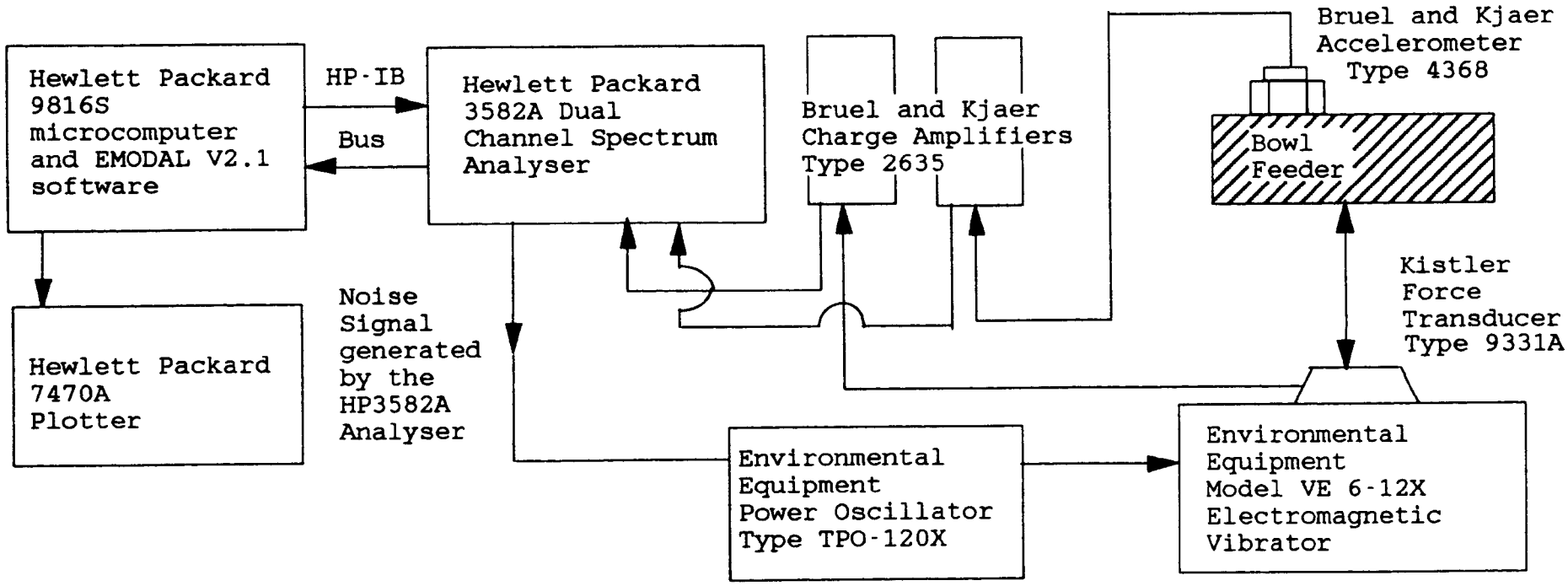

Fig.4.1 Block diagram of experimental apparatus and instrumentation used in modal testing

4.3 Suspension and Excitation of the Structure

In carrying out a modal test, one of the first aspects which requires consideration is the mechanical means of supporting and (correctly) exciting the structure. The method of support is determined by various factors such as the boundaries of the theoretical model which the test is designed to verify, whether it is required to isolate the behaviour of an individual component or to consider a system as a whole, and the mass and fixings of a strucure which may prevent it from being tested other than in-situ.

Since the boundaries of the numerical model of the bowl feeder were free, and it was the characteristics of the feeder structure itself which were of interest, it was decided that the most appropriate form of support was as a free structure. This was achieved by hanging the feeder from a square-section welded framework using 'soft' springs chosen to give a rigid body mode well below the frequency range of interest during testing. The points of suspension were three equidistant points on the floor of the bowl. A photograph of the test rig is given as Plate 4.1.

Plate 4.1 Experimental arrangement for modal testing

Given that the analysis of the mobility measurements was to be carried out using a digital frequency analyser, there were two possible methods of excitation available: an impulse from an instrumented impact hammer or bandwidth limited random noise. However, the HP3582A had certain limitations in terms of its signal-conditioning capabilities which made it unsuitable for taking accurate measurements from a transient signal. These were:

i) It was not possible to specify different time lengths for the windows applied to the input and output signals. The window length used was a direct function of the frequency range selected for analysis. For a long sample length and a short impact, this could produce unacceptable values of the signal-to-noise ratio;

ii) It was not possible to select any pre-trigger for the input signal. Depending on the trigger level being used, this could result in part of the input signal being 'lost' thus further degrading the s-n ratio; and

iii) The only window function available on the HP3582A for use with transient signals was a Uniform passband, which is the result of using no time

domain 'window' weighting. A better choice for the transient signal generated by an impact hammer is the Exponential window, which would have reduced leakage by concentrating on the more important information in the initial part of the time record.

In addition, the HP3582A offered the facility of a built-in noise source which was bandwidth limited to the frequency range selected for analysis. This would ensure that, unlike the impulse provided by the impact hammer, no energy was input into the structure outside the frequency range of interest. Since this is good practice when zooming-in on measurements in order to achieve higher resolution, this made the choice of random noise as a method of excitation even more attractive.

The HP3582A also offered the choice of two 'random' noise sources, a periodic-random source, and a 'true' random source. The periodic-random source is based on the pseudo-random source which involves the generation of a random mixture of amplitudes and phases for all the frequency components in the range of interest with some specific requirement such as equal energy at each frequency. A sample of pseudo-random excitation is generated, and after a few cycles, a measurement of the steady-state response is made. A different pseudo-random

sequence is then generated and the procedure repeated. Because of the essentially periodic nature of the signal, and the fact that there is synchronisation with the analysis part of the process, there are no leakage or bias errors in any of the measurements. It was felt that the periodic-random source would probably yield the most accurate results. However, it should be remembered that it is best to verify such an assumption by carrying out initial investigations using both forms of excitation, and by checking the results obtained close to the resonant frequencies using sinusoidal excitation.

The drive itself was provided by an electromagnetic vibrator, and the forcing function transmitted via a drive rod. In order to prevent any bending constraints between the feeder and the exciter, which would introduce unknown forces into the input measurement, a small drive pin was inserted between the two. This was made by reducing a short length of the drive rod to 1 mm in diameter. A photograph of the drive rod and pin is shown as Plate 4.2.

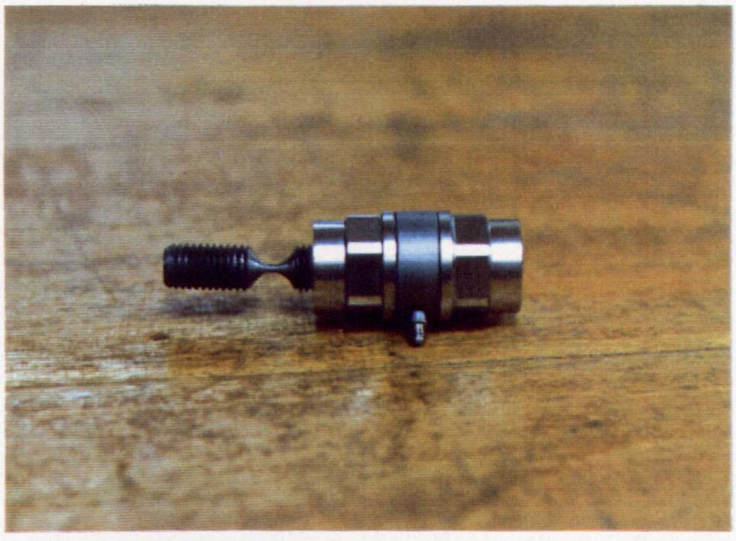

Plate 4.2 Drive rod and force transducer

The point of attachment of the exciter was chosen as the centre of the base of the feeder. The electromagnetic coil which provides the driving force during normal operating conditions has its armature attached to the bowl and its coil attached to the base; thus the centres of either the bowl or the base would have been suitable points of excitation during modal testing.

Because the modal testing was to use an alternative form of excitation from the electromagnetic coil which provides the driving force during normal operating conditions, and because this coil is not included as part of the numerical model, this was removed during testing. This also made access to measurement and excitation points easier.

4.4 Transducers and Amplifiers

In order to make mobility or FRF measurements, it is necessary to measure both the force input and the corresponding response. The input force was measured using a piezoelectric force transducer; this was mounted at the end of the drive rod, between the narrow drive pin and the base of the feeder. It is important that the transducer is mounted as near as possible to the structure under test in order to take an accurate

measurement of the actual forcing function. The response of the structure was measured using a piezoelectric accelerometer. There are two important considerations in this connection:

i) The mounting of the accelerometer. As detailed in the Bruel and Kjaer handbook (19) the use of different methods of mounting can significantly alter the frequency response characteristics of the accelerometer assembly by reducing the first resonant frequency. This needed to be balanced with ease of manouvrability during testing when it was necessary to take a number of transfer mobility readings. Mountings such as a threaded magnetic base or double sided tape offered flexibility of movement of the transducer, but reduced the resonant frequency from 32 kHz to between 7 and 8 kHz, giving an operating range of 0-2 kHz. Since the frequency range which was of interest during the modal test was only 0-1250 Hz, it was felt that these methods of mounting provided an appropriate solution.

   Irrespective of the method to be used, correct mounting of the accelerometer is crucial if accurate

measurements are to be taken. Surfaces should be flat and clean in order to prevent any 'base bending'.

ii) The quantity to be measured by the accelerometer. Although the accelerometer measures acceleration directly, it is also possible by the use of integrating circuits to obtain both velocity and displacement as outputs. The choice of parameter is based on the consideration of two factors. The first of these is the curve-fitting algorithms which were available as part of the Entek modal analysis software EMODAL V2.1(20). Both SDOF 'peak-amplitude' and 'circle-fit' routines could be used, the circle-fit method offering advantages when separating out coupled modes and allowing a more interactive approach to curve-fitting from the user. Texts such as Ewins(21) show that for a viscous damping model a Nyquist plot of mobility gives an exact circle for a SDOF system, whereas for structural or hysteretic damping a Nyquist plot of receptance gives an exact circle. Mobility and receptance are defined as:

$$\text{mobility} = \frac{\text{velocity}}{\text{force}}$$

$$\text{receptance} = \frac{\text{displacement}}{\text{force}}$$

A viscous damping model was assumed, and it was therefore more appropriate to measure velocity. In addition, the frequency range of interest also needed to be considered. The correct measurement parameter needs to be selected in order to give the flattest frequency spectrum and therefore the best dynamic range in the band chosen for analysis. Measurement of displacement will give low frequency components most weight and conversely acceleration measurements will weight the level towards the high frequency components. Brüel and Kjær handbooks(22,23,24) suggest that in the range from 10 to 1000 Hz a measure of vibration velocity gives the best indication of a vibration's severity, and correspondingly the flattest spectrum. It was therefore decided on these two counts that the measured response parameter would be velocity.

Mobility measurements were taken in the x,y and z directions for all points on the structure by attaching the accelerometer to the three perpendicular faces of a

mounting block or cube which could be bolted onto the bowl or base at the measurement locations. A photograph of this is shown as Plate 4.3.

Signals from both the force transducer and the accelerometer were conditioned using charge amplifiers. These contained integrating networks to convert the acceleration signal to either velocity or displacement proportional signals.

4.5 Spectrum Analyser

The Hewlett Packard 3582A is a dual channel digital frequency analyser. It enables two signals captured simultaneously in the time domain to be analysed in the frequency domain using the Fast Fourier Transform algorithm developed by Cooley and Tukey(25). In the dual channel operating mode it calculates frequency spectra with 256 spectral lines.

The basic process of spectral analysis involves the following stages:

i) The analogue input signals are filtered, sampled and digitised to give a series of time records. The sampling rate and the record lengths determine the frequency range and the resolution of the analysis.

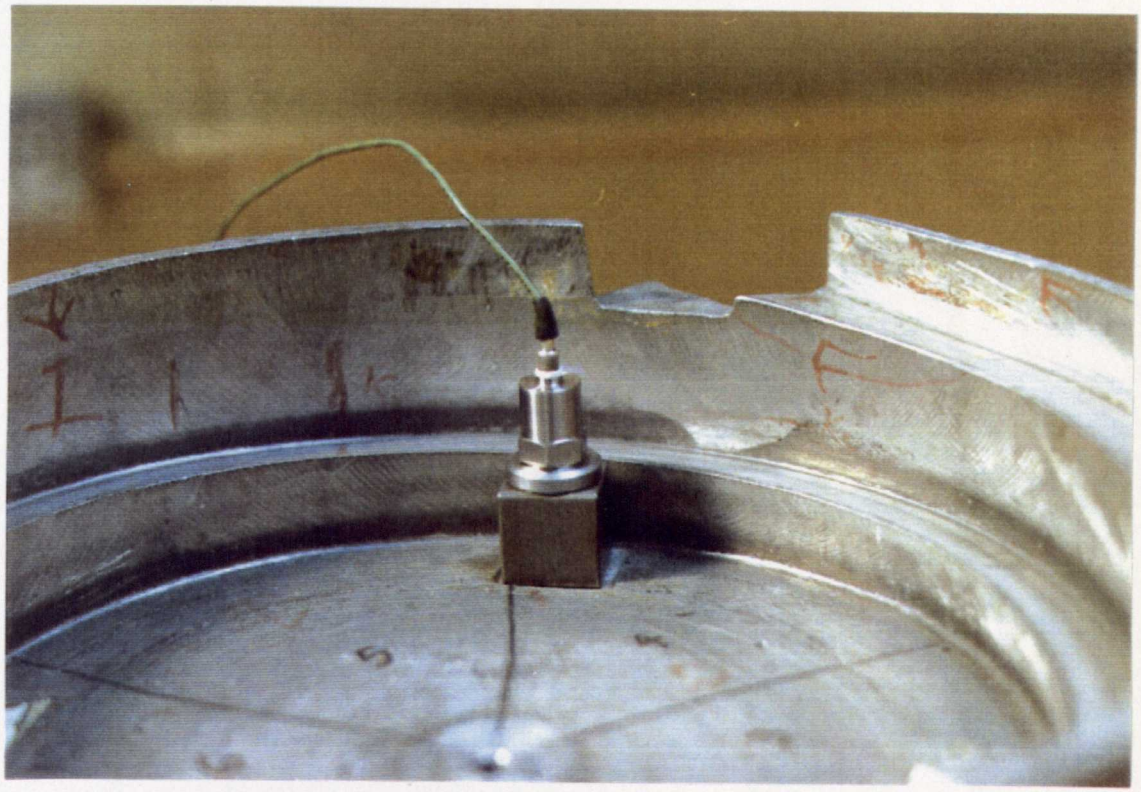

Plate 4.3 Accelerometer mounting block

ii) Each digital sequence is transformed into the frequency domain as a complex spectrum by the use of a Discrete Fourier Transformation.

iii) Further post processing is carried out on the two signals to give magnitude and phase information of the transfer function, $H(j\omega)$.

In order to be able to take accurate measurements, it is important that the analysis which is carried out and any possible errors which may occur are understood. For a random signal, it is not possible to carry out the usual Fourier Transform because its inherent properties violate the Dirichlet condition. Instead, the autocorrelation function (ACF), $r_{ff}(\tau)$, defined as the 'expected' (or average) value of the product $(f(t).f(t+\tau))$ computed along the time axis is used.

$$r_{ff}(\tau) = \int_{-\infty}^{\infty} f(t).f(t+\tau)\ dt \qquad (4.2)$$

This will always be a real and even function of time, and will generally take the form illustrated in Fig.4.2 a). The ACF, unlike the original signal f(t), does satisfy the requirements for Fourier transformation and thus its Fourier Transform can be obtained by the usual equation.

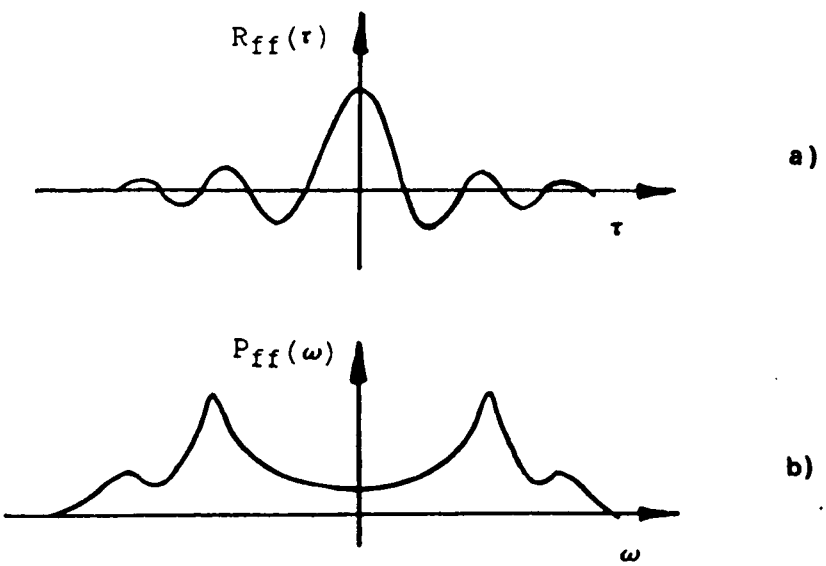

Fig.4.2 Basic Ingredients of Random Signal Description

a) Autocorrelation function

b) Power Spectral Density

The resulting parameter is called the Auto- or Power Spectral Density (PSD), which is defined as:

$$P_{ff}(\omega) = (1/2\pi) \int_{-\infty}^{\infty} r_{ff}(\tau) . e^{-j\omega\tau} \, d\tau \qquad (4.3)$$

The Power Spectral Density is a real and even function of frequency, and generally takes the form shown in Fig.4.2 b).

Similar quantities exist for a pair of functions such as $f(t)$ and $x(t)$ and are called the cross correlation $r_{xf}(\tau)$ and the Cross Spectral Density (CSD) Function $P_{xf}(\omega)$, where

$$r_{xf}(\tau) = \int_{-\infty}^{\infty} x(t) . f(t+\tau) \, dt \qquad (4.4)$$

and

$$P_{xf}(\omega) = (1/2\pi) \int_{-\infty}^{\infty} r_{xf}(\tau) . e^{-j\omega\tau} \, d\tau \qquad (4.5)$$

Cross correlation functions are real, but not always even functions of time, and cross spectral density functions are generally complex functions of frequency with the conjugate property that

$$P_{xf}(\omega) = P_{fx}^{*}(\omega) \qquad (4.6)$$

By considering the impulse response of a system and its ACF, three important results are derived, as shown in various texts (26,27):

$$P_{xx}(\omega) = P_{ff}(\omega) . |H(j\omega)|^2 \qquad (4.7)$$

$$P_{xf}(\omega) = P_{ff}(\omega) . H(j\omega) \qquad (4.8)$$

$$P_{fx}(\omega) = P_{xx}(\omega) . H(j\omega) \qquad (4.9)$$

The first equation (4.7), although apparently convenient, cannot be used to derive the FRF from measurements of input and response, because it contains only the modulus of $H(j\omega)$. It is therefore necessary to use one of the other expressions (4.8) or (4.9). In theory, both should yield the same value of $H(j\omega)$ but this is not the case in practice. It is useful to consider why this is so, since it introduces an important quantity in the field of vibration measurement.

Consider the case where there is noise in the response signal (this may be mechanical noise, including non-linear behaviour, electrical noise in the instrumentation, or limited analysis resolution).

The better FRF estimator is

$$H(j\omega) = \frac{P_{fx}(\omega)}{P_{ff}(\omega)} \qquad (4.10)$$

which is normally called H_1: this is because random noise in the output is removed during the averaging process of the cross spectrum.

Where there is noise in the input, the FRF estimator which minimises the effect of this is

$$H(j\omega) = \frac{P_{xx}(\omega)}{P_{xf}(\omega)} \qquad (4.11)$$

which is normally referred to as H_2.

Generally, it is easier and therefore cheaper to calculate H_1, and so this is the algorithm used by most spectrum analysers. An additional reason for using this estimator is that when an excitation force is being measured, the transducer is directly connected to the structure under test, and the only noise present in the input is some very low level electrical noise, making H_1 a more useful measurement.

However, when noise is present at both input and output, H_1 and H_2 can be used to find a confidence level for the true H. This is called the coherence function, and is defined as

$$\gamma(j\omega)^2 = \frac{P_{xf}(\omega)^2}{P_{xx}(\omega) \cdot P_{ff}(\omega)} \qquad (4.12)$$

a more rigorous derivation of which is given in texts such as Newland(28). The Cross Spectrum inequality

$$P_{xf}(\omega)^2 < P_{xx}(\omega) \cdot P_{ff}(\omega) \qquad (4.13)$$

states that if any of the Auto-Spectra contain non-coherent noise, then the magnitude of the Cross Spectrum squared is smaller than the product of the Auto-Spectra. This is because non-coherent noise contributions are averaged out of the Cross Spectrum.

The coherence function lies between 0 and 1, where 1 indicates no noise in the measurement, and 0 pure noise. The interpretation of the coherence function is that for each frequency ω it shows the degree of linear relationship between the measured input and output signals.

When making mobility measurements, the coherence function is an extremely powerful property in detecting a number of possible errors.

As well as being aware of possible sources of error in the measurements taken and the corresponding checks which can be performed, errors can also occur in the processing of data, which therefore needs consideration. Most modern analysers are fitted with non-optional anti-aliasing filters, but suitable windows need to be applied to the signals captured in order to minimise leakage errors. Leakage occurs because of discontinuities which may arise at the end of the finite length of time data taken, and results in energy 'leaking' into other spectral lines close to the true frequency components of the signal. Windowing involves the imposition of a prescribed profile on the time signal prior to performing the Fourier Transform. This weights the time data, reducing the effects of discontinuities where the signal is truncated, or, in the case of a Force window, improving the signal to noise ratio by imposing an exponential decay. For the random excitation and response in this test a Hanning window was used.

One further point which merits mentioning is the use of averaging during the acquisition of measurement data. Where errors present in a measurement are random, these can be removed by averaging and statistical confidence improved. However, there are other sources of error which are systematic in nature and therefore do not respond to averaging. This is an important distinction. With the HP3582A Analyser RMS averaging was used; this smooths out the noise variations in a measurement and must be used when making coherence measurements.

4.6 Controlling Microcomputer and Software

In order to carry out the successful implementation of a modal test, each stage of the procedure needs to be controlled and coordinated. In the experimental arrangement used here, this was carried out by a Hewlett Packard 9816S microcomputer running Entek EMODAL V2.1(20) modal analysis software. The 9816S has two floppy disk-drives, and an extra 256K RAM board had to be installed to run the software. The microcomputer was interfaced with the spectrum analyser via an HP-IB interface bus. This enabled the microcomputer to remotely control the acquisition of measurement data during testing. The software was menu-driven by using the soft-keys on the keyboard.

4.7 Modal Testing Procedure

A flow chart of the steps involved in a modal test is shown as Fig.4.3. These will now be considered in more detail, paying particular attention to the testing of the bowl feeder structure.

4.8 Definition of Measurement Locations

Having decided on the excitation and suspension points of the structure, it is also necessary to decide on measurement locations where transfer mobilities will be measured. This is usually determined by the type of behaviour which a test is being designed to model e.g. a fine mesh is required when trying to capture high frequency panel resonances. Since the numerical model which this test was designed to verify was based on a lumped parameter approach, it was decided to restrict this analysis to the consideration of the feeder as a rigid bowl and base with all the flexibility concentrated in the springs. Thus the bowl and base were represented by simple triangles, the corners being the points of attachment of the springs as shown in Fig.4.4.

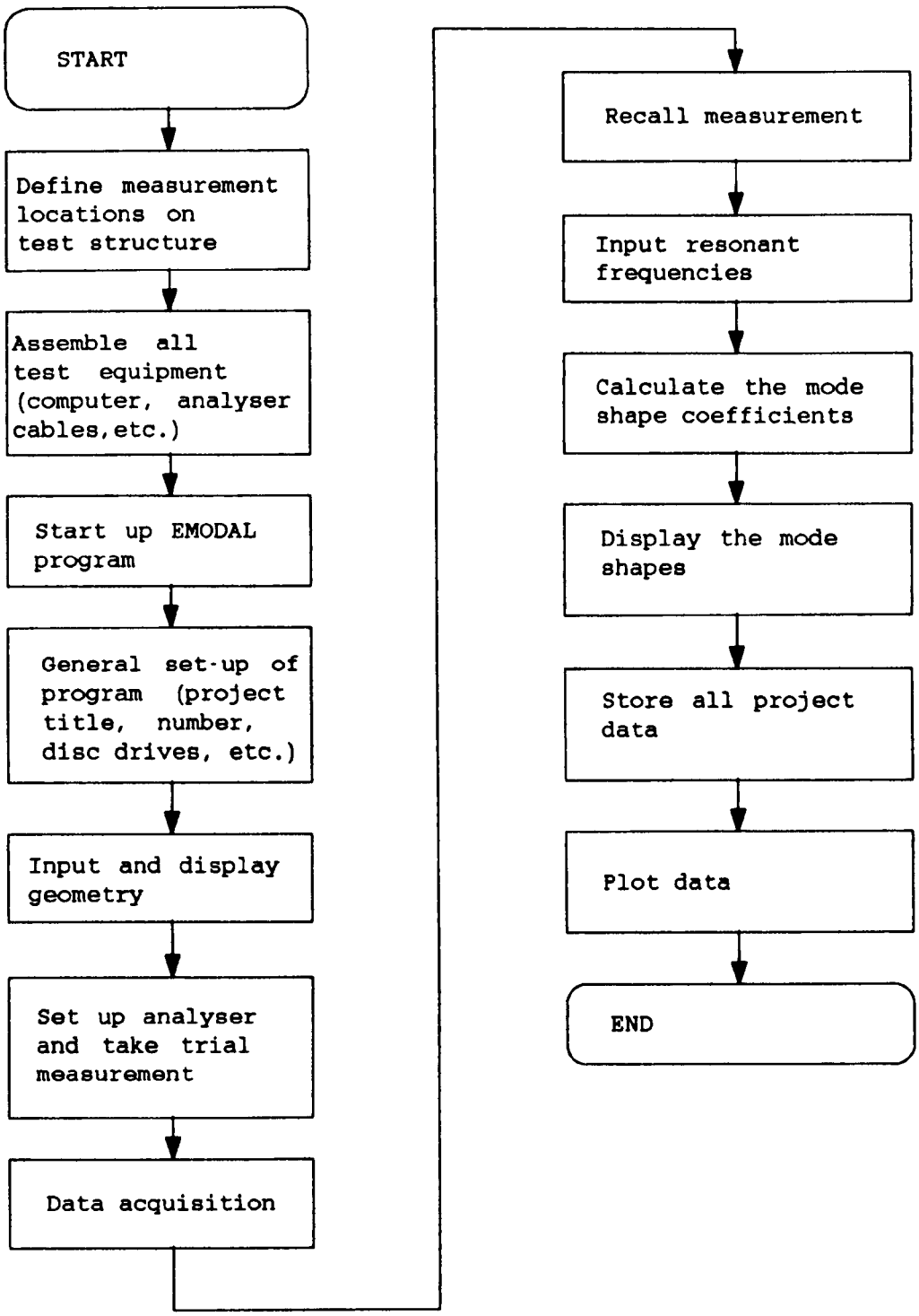

Fig.4.3 Flow Diagram for Experimental Modal Analysis

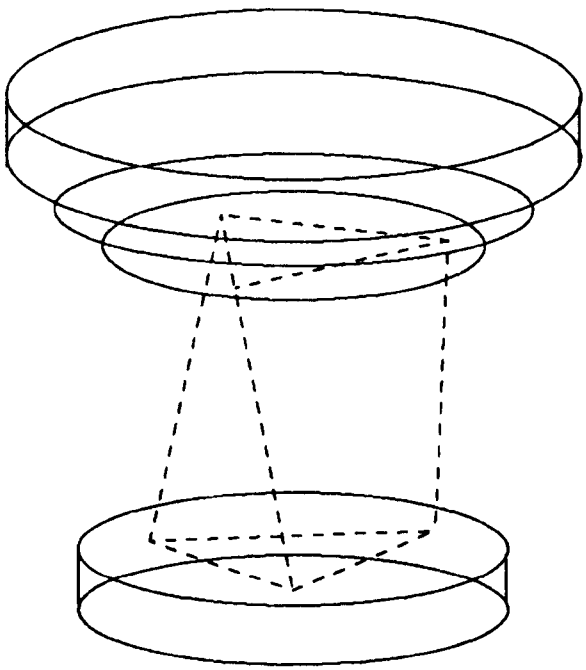

Fig.4.4 Modal Analysis Mesh

The geometry of all the excitation and measurement locations or nodes were input into the computer and stored on floppy disk. In addition, 'links' between nodes were also defined and entered; these would enable the mode shapes obtained from the test to be viewed, both in deflected and animated forms.

4.9 Data Acquisition

Before taking the actual mobility measurements which will be stored and analysed as part of the modal test, it is necessary to take some trial measurements. These enable checks to be carried out in an effort to ensure that the measurements made are 'good', and to maximise the accuracy.

Prior to dealing with any random or bias errors which may be degrading the quality of the measurements, it is important that the sensitivities of the charge amplifiers have been correctly specified and that the settings on the analyser have been adjusted to avoid overload but to maximise dynamic range. Initial measurements enable checks to be made on the sensitivity settings of the amplifiers; a rough calculation of expected values of force and velocity can be compared with measured values to give at least the same order of magnitude.

Initial measurements also enable the frequency range to be used during testing to be established. Whilst the broad band of analysis is likely to have been decided on before the test, examination of measurements indicates those parts of the range which exhibit the desired resonant frequencies and therefore require closer analysis. Initial measurements of the bowl feeder structure showed two separate ranges with distinct resonances and antiresonances. These were:

0 - 150 Hz

470 - 650 Hz.

These ranges were subsequently used for narrowband measurement and analysis of the feeder structure.

The checks which are performed on trial FRFs are as follows:

i) A freely suspended structure should exhibit a rigid body mode at a very low frequency (considerably lower than the first resonant frequency).

ii) The incidence of resonances and antiresonances can be checked. For a point mobility there must be an

antiresonance after every resonance, whereas for transfer mobilities between two points well-separated on the structure there should be more minima than antiresonances.

iii) A Nyquist plot can be checked so that in each resonance region the curve traces out at least part of a circular arc. Curves which are not smooth may be due to insufficient frequency resolution.

iv) The coherence level should be close to 1 across the frequency range. Causes of low coherence levels are:

a) Noise at the output. This may be a response to unmeasured forces, or it can occur at an antiresonance.

b) Noise at the input. This can occur at the resonant frequencies, but may also be caused by mechanical damage to the exciter.

Both a) and b) can be caused by electrical noise in the instrumentation. A common cause is problems with cables, which may result from a breakdown in the shielding or from excessive motion of the cable which can be

cured by securing it to the supporting structure or foundations. Another cause is damaged instrumentation.

c) Non-linear behaviour of the system.

d) Insufficient resolution. This can be solved by 'zooming' in on a smaller frequency range.

e) Poor mounting of the accelerometer which causes 'base bending'. Mounting points need to be clean and flat.

Some errors are random and can be averaged out by taking a number of measurements. As stated earlier this is not true for systematic errors. With random excitation it is always good practice to make several successive measurements and to accumulate a running average of the FRF estimate and the coherence. An average of 8 measurements was found necessary with the bowl feeder structure.

Once satisfactory trial measurements have been obtained the data acquisition stage of the process can be carried out. A measurement location and direction is entered into the microcomputer before each FRF is obtained and subsequently stored on floppy disk.

Mobility measurements were taken in the x,y and z directions for all points on the structure.

Point and transfer mobility measurements in the two frequency ranges are given as Figs. 4.5, 4.6, 4.7 and 4.8.

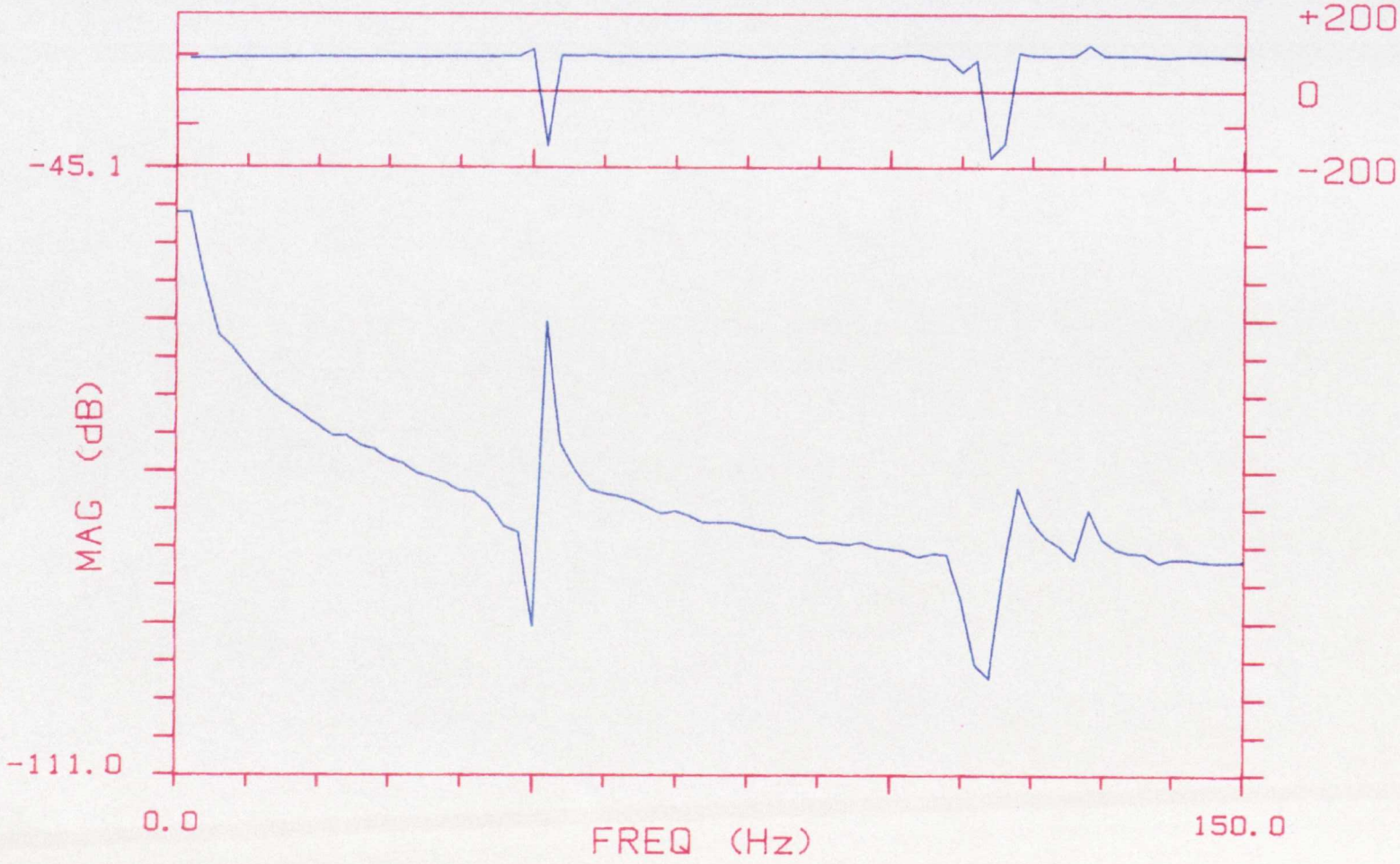

Fig.4.5 Point mobility measurement in the range 0 - 150 Hz

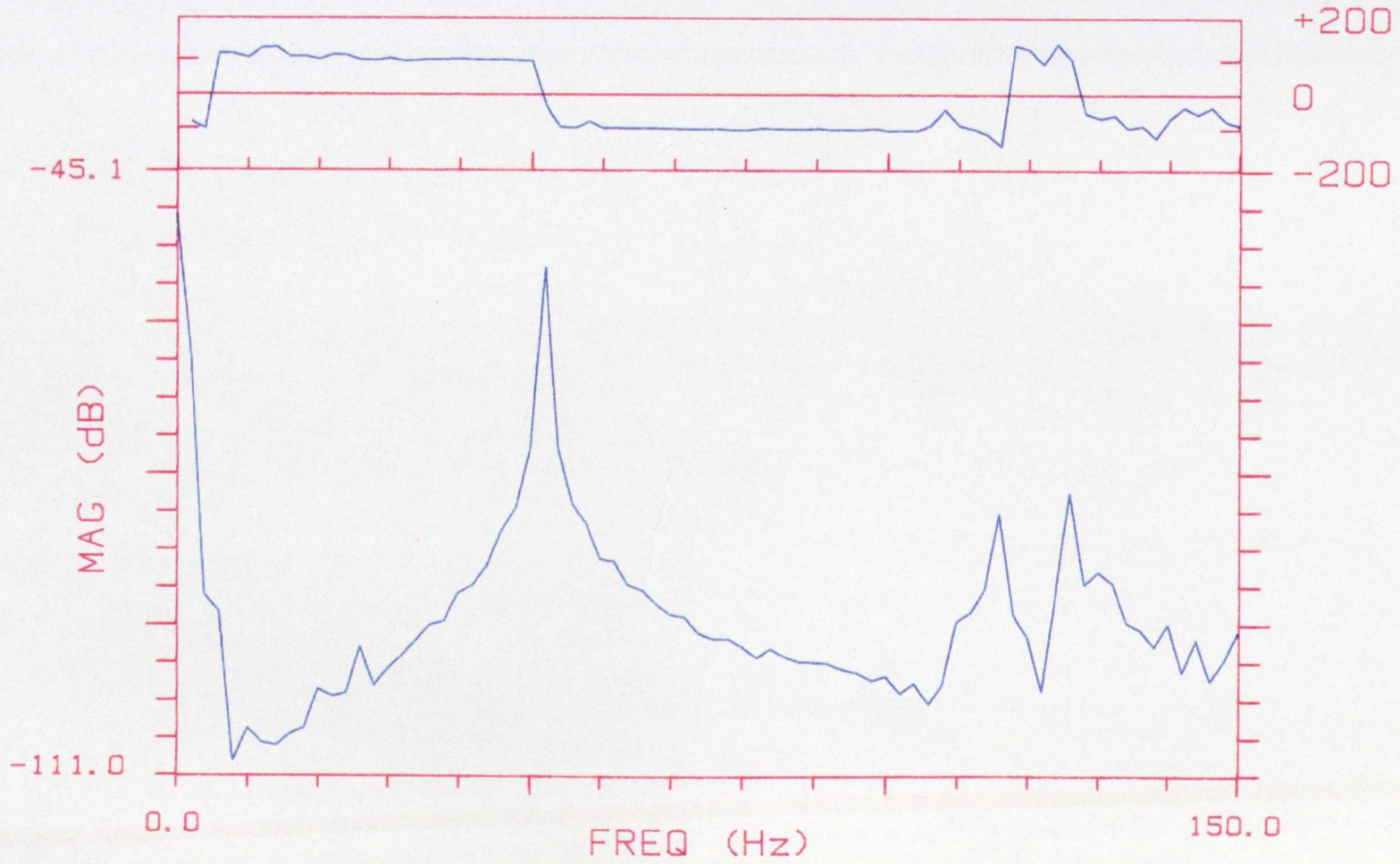

Fig.4.6 Transfer mobility measurement in the range 0 - 150 Hz

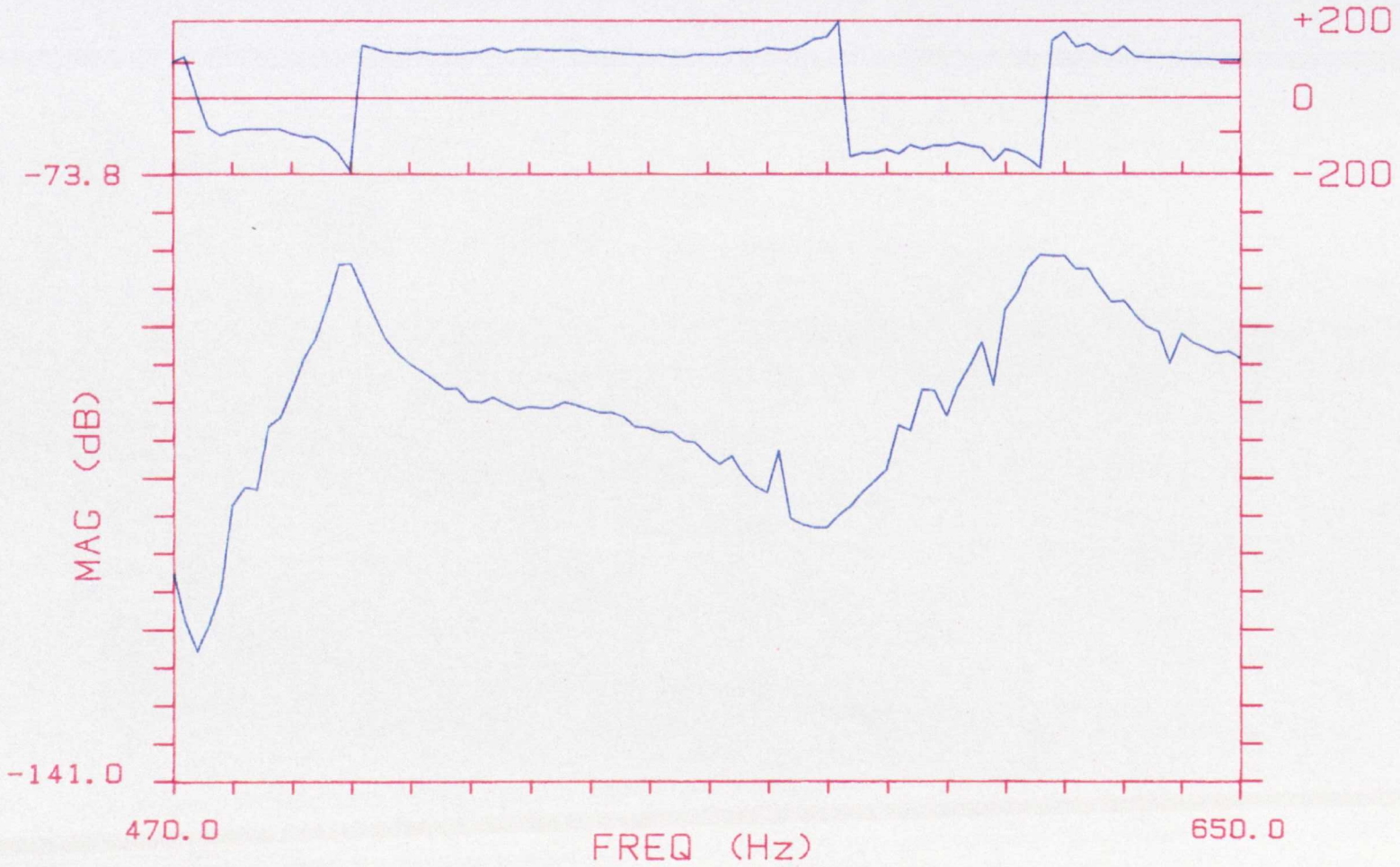

Fig.4.7 Point mobility measurement in the range 470 - 650 Hz

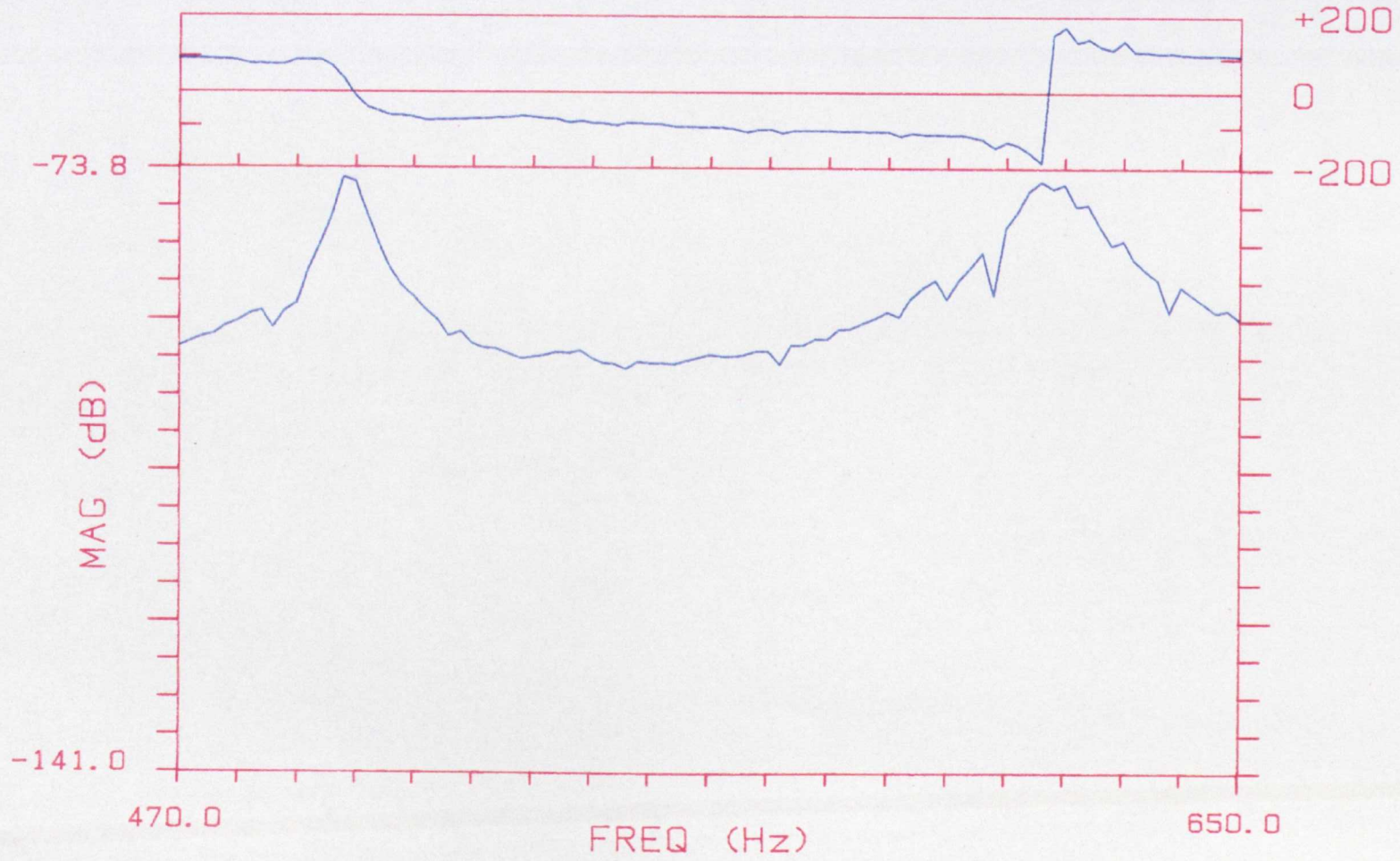

Fig.4.8 Transfer mobility measurement in the range 470 - 650 Hz

4.10 Extraction of Modal Parameters

This stage of the modal test procedure is concerned with the analysis of the measurement data obtained in the previous section in order to estimate the modal parameters of the system. This involves carrying out a curve-fit on the data, assuming that the mobility function at a frequency ω is of the form given in equation (4.1) or the alternative expression

$$Y_{jk}(\omega) = \left(\frac{x_j}{f_k}\right) = i\omega \sum_{r=1}^{N} \left[\frac{{}_rA_{jk}}{(\omega_r^2 - \omega^2)}\right] \qquad (4.14)$$

where ${}_rA_{jk}$ is termed the Modal Constant (sometimes referred to as the Residue). This is the specific mobility linking coordinates j and k for the rth mode.

The purpose of the curve-fitting is to establish values of ${}_rA_{jk}$, and the Pole or natural frequency ω_r (note that the above equation is for an undamped system).

It is now worth considering the various curve-fit algorithms which were available as part of the EMODAL

software. These were:

i) Quadrature extraction;

ii) SDOF-finite difference;

iii) Complex division; and

iv) SDOF Circle fit.

i) and iii) are somewhat crude and are only useful for fairly straightforward structures whose FRFs exhibit low modal density. ii) is also known as the peak-amplitude method and is carried out on the Bode plot of the mobility. The estimates it obtains depend heavily on the accuracy of the maximum FRF levels. Since most of the errors in mobility measurements are concentrated around the resonance regions, particularly with lightly damped structures, the accuracy of this method has limitations. In addition, the assumption of a SDOF model tends to cause equally serious limitations. Even with clearly-separated modes it is found that the neighbouring modes do contribute a significant amount to the total response at the resonance of the mode being analysed. Method iv) was originally developed to deal with this problem, and is therefore a better choice for more complex structures with higher modal density. It also produces more accurate results with lightly damped structures. Another advantage is that the routine used in

the EMODAL package offers the user a more interactive curve-fit procedure, where it is possible to accept, reject or modify the microcomputer-generated fit. It was therefore decided that the most appropriate method was the SDOF circle fit.

It should be noted that all the algorithms available in the EMODAL package are SDOF routines, whereas equation (4.14) is for a MDOF system. This simplification of the analysis also has limitations. It does not offer the facility of estimating each resonant frequency from all the measurements taken; instead a local curve-fit is carried out where the user specifies the resonant frequency from a single measurement and the frequency span around each modal frequency over which the circle fit model is applicable. This is always a compromise between including as many data points as possible and moving so far away from the resonance that other modes become dominant.

It is now worth considering the actual properties of the modal circle.

For a system with damping equation (4.14) can be rewritten as:

$$Y_{jk}(\omega) = j\omega \sum_{r=1}^{N} \left[\frac{{}_rC_{jk} \exp j\theta_r}{(\omega_r^2 - \omega^2) + 2j\omega\omega_r\zeta_r} \right] \qquad (4.15)$$

where ζ_r is the viscous damping ratio of the rth mode.

The inclusion of damping results in the complex form of the modal constant. At frequencies very close to the resonant frequency ω_r, this equation becomes:

$$Y_{jk(\omega=\omega r)} \approx j\omega \left[\frac{{}_rC_{jk} \exp j\theta_r}{(\omega_r^2 - \omega^2) + 2j\omega\omega_r\zeta_r} \right] + {}_rD_{jk} \qquad (4.16)$$

where all other modes combine to form a complex quantity ${}_rD_{jk}$ which may be treated as being constant over the narrow frequency range of the ω_r resonance.

This can now be related to a Nyquist plot of mobility as shown in Fig.4.9. The first term of the equation results in a circle of diameter ${}_rC_{jk}/2\omega\omega_r\zeta_r$ which is rotated through an angle θ_r. The second term displaces the circle by an amount ${}_rD_{jk}$.

It can therefore be seen that once the resonant frequency ω_r and damping ratio ζ_r have been determined from a single measurement, the modal constant ${}_rC_{jk}\exp j\theta_r$ can be identified by constructing the best-fit circle through the selected points near resonance and finding the diameter and rotation of this circle.

The mode shape vector ${}_r\phi_k$ can be determined from the point mobility measurement Y_{kk} and its corresponding modal constant ${}_rC_{kk}\exp j\theta_r$. From this and the transfer mobility measurement Y_{jk}, the mode shape vector ${}_r\phi_j$ can be found.

Plots of the mode shapes can either be displayed in a static, deflected or an animated form. These can then be dumped to a graphics plotter to obtain a hard copy.

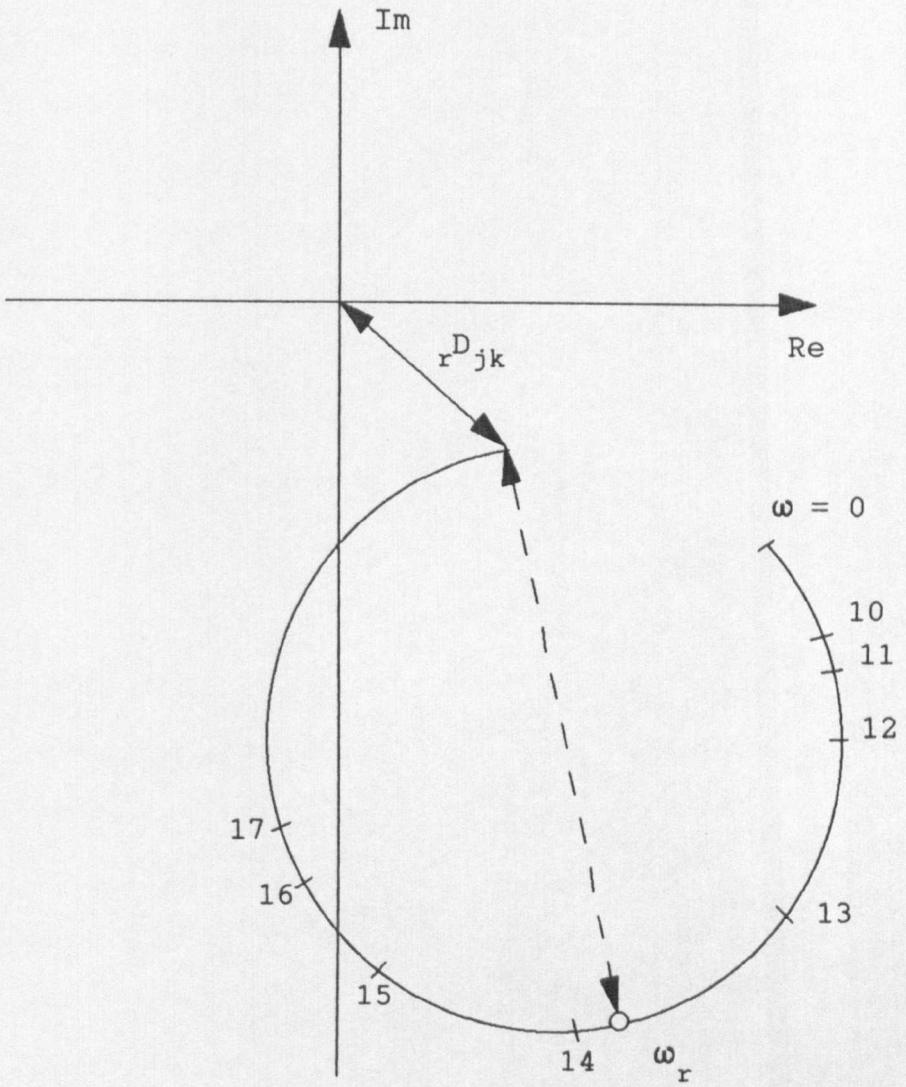

Fig.4.9 Nyquist plot of a modal circle

5. RESULTS OF THE NUMERICAL MODEL AND MODAL ANALYSIS

In order to verify the numerical model described in Chapter 3, this was run for a bowl feeder which is part of the standard product range manufactured by Aylesbury Automation Ltd. These results were then compared with experimental modal analysis of the feeder which was carried out as described in Chapter 4.

5.1 Description of the Bowl Feeder and its input parameters

The bowl feeder used in this phase of the project was a model 15 feeder manufactured by Aylesbury Automation Ltd. This is a medium-sized feeder with a cast aluminium bowl which is normally used for feeding components such as small items of industrial hardware e.g. bolts and other fixings. The dimensions and physical properties which were required as input data for the numerical model are:

Spring length = 0.176 m

Spring width = 0.01925 m

Spring thickness = 0.00323 m

Spring spacing = 0.00087 m

Bowl offset angle, ϕ_1 = 0.003 rad

Spring angle = 1.1345 rad

Radius of spring attachment points on bowl = 0.087266 m

Young's modulus (springs) = 210 GN/m^2

Shear modulus (springs) = 81 GN/m^2

Bowl mass = 10.75 kg

Base mass = 24.1 kg

Bowl radius for inertia calculation = 0.22 m

Base radius for inertia calculation = 0.145 m

Bowl height = 0.11 m

Base height = 0.055 m

Vertical thickness of bowl = 0.003 m

Horizontal thickness of bowl = 0.005 m

Radius of bowl fixing plate = 0.09 m

Thickness of bowl fixing plate = 0.02 m

Spring length is taken as being the distance between the centres of the fixing bolts at the ends of a leaf spring.

5.2 Results

A table comparing the natural frequencies predicted by the numerical model and the experimental modal analysis are given in Table 5.1. The mode shapes predicted by the numerical model are shown in Figs.5.1 and 5.2. The solid line represents the undeformed shape, and the dotted line the deformed shape. It should be noted that although

there are only six natural frequencies there are eight different mode shapes. This is because the 'tipping'modes (about the x and y axes) occur in pairs, the first tipping modes occuring at 103.0 Hz, and the second at 580.4 Hz.

The mode shapes obtained from the experimental modal analysis are shown in Figs.5.3, 5.4, 5.5, 5.6 and 5.7. In this case, the dotted lines represent the undeformed shape and the solid lines the magnified deformed shape at the extreme of vibration. The two plots given for each mode shape show the deformed shape at the two extremes of vibration.

Natural Frequency (Hz)		
Numerical Model	Modal Analysis	
0.0		rigid body mode
56.0	52.0	axial
103.0	118.0	tipping
103.0		
113.8	128.0	axial
580.4	500.0	tipping
580.4		
820.8	618	axial

Table 5.1 Natural frequencies of a bowl feeder

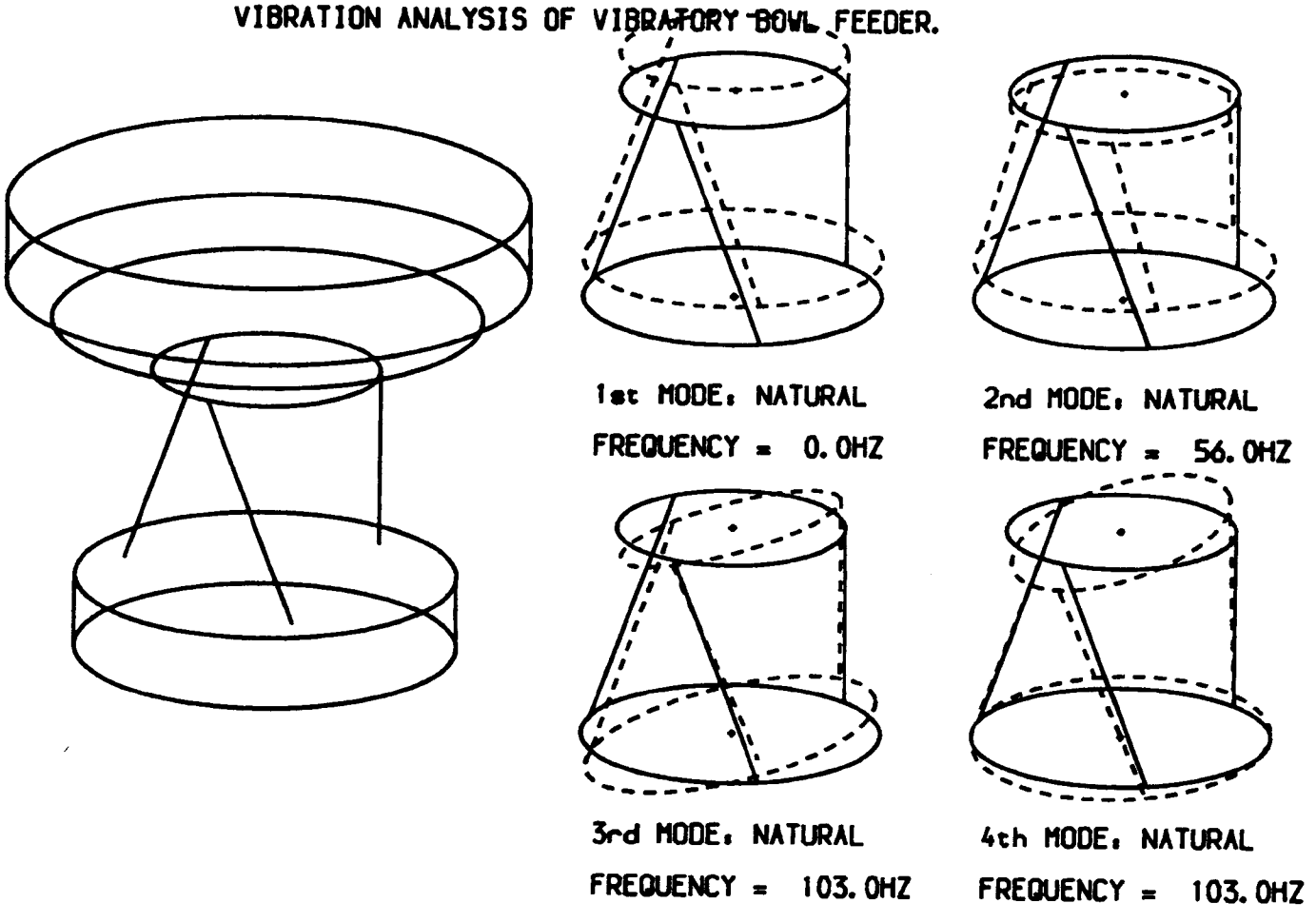

Fig.5.1 1st four predicted mode shapes

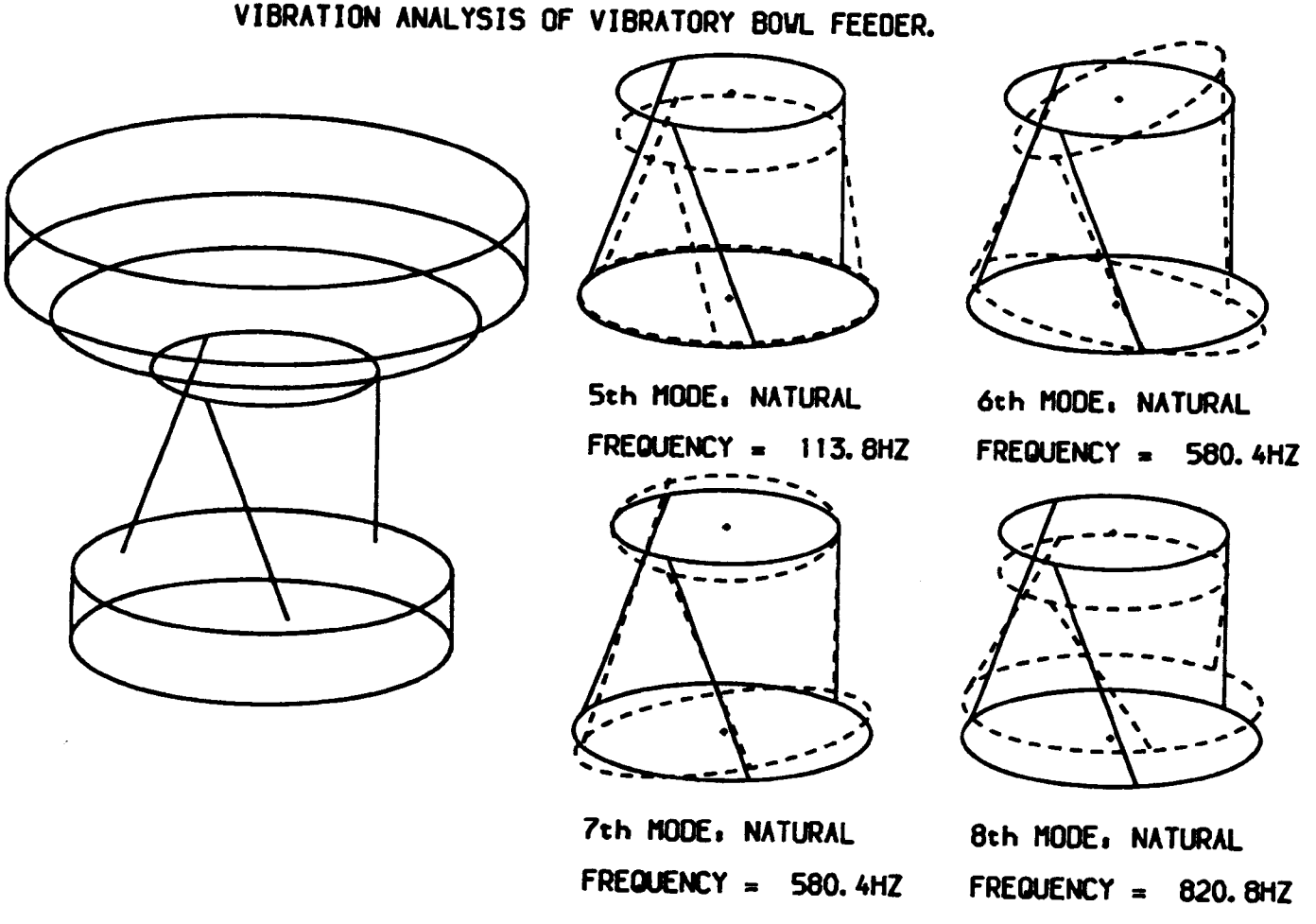

Fig.5.2 2nd four predicted mode shapes

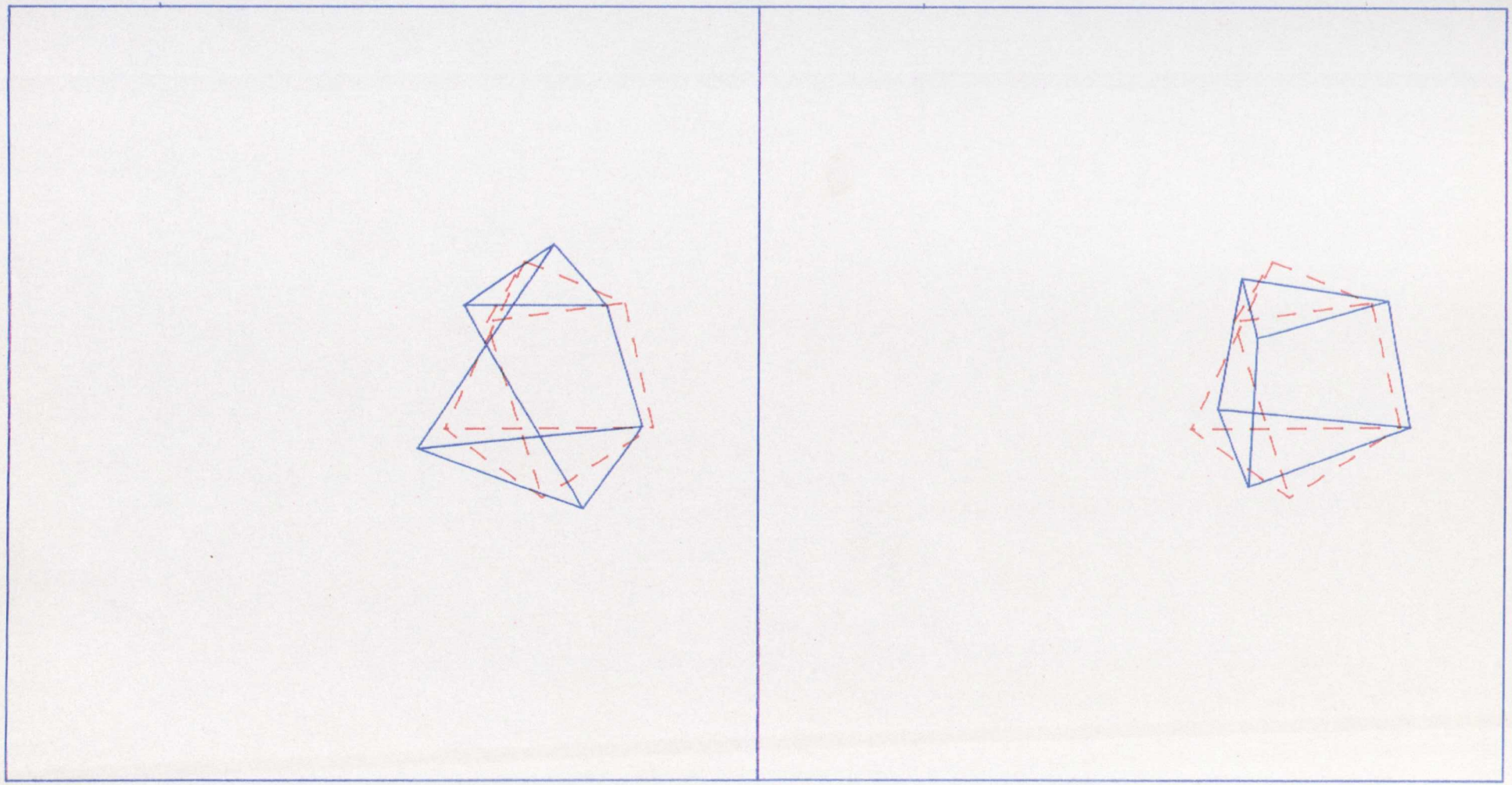

Fig.5.3 Experimental mode shape at 52.0 Hz

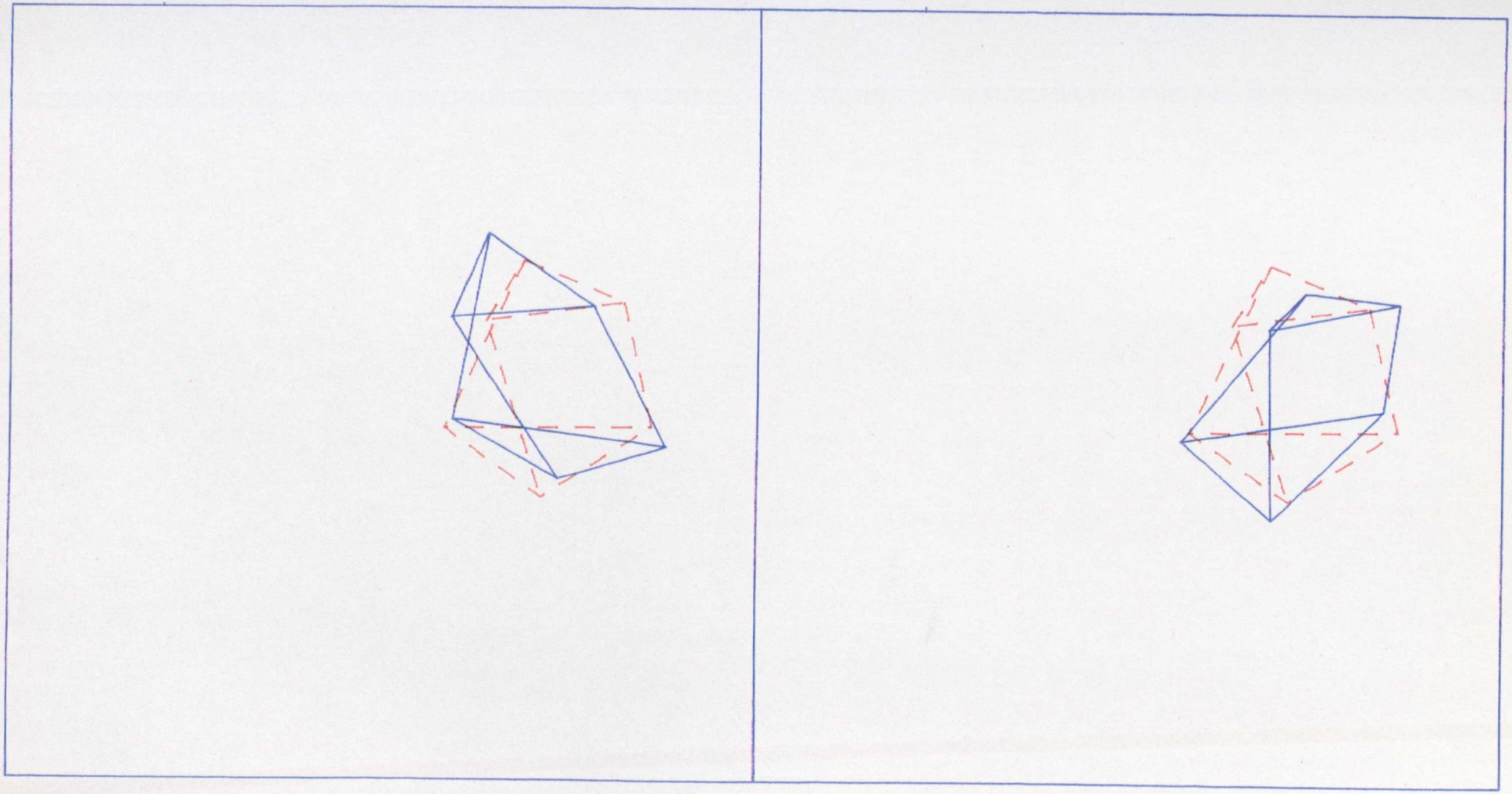

Fig.5.4 Experimental mode shape at 118.0 Hz

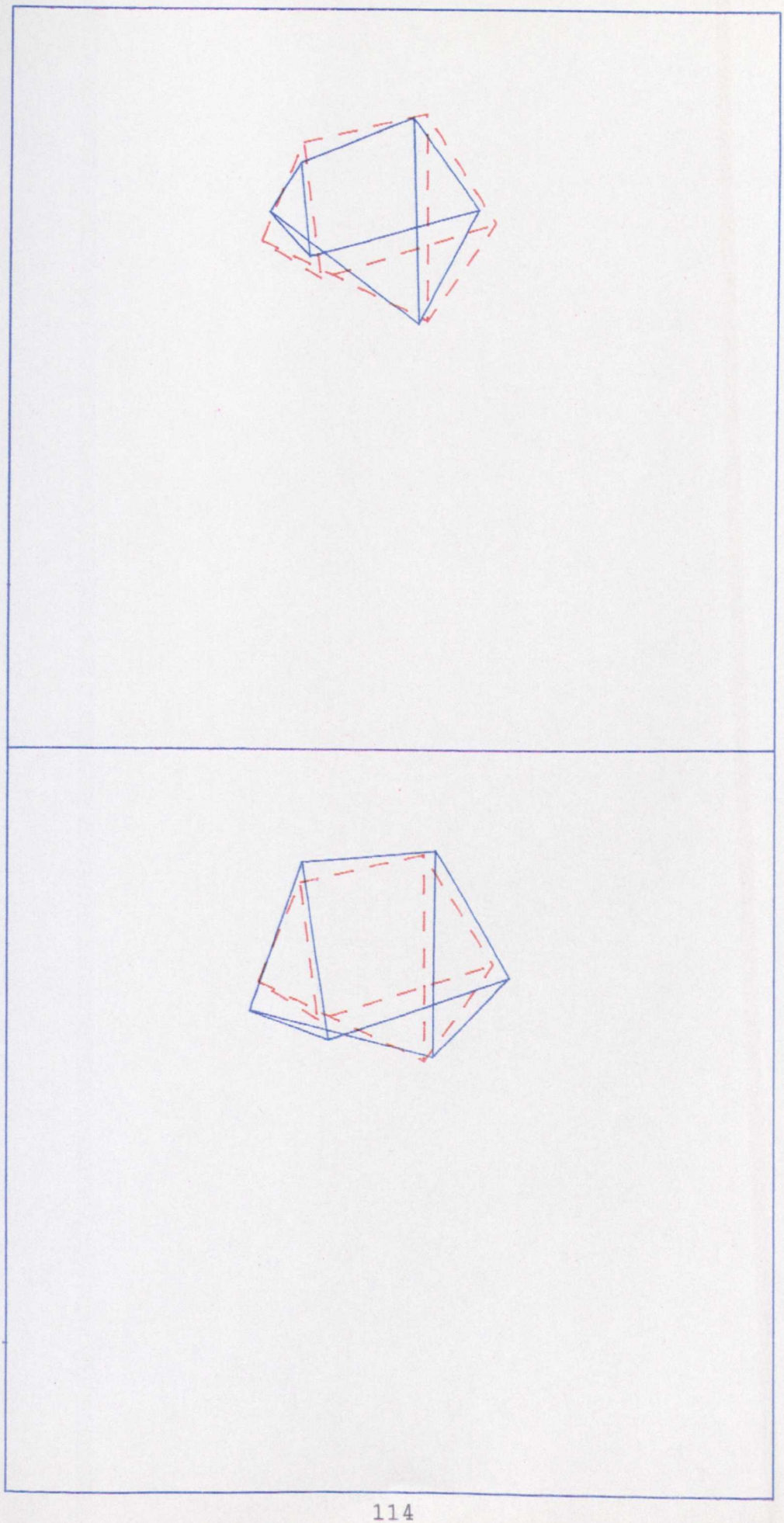

Fig.5.5 Experimental mode shape at 128.0 Hz

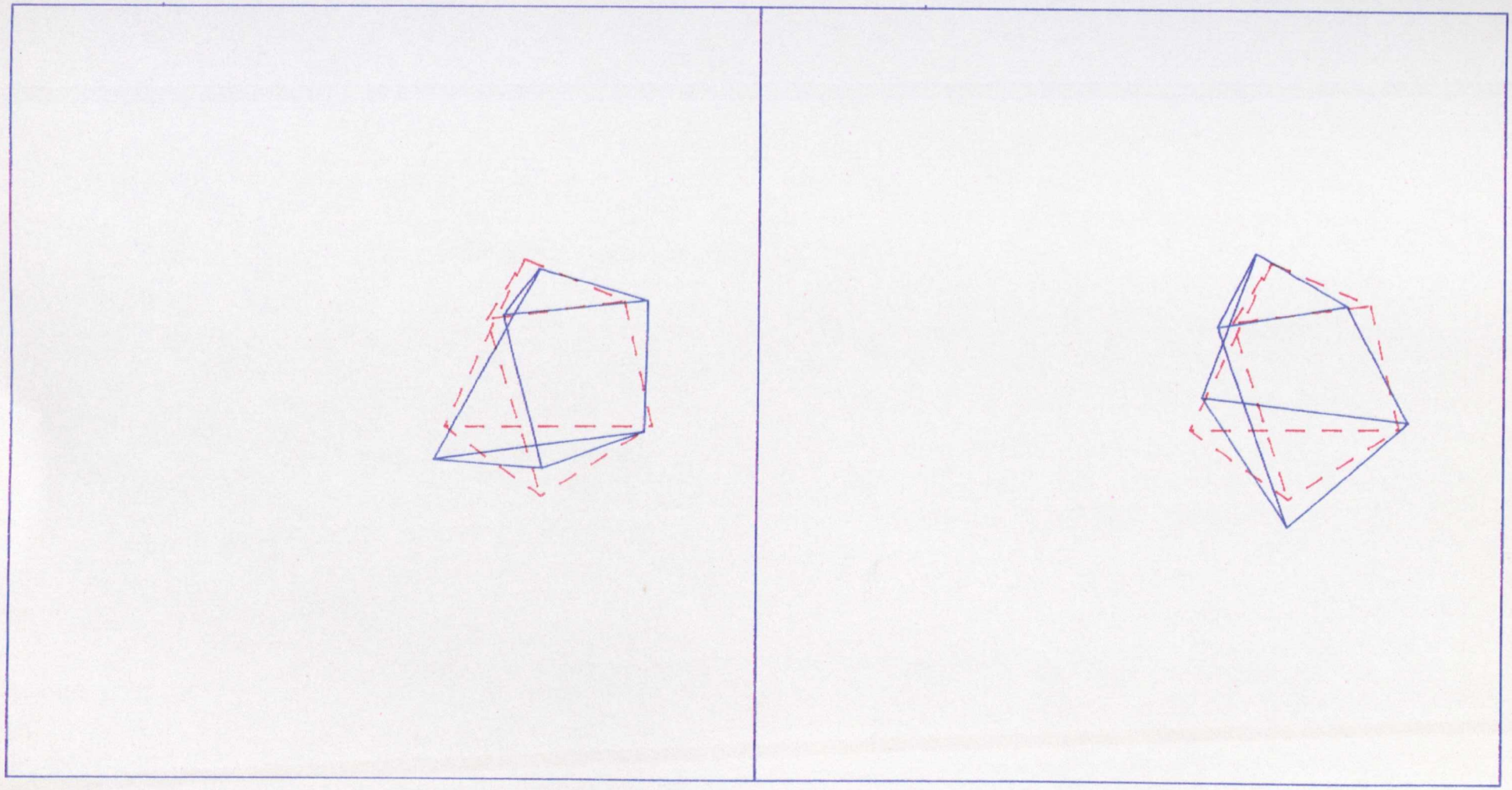

Fig.5.6 Experimental mode shape at 500.0 Hz

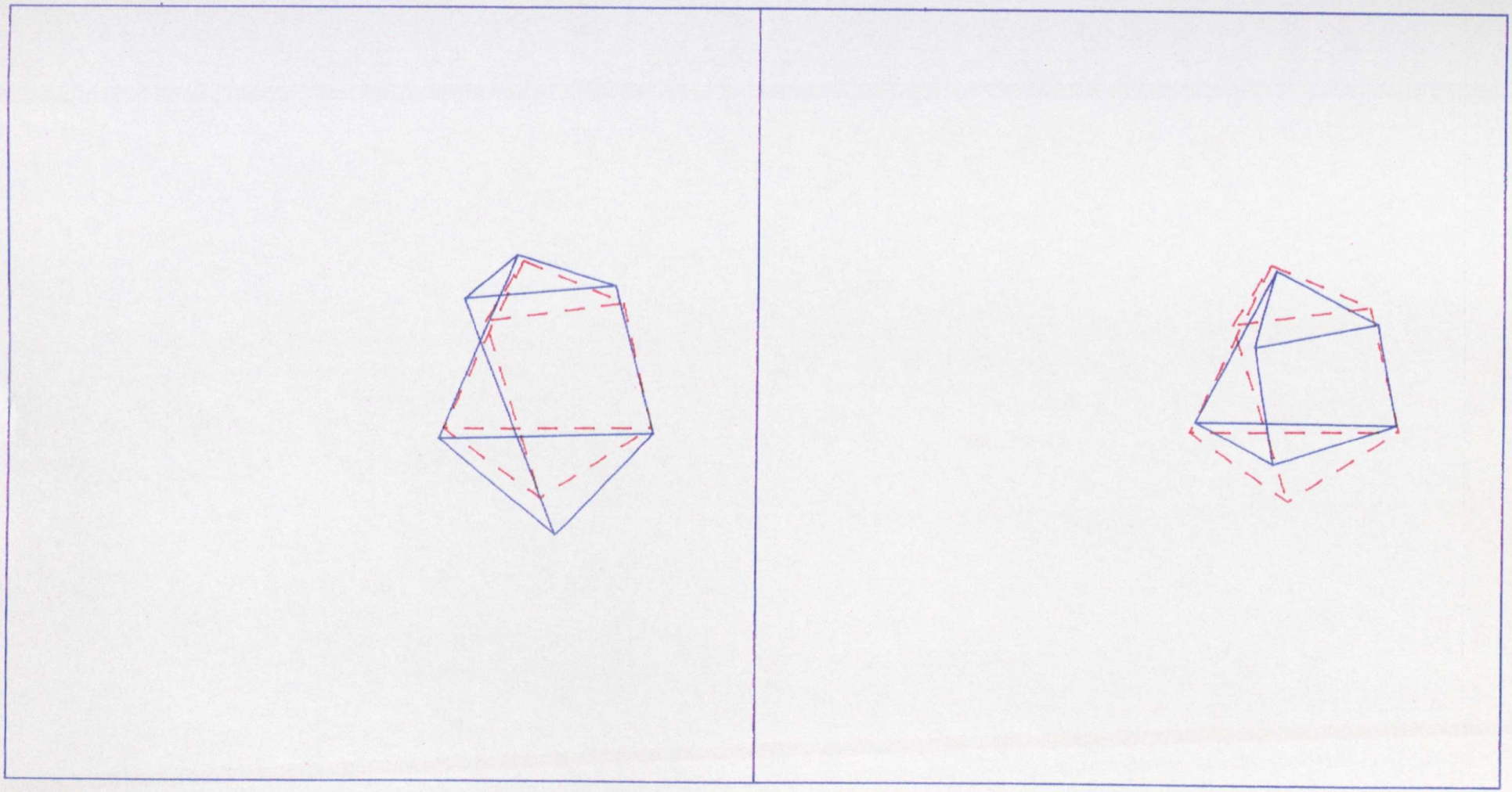

Fig.5.7 Experimental mode shape at 618.0 Hz

5.3 Discussion

From Table 5.1 it can be seen that good agreement is obtained between the numerical and experimental results for the first two axial modes and the first tipping mode. It is quite clear from the experimental mode shapes that transverse deflections have been excited at the first tipping mode; there is also some transverse motion at the other modes. This may be due to imbalances in the inertias of the bowl and base, or because of differences in spring stiffnesses between the three banks of springs.

In considering the higher frequency modes, there is still good agreement between the predicted mode shapes but the natural frequencies computed from the numerical model are excessively high when compared with the experimental results. This would indicate that the numerical model is overconstrained; this is probably because the lumped parameter assumption is no longer valid and the bowl and base no longer behave as rigid bodies.

Despite the limitations at higher frequencies, the numerical model provides three accurate natural frequency computations in the lower frequency range, and close to the driving frequency of 50 Hz.

5.4 Natural frequency of the bowl

In order to investigate the discrepancy between the numerical and experimental values obtained for the higher natural frequencies of the bowl feeder, the natural frequency of the bowl was calculated treating this as a continuous structure undergoing flexural vibration. This was a departure from the assumption made in the numerical model that the bowl behaved as a rigid body.

It was decided in the first instance to analyse the bowl as a circular plate. A formula for the natural frequency of circular plates was extracted from Blevins(33). This was:

$$f_n = \frac{\lambda^2}{2\pi b^2} \sqrt{\left\{ \frac{Eh^3}{12\rho(1 - \upsilon^2)} \right\}} \qquad (5.1)$$

where E is Young's modulus, h is thickness of the plate, b the radius of the plate, ρ the mass per unit area of the plate, υ is Poisson's ratio, and λ is a constant extracted from the tables in Blevins. For the first mode of a plate with simply-supported edges $\lambda = 4.977$; and thus substituting values of bowl geometry given earlier in this chapter, an estimate of the natural frequency of

the bowl is

$$f_n = \frac{(4.977)^2}{2\pi\,(0.22)^2}\sqrt{\left\{\frac{71 \times 10^9 \times (0.003)^3}{12 \times 27.1 \times (1 - 0.34^2)}\right\}}$$

$$= 384 \text{ Hz}$$

For a circular plate with a clamped edge, $\lambda = 10.22$, which gives a value of $f_n = 1619$ Hz.

The edge support conditions of the bottom of the bowl will lie somewhere between these two idealised cases, and it can therefore be seen that it is likely that flexure of the bowl itself may occur in the same frequency range as the two higher natural frequencies of the lumped parameter system.

It would not be possible to extract a mode shape involving flexure of the bowl using the coarse mesh of measurement points defined in the experimental modal analysis. This would require a finer mesh of measurement points. It is therefore possible that the higher modes did involve some flexure.

6. NUMERICAL MODEL FOR THE FORCED RESPONSE OF A FEEDER

Having developed a numerical model of the bowl feeder structure which accurately models its dynamic characteristics, it was then necessary to reconsider the original aims and objectives of the project before proceeding further. Initial work had been carried out in response to clear development needs of both the manufacturers and customers, namely the desire for:

i) an increase in the feed rate of components;

ii) a reduction of the power input and running costs;

iii) a quieter and smoother running feeder; and

iv) a feeder which is easier to tune.

The consideration of these objectives was essential in focussing the direction of the next stage of the programme of work. The aims of this were therefore:

i) optimisation of the geometric parameters of the bowl feeder structure in order to achieve an increase in feed-rate; smoother, quieter running, and lower power consumption; and

ii) the production of a 'portable', user-friendly design tool which would enable development engineers to investigate the performance characteristics of alternative structures and arrangements.

In response to the second objective, it was decided to adapt the numerical model already developed to run on a spreadsheet package on a microcomputer. This offered the following advantages:

i) it would allow easy transfer of the software for design and development engineers working in the field;

ii) it offers user-friendly facilities such as 'pop-down' menus, 'dialog-boxes' and overlay windows, making the software easier to access and use; and

iii) a spreadsheet package allows calculations of the 'what-if?' type, where parameters are varied over a specified range, to be easily and readily performed.

However, at this stage, the numerical model was only capable of predicting the natural frequencies and mode shapes of the bowl feeder. In order to fulfill the first objective for this part of the project, it was necessary to be able to predict the feed rate of the feeder, or some other parameter that was directly related to feed rate. It was therefore necessary to consider the forced response of the feeder, and so this chapter, in addition to covering the transfer of the model to a spreadsheet package, deals with this area.

6.1 The Spreadsheet Model

In transferring the numerical model to the spreadsheet package, it was decided to constrain the system to a four degree-of-freedom model, allowing for vertical motion, rotation about a vertical axis and in-plane tipping of just the bowl. Since the motion of the bowl provides the driving force for the components, and for feeders operating in the field every effort is made to prevent any motion of the base by rigidly clamping this to a supporting stand, it was felt that a valid assumption would be to neglect the movement of the base.

The spreadsheet package used was the MICROSOFT EXCEL spreadsheet (29) running on the Apple Macintosh Plus. The Macintosh computer was chosen because of the user-friendly facilities which it offers. The spreadsheet gives a wide range of graphics and database facilities which will be described in more detail in later sections. It also allows high-level programs to be written within the spreadsheets using 'Macros', and for special-purpose menus and dialog-boxes to be added to enhance software for a particular requirement.

6.2 Forced Response of the Model using Modal Analysis

Having determined the modal parameters of the system, it now becomes possible to predict the response to a defined forcing function, {F}, which is an arbitrary function of time (a special case of which is a harmonic or periodic function). A more general presentation is given in the text by Craig(30).

Considering the equation of motion for an n degree-of-freedom forced system:

$$[M]\{\ddot{x}\} + [K]\{x\} = \{F\} \qquad (6.1)$$

where the symbols have their usual meaning. For clarity,

the undamped case will be considered first, but for an accurate prediction of the response it will be necessary to include the damping of the system. This will be covered later in this section.

The solution of the eigenvalue problem

$$[M]\{\ddot{x}\} + [K]\{x\} = 0 \tag{6.2}$$

yields the matrix of the eigenvectors, the modal matrix [P], and the diagonal matrix of the eigenvalues, the spectral matrix $[\Lambda]$. The response of any system to a particular excitation function may be described as a superposition of the normal modes of the system [P], by writing this in the form

$$\{x(t)\} = [P]\{n(t)\} \tag{6.3}$$

where $\{n(t)\}$ is the column matrix of the set of normal or principal coordinates. The orthogonality property states that

$$[P]^T[M][P] = [M] \tag{6.4}$$

$$[P]^T[K][P] = [K] \tag{6.5}$$

where $[M]$ and $[K]$ are diagonal matrices.

However, if the modal matrix is normalised according to the equation

$$\{P_r\}^T[M]\{P_r\} = 1 \tag{6.6}$$

then equations (6.4) and (6.5) can be written in the form

$$[P]^T[M][P] = [I] \tag{6.7}$$

$$[P]^T[K][P] = [\lambda] \tag{6.8}$$

A consequence of this is that the normal modes can be used to uncouple the equations of motion of a system. Equation (6.1) can be rewritten as

$$[M][P]\{\ddot{n}\} + [K][P]\{n\} = \{F\} \tag{6.9}$$

Premultiplying throughout by $[P]^T$ gives

$$[P]^T[M][P]\{\ddot{n}\} + [P]^T[K][P]\{n\} = [P]^T\{F\} \tag{6.10}$$

Using the results of the orthogonality relations, equations (6.4) and (6.5), and introducing a column matrix of normalised or principal forces, $\{N\}$, equation (6.10) becomes

$$[M]\{n\} + [K]\{n\} = \{N\} \tag{6.11}$$

This represents a set of n uncoupled differential equations of the type

$$\ddot{n}_r(t) + \omega^2_r \dot{n}_r(t) = Q_r(t), \quad r = 1,2,\ldots,n \qquad (6.12)$$

It is useful at this point to consider the effect of the inclusion of damping in the model. A model of proportional damping was assumed; further details of this are given in the text by Tse, Morse and Hinkle(39). The damping matrix $[C_p]$ is defined as

$$[C_p] = \alpha[M] + \beta[K] \qquad (6.13)$$

The equation of motion (6.1) becomes

$$[M]\{\ddot{x}\} + [C_p]\{\dot{x}\} + [K]\{x\} = \{F\} \qquad (6.14)$$

Since the damping matrix $[C_p]$ is proportional to the mass and stiffness matrices, the orthogonality relations can also be used to uncouple this. The argument given above results in a set of n damped uncoupled equations of the form

$$\ddot{n}_r(t) + (\alpha + \beta\omega^2_r)\dot{n}_r(t) + \omega^2_r n_r(t) = Q_r(t) \qquad (6.15)$$

Also, consider a periodic forcing function of the form

$$Q_r(t) = \frac{\tilde{q}_r}{\tilde{m}_r} \cos \Omega t \qquad (6.16)$$

where $\tilde{m}_r$ is the rth element in the diagonal mass matrix $[M]$ given by

$$\tilde{m}_r = \{x_r\}^T [M] \{x_r\} \qquad (6.17)$$

The solution of equation (6.15) can be obtained by means of the Laplace Transform method. Transforming both sides of (6.15) and given that only the steady-state solution is required, terms involving initial conditions $n_r(0)$ and $\dot{n}_r(0)$ are neglected, giving

$$s^2\tilde{n}_r(s) + (\alpha + \beta\omega^2_r)s\tilde{n}_r(s) + \omega^2_r\tilde{n}_r(s) = \frac{\tilde{q}_r}{\tilde{m}_r} \cdot \frac{s}{s^2+\Omega^2} \qquad (6.18)$$

where $\tilde{n}_r(s)$ is the Laplace Transform of $n_r(t)$. The subsidiary equation is

$$\tilde{n}_r(s) = \frac{\tilde{q}_r}{\tilde{m}_r}\left\{\frac{s}{(s^2 + \Omega^2)(s^2 + (\alpha+\beta\omega^2_r)s + \omega^2_r)}\right\} \qquad (6.19)$$

and this has a steady-state solution of the form

$$n_r = \left[\frac{\tilde{q}_r}{\tilde{m}_r[((\omega^2_r - \Omega^2)^2 + (\alpha + \beta\omega^2_r)^2\Omega^2)]} \right] \cos(\Omega t - \phi) \qquad (6.20)$$

where the phase angle ϕ is given by

$$\tan \phi = \left(\frac{(\alpha + \beta\omega^2_r)\Omega}{(\omega^2_r - \Omega^2)} \right) \qquad (6.21)$$

The n equations given by (6.19) can be combined and written as a matrix [S] which is given by

$$\{n\} = [S] \{Q_r\}$$

or

$$\{n\} = \left[\frac{\cos(\Omega t - \phi_r)}{\{x_r\}^T[M]\{x_r\}((\omega^2_r - \Omega^2)^2 + (\alpha + \beta\omega^2_r)^2\Omega^2)}, \ldots\ldots \right] \{Q_r\} \qquad (6.22)$$

where [S] is diagonal, and

$$\phi_r = \tan^{-1}\left(\frac{(\alpha + \beta\omega^2_r)\Omega}{(\omega^2_r - \Omega^2)} \right) \qquad (6.23)$$

However, from equation (6.11) and (6.3)

$$\{N\} = [P]^T\{F\} \qquad \text{and}$$

$$\{x\} = [P]\{n\} \qquad (6.24)$$

Thus an expression for the response vector {x} can be found by substituting these in equation (6.22)

$$\{x\} = [P]\left[\frac{\cos(\Omega t - \phi_r)}{\{x_r\}^T[M]\{x_r\}\quad((\omega^2_r - \Omega^2)^2+(\alpha+\beta\omega^2_r)^2\Omega^2)}, \ldots\right][P]^T\{F\} \qquad (6.25)$$

The Laplace Transform manipulation presented here gives the response of the system as a displacement vector {x}. A similar analysis shows that the acceleration of the system, $\{\ddot{x}\}$, is related to the displacement, {x}, for a harmonic input at a frequency Ω by

$$\{\ddot{x}\} = -\Omega^2\{x\} \qquad (6.26)$$

In predicting the response of the bowl feeder, it is more useful to predict the resulting acceleration vector rather than the displacement vector. This is because earlier work by Redford and Boothroyd(2) investigating the mechanics of components in vibratory conveying, showed that there was an approximately linear relationship between the normal acceleration of the conveyor and the mean conveying velocity of the components, as shown in Fig.2.2.

The normal acceleration A_n is the acceleration perpendicular to the track i.e. if the vertical acceleration of the bowl is A, then

$$A_n = A \cos \theta \qquad (6.27)$$

where θ is the angle of the track. This varies from 0° at the bottom of the bowl to $\approx$ 4° higher up the track. Since feeding often occurs by 'shoving' of components higher up the track by those in the bottom of the bowl, it was decided to use the maximum value of A_n given by taking $\theta = 0°$.

The relationship between the bowl acceleration and the mean feeding velocity allows predictions of the feeder response in terms of acceleration to be used as an indication of how any design modifications might affect the component feed-rate. Care should be taken regarding this linear relationship, however. Large changes in acceleration values may take the operating point of the feeder outside the range within which an assumption of linearity is valid, and poor feed conditions may result, rather than an improvement.

6.3 Development of the Spreadsheet Model

Having established equations for the response of a multi degree-of-freedom system to an excitation vector {F}, the next stage was to implement this using the spreadsheet. This involved two distinct stages:

i) the development of a 'worksheet' which calculated the modal properties of the feeder from all the input parameters; and

ii) the development of high-level 'Macros' which are called and executed from the worksheet in i) to calculate the response of the system to a harmonic excitation.

These will now be dealt with separately.

6.4 Worksheet for the calculation of modal properties

As discussed in section 6.1, the numerical model to be used in the spreadsheet is a four degree-of-freedom version of the model described in Chapter 3, constraining motion of the base but allowing the bowl to move in the four modes of vertical displacement, rotation about the vertical axis and in-plane tipping about the x and y axes.

The procedures used in formulating the global mass and stiffness matrices are the same as those given in the flow charts Fig.3.7 and Fig.3.8, using the matrix manipulation functions MMULT, MINVERSE, and TRANSPOSE of the spreadsheet to perform matrix manipulation, inverse and transpose respectively(31). Table 6.1 shows the input parameters as they are entered into the spreadsheet.

Since the purpose of finding the response of the feeder to a forcing function was to be able to predict changes in performance, it was felt that it was only necessary to consider those modes of vibration of the bowl which directly contributed to the motion of the fed parts, namely vertical displacement and rotation about the vertical axis. Prior to calculation of the eigenvalues and eigenvectors for use in the modal analysis, the model was constrained further, resulting in (2 x 2) mass and stiffness matrices. A flow chart for the solution of this eigenproblem is presented as Fig.6.1.

Spring Dimensions and Parameters :	
Length =	0.176
Width =	0.01925
Thickness =	0.00323
Spring spacing =	0.002
Spring Angle =	1.1344640138
Young's Modulus =	2.10E+11
Shear Modulus=	8.10E+10
Thickness of spring bank =	0.01369
Number of Spring banks=	3
Ix =	5.760162E-09
Iy =	1.862908E-09
J =	3.965433E-09
Bowl Dimensions:	
Mass =	10.8
Radius =	0.087266
Radius Angle =	0.003
Moment of Inertia =	0.3739999987
MIx=MIy=	0.179

Table 6.1 Input parameters for spreadsheet

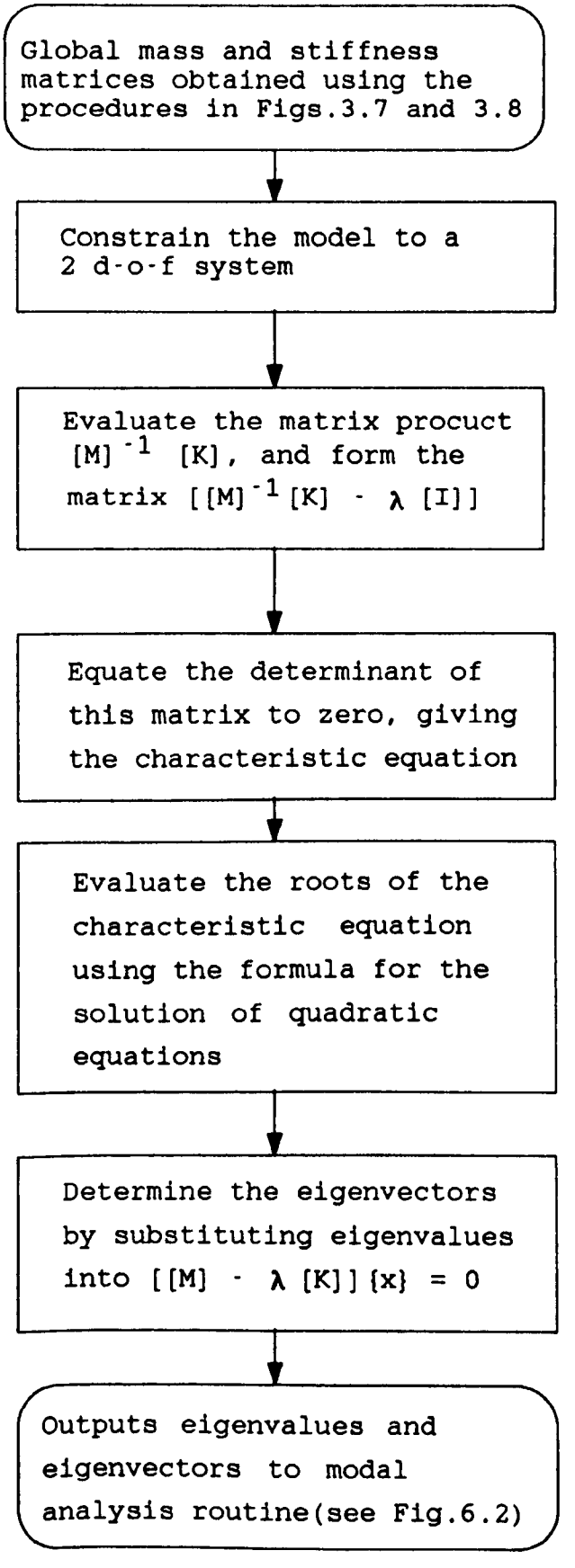

Fig.6.1 Flow chart of procedures for evaluation of eigenvalues and eigenvectors

From the results given in Chapter 5, it can be seen that for the first natural frequency there is a variation between the measured and predicted values of 4.0 Hz (numerical model = 56.0 Hz; experimental = 52.0 Hz). For the predictions of the forced response of the feeder to be accurate in the frequency range of interest, which is close to 50 Hz, it was important that the accuracy of this first natural frequency was improved. The various input parameters to the numerical model were considered, and in particular those which it was felt were difficult to measure accurately. The spacing between the individual springs in a spring bank does not remain fixed when the bowl feeder is executing its motion, and so it was felt that a change in this parameter may result in a significant improvement. Measurement of the spacers used between springs indicated a range of values from 0.8 to 2.0 mm. It was decided to use a value of 2.0 mm which gave a first natural frequency of 52.7 Hz.

6.5 Forced Response using spreadsheet 'Macros'

The next stage was the implementation of the modal analysis routine to find the output of the system in response to an excitation of the form $\{f\} \cos \Omega t$. The required input parameters were:

i) the (2 x 1) vector of the amplitudes of the input forces, {f}, where the two elements represent a linear force in the vertical direction and a torque about the vertical axis respectively;

ii) the frequency of the forcing function, Ω; and

iii) the damping constants of the system. The modal analysis routine assumes a model of proportional damping, and this is related to the viscous damping ratio for the rth mode ζ_r by:

$$\alpha + \beta\omega_r^2 = 2\zeta_r\omega_r \qquad (6.28)$$

It is usual with viscous damping to adopt a model of the form:

$$[C_p] = \beta\,[K] \qquad (6.29)$$

and so equation (6.28) becomes

$$\beta = \frac{2\zeta_r}{\omega_r} \qquad (6.30)$$

The value entered as an input parameter on the spreadsheet is the viscous damping ratio, ζ_r.

The prediction of the forced response of the system is carried out by a 'Macro' which is called and executed by the spreadsheet described in section 6.4. MICROSOFT EXCEL Macros (31) are programs written in the Microsoft Excel Macro Language to enable the spreadsheet to carry out user-defined tasks or calculations which are not available as part of the standard software. There are two types of macros: command macros carry out a sequence of commands for the user automatically; and function macros perform a specified calculation, returning the value to a formula on the calling worksheet. The Macro language contains a wide range of functions and commands, enabling the standard operations offered by high-level languages such as input and output of data, arithmetic and logical operations, conditional statements, and repetitive or iterative calculations to be performed.

A flow chart of the procedure used in the calculation of the response of the feeder to an excitation is given in Fig.6.2, and a copy of the macro used to perform this is given in Appendix 4.

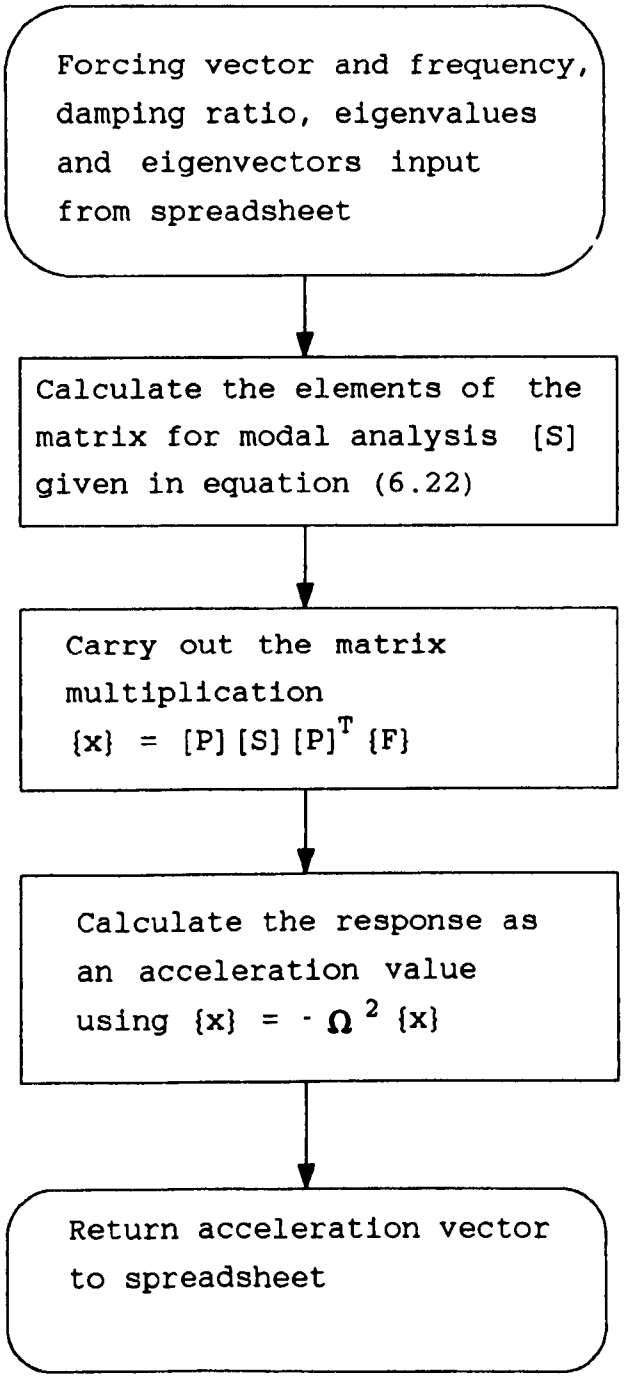

Fig.6.2 Flow chart of procedures to determine the forced response of the system using modal analysis

The output of the macro is a (2 x 1) column vector of bowl accelerations, the first element being acceleration in the vertical direction, and the second the angular acceleration of the bowl about its vertical axis. This vector is returned to the calling spreadsheet and entered into those cells which had originally called the macro. In using these acceleration values to predict the performance of the feeder by relating this to the feeding velocity of components, as described in section 6.2, the first element of the vector, namely acceleration in the vertical direction, is the required parameter.

7. EXPERIMENTAL INVESTIGATION OF THE FORCED RESPONSE OF A FEEDER

In order to verify the results of the forced response analysis described in Chapter 6, it was necessary to undertake a programme of experimental work. The source of driving power to the feeder used during normal operating conditions, the electromagnetic coil, was removed, and replaced with a drive rod arrangement from an electromagnetic vibrator capable of inputting harmonic forcing functions with a range of amplitudes and frequencies.

7.1 Experimental Apparatus

A block diagram of the apparatus and instrumentation used in this phase of the work is shown in Fig.7.1. The bowl feeder used was the same as that described in Chapter 5, a Model 15 Aylesbury Automation feeder.

In order to prevent any motion of the base of the feeder, this was rigidly bolted at three equidistant points to the supporting framework which was fabricated from square section steel, with two large U-channel cross members providing the platform on which the feeder was mounted. A photograph of this arrangement is given as Plate 7.1.

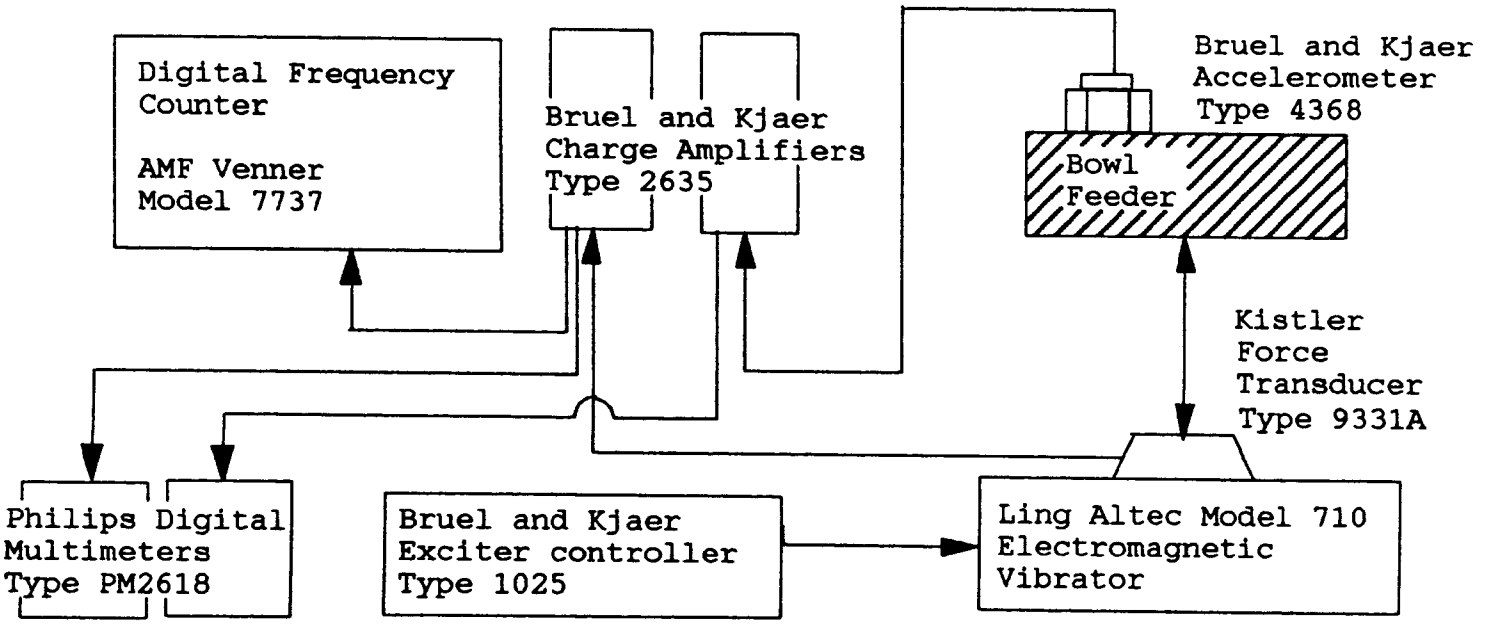

Fig.7.1 Block diagram of experimental apparatus and instrumentation used in testing the forced response of the bowl feeder

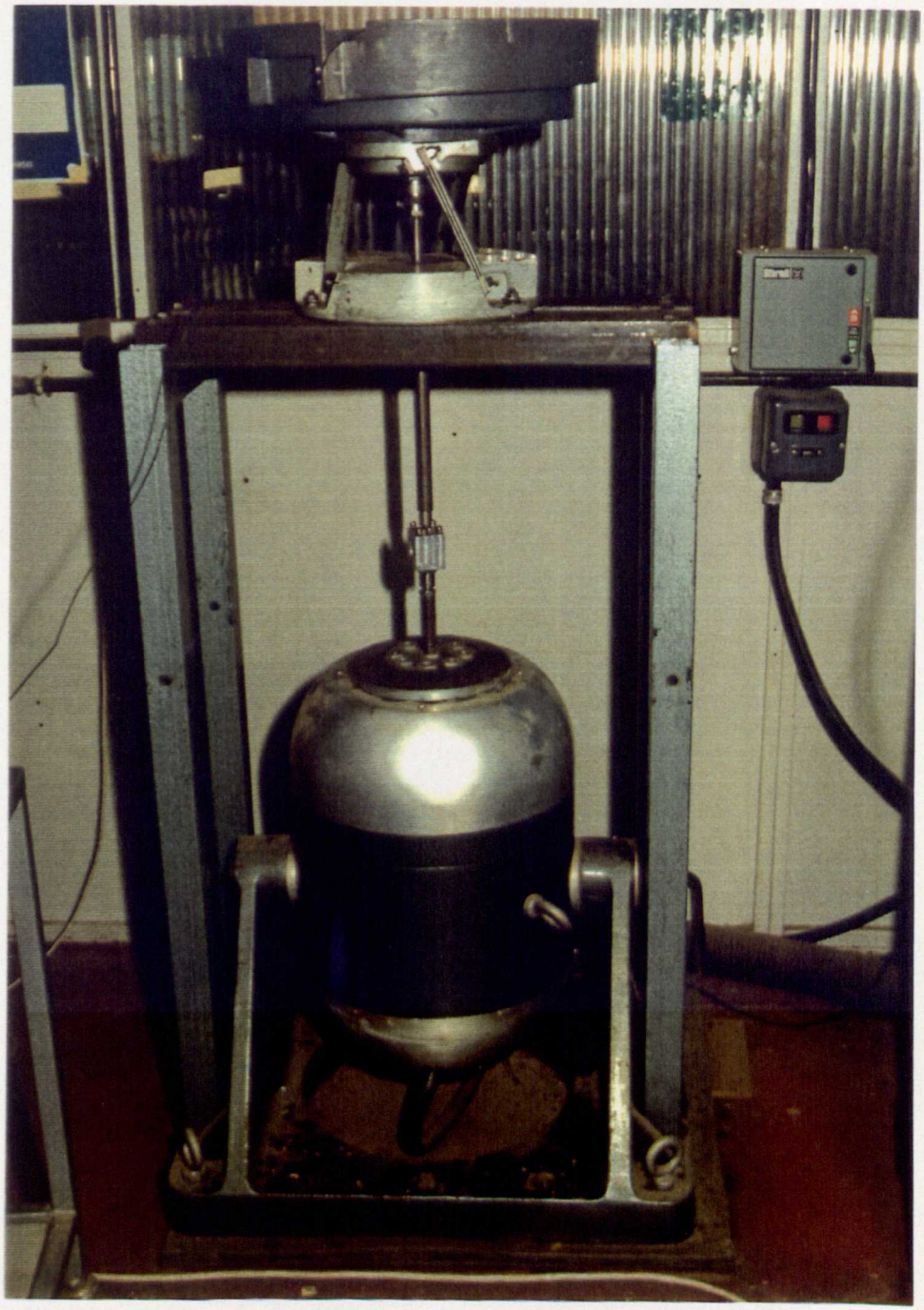

Plate 7.1 Experimental arrangement for testing of forced response

The driving force for the feeder was provided by a Ling Altec model 710 electromagnetic vibrator. This was chosen because forces in excess of 200 N were required in order to drive the feeder within its operating range. This value was arrived at by considering acceleration values which had been measured for feeders during normal operation, and taking a bowl mass of approximately 10kg. From Newton's Second Law

$$F = ma = 10 \text{ kg} \times 20 \text{ m/s}^2 = 200 \text{ N}$$

The Ling Altec was the only exciter available which was capable of providing this magnitude of force output. The forcing function used was a harmonic waveform provided by a sinewave generator contained within the exciter control unit.

The drive itself was provided through a circular cross section drive rod threaded into the underside of the bowl. This incorporated a thrust bearing, allowing both rotation and vertical motion of the bowl during excitation. A photograph of this is shown as Plate 7.2. A piezoelectric force transducer was placed in the drive rod directly below the bowl to measure the input force.

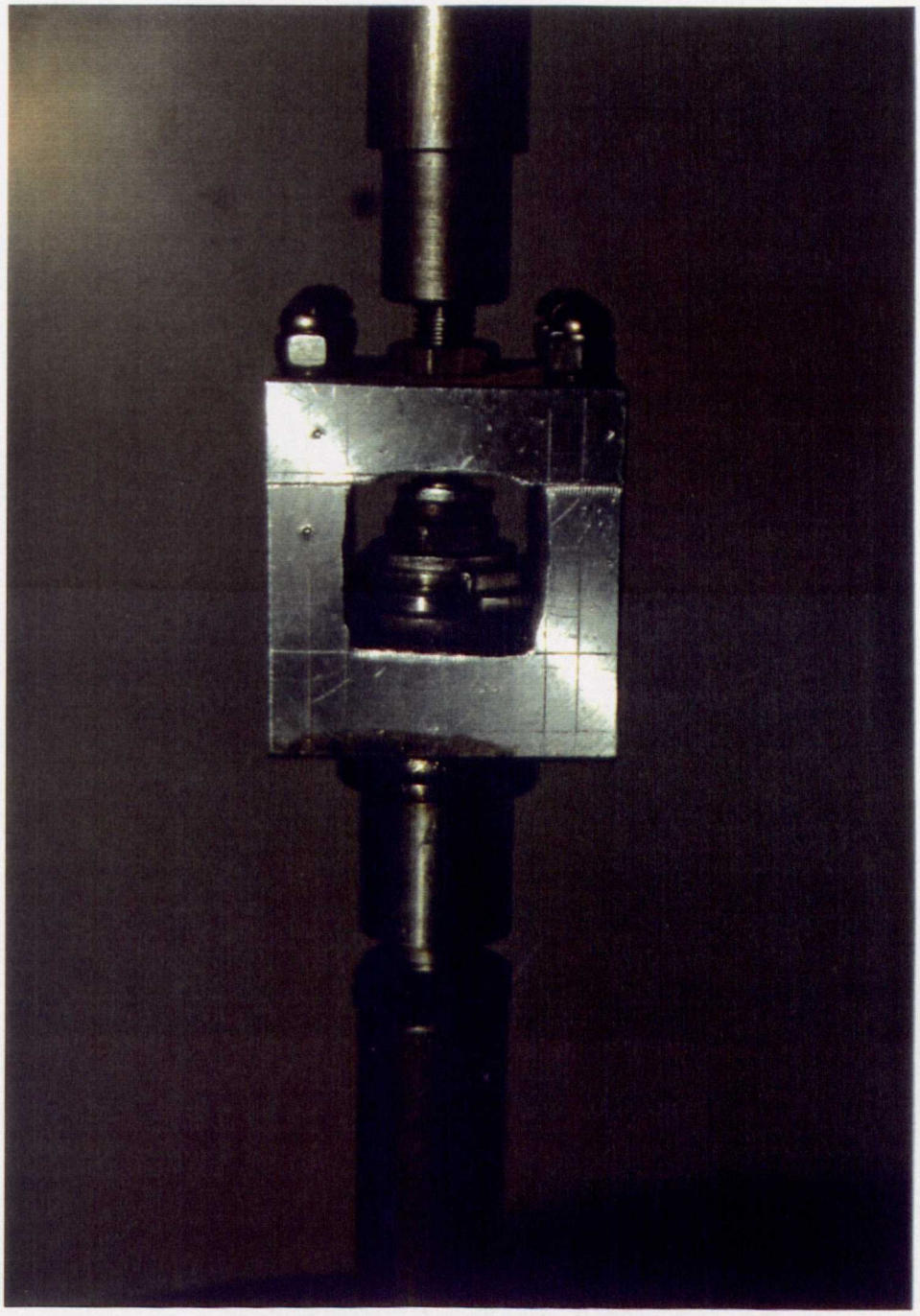

Plate 7.2 Drive rod incorporating thrust bearing

A Brüel and Kjær piezoelectric accelerometer was used to measure the response of the bowl, and this was attached using the threaded magnetic base described in Chapter 4. Mounting blocks were made up for this test, one for attaching the accelerometer at the centre of the bowl, which was inserted into a threaded hole; and another block which clamped onto the outside rim of the bowl. A photograph of these is shown as Plate 7.3.

Both the input and output signals were viewed on an oscilloscope to check for any deviation or distortion from a 'true' sinusoidal waveform, and the r.m.s. values of these were measured using digital multimeters. The frequency of the input signal was measured using a digital frequency counter.

7.2 Experimental Procedure

Since the modal analysis model described in Chapter 6 for the prediction of the forced response of the feeder was for a harmonic forcing function, the input chosen for the experimental tests was a sinewave. The amplitude of the input force was varied from 350 to 650 N in steps of 50 N for a range of input frequencies from 45 Hz to 52.5 Hz in steps of 2.5 Hz.

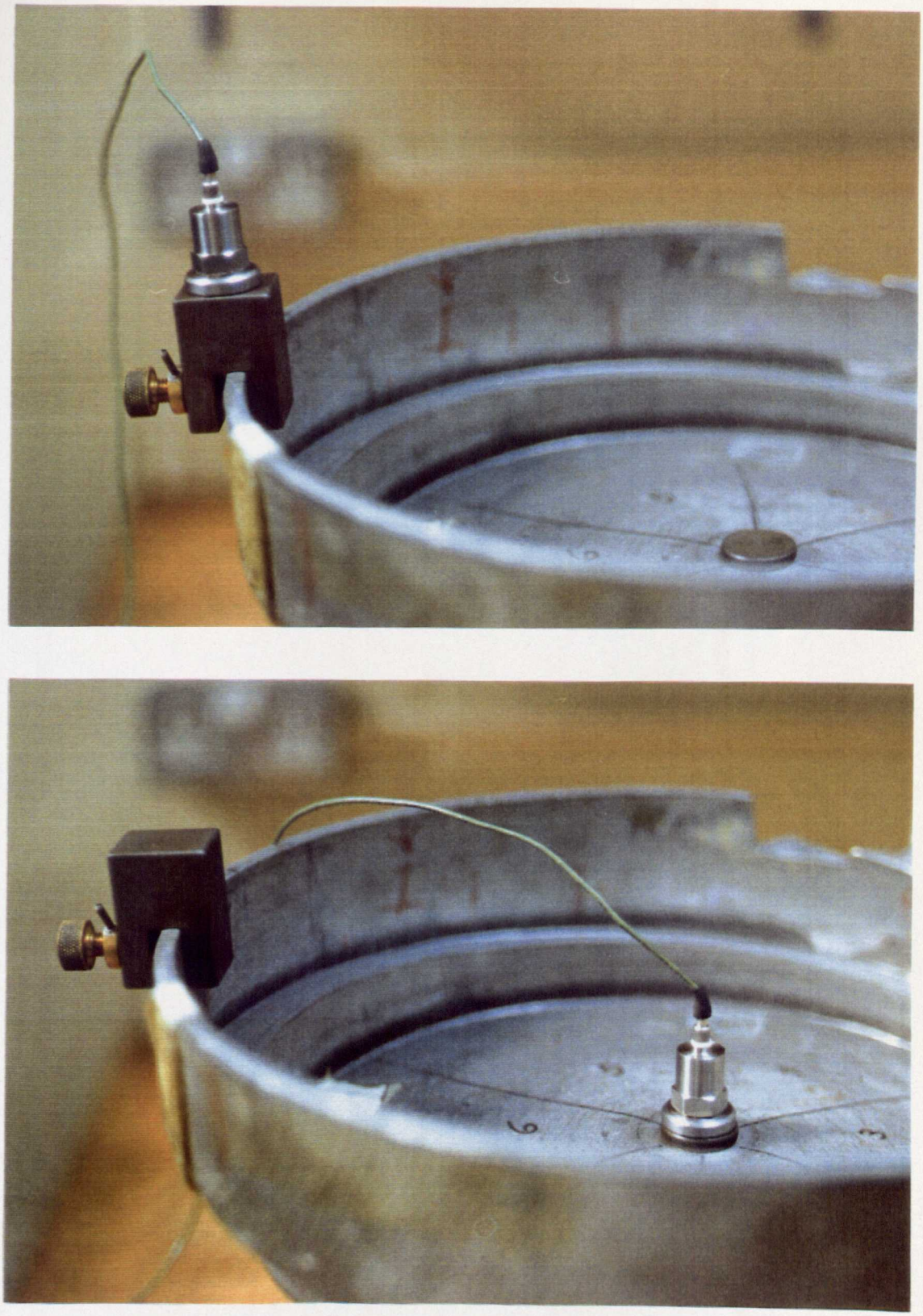

Plate 7.3 Accelerometer mounting blocks

After each frequency change, acceleration readings were taken at four equidistant points on the rim of the bowl and at the centre of the bowl to ensure uniform readings across the bowl, indicating that the bowl was correctly tuned and that it was only necessary to take readings at one point. When this had been established, acceleration readings were taken at the centre of the bowl. To ensure repeatability of results, readings were taken both running up from 350 to 650 N, and running down again. This allowed any discrepancies to be checked, and, where these were small, an average of the two readings was taken.

7.3 Analysis of response using the spreadsheet model

In order to be able to predict the acceleration response of the feeder, an estimate of its damping ratio was required. This was estimated for the first mode of vibration at 52 Hz using two different methods:

i) Logarithmic decrement. For a single degree-of-freedom system, or a system with well separated modes, the impulse response in the time domain will be of the form of an exponentially decaying sinewave which can be represented mathematically by the equation

$$x = X\, e^{-\zeta\omega_n t} \sin\left(\omega_n t \sqrt{(1 - \zeta^2)} + \phi\right) \qquad (7.1)$$

The logarithmic decrement δ is defined as the natural logarithm of the ratio of any two successive amplitudes. A standard result given in the text by Thomson (32) is that this ratio reduces to the form

$$\delta = \zeta\omega_n\tau_d \qquad (7.2)$$

where τ_d is the damped period of the oscillations.

For small ζ, $\omega_n \approx \omega_d$, and the equation becomes

$$\delta = 2\pi\zeta \qquad (7.3)$$

Successive ratios are given by

$$\frac{x_o}{x_1} = \frac{x_1}{x_2} = \frac{x_2}{x_3} \ldots\ldots = \frac{x_{n-1}}{x_n} = e^{\delta} \qquad (7.4)$$

The ratio x_o/x_n can be written as

$$\frac{x_o}{x_n} = \frac{x_o}{x_1}.\frac{x_1}{x_2}.\frac{x_2}{x_3} \ldots\ldots \frac{x_{n-1}}{x_n} = (e^{\delta})^n = e^{n\delta} \qquad (7.5)$$

Thus the logarithmic decrement after n cycles is given by

$$\delta = \frac{1}{n} \ln\left(\frac{x_o}{x_n}\right) = 2\pi\zeta \qquad (7.6)$$

An impulse was applied to the bowl feeder with an accelerometer mounted at the centre of the bowl. The waveform which resulted from the applied impulse was stored on a digital oscilloscope and a plot of this is given as Fig.7.2. The resulting waveform is not the pure sinewave which would be produced by a single degree-of-freedom system. However, by averaging over 10 cycles, the fundamental frequency of the trace can be seen to be 52 Hz. The actual waveform appears to be due to another sinewave at a frequency of slightly more than twice the fundamental being superposed on this. These findings would seem to agree with the results given in Chapter 5.

Despite this departure from the behaviour of a single degree-of-freedom system, it is still possible to clearly identify the cyclic variations at 52 Hz and their decaying amplitudes.

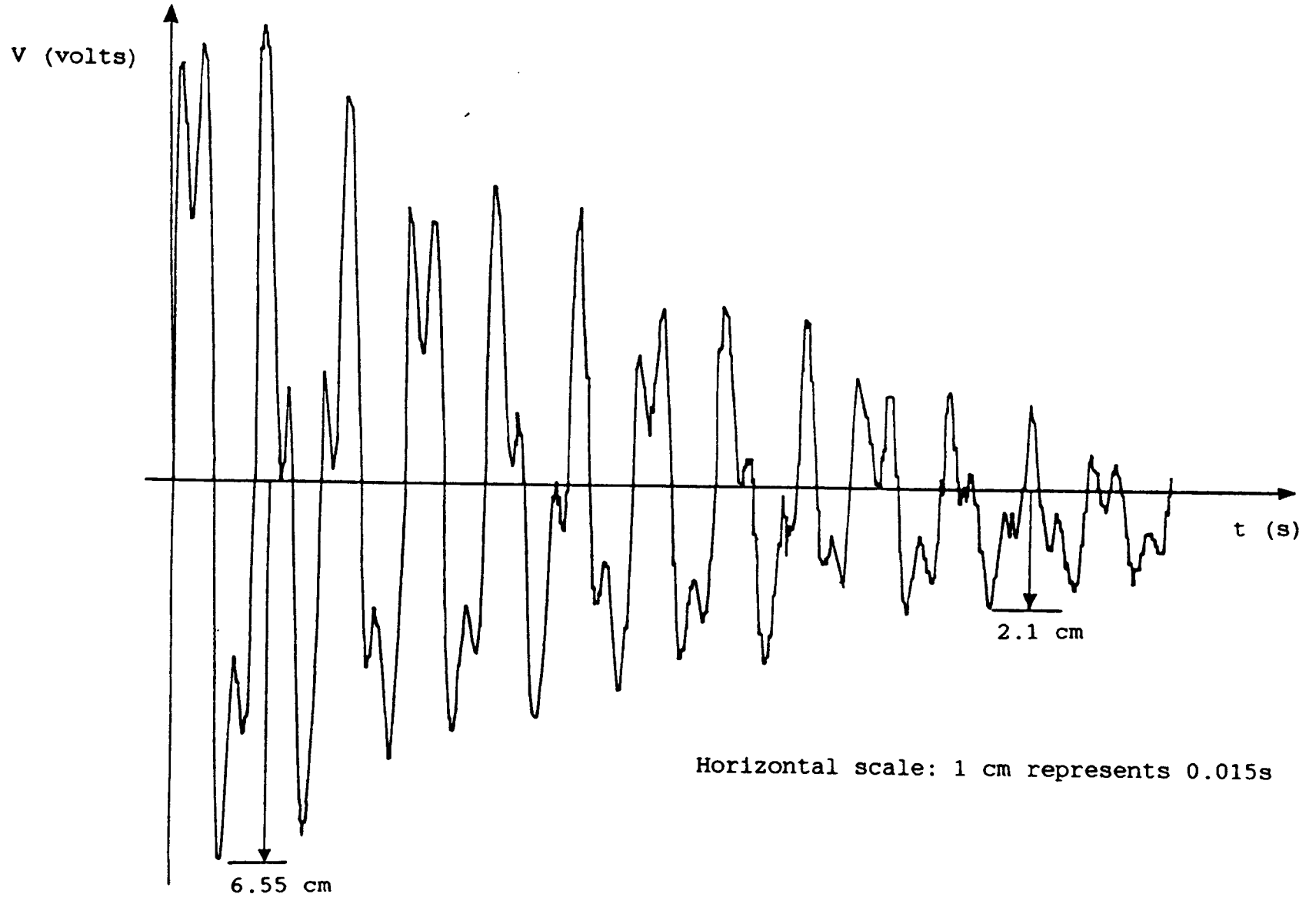

Fig.7.2 Impulse response of a bowl feeder

Thus the logarithmic decrement after 10 cycles can be obtained

$$\frac{x_o}{x_{10}} = \frac{6.55 \text{ cm}}{2.1 \text{ cm}} = 3.119$$

and so

$$\zeta = \frac{1}{2\pi.10} \ln(3.119) = 0.018$$

ii) From the frequency domain plots obtained in the modal testing described in Chapter 4. When the resonant frequencies and the frequency range over which curve-fitting is to take place are specified by the user as outlined in section 4.10, the modal testing software extracts the damping ratios at each mode using the half power points in the frequency domain. These values are then stored in a frequency and damping table, which can easily be accessed. The damping ratio stored for the mode at 52 Hz was ζ = 0.025.

From these two estimates, an average value of ζ = 0.021 was taken for use in the forced response model.

Since the force applied to the bowl was purely in the vertical direction and there were no restraining torques, the force vector {f} contained a zero element for the applied torque such that

$$\{f\} = \{f_1, 0\}$$

where f_1 is the applied force.

The input parameters of the bowl and base for the spreadsheet model were presented as Table 6.1, and are identical to those used in the experimental modal testing and given in section 5.1.

7.4 Results

A table of the experimental and numerical results is given as Table 7.1, and these are presented in graphical form in Fig.7.3.

Force Input (N)	Bowl Acceleration (m/s^2)							
	45 Hz Expt	45 Hz Predict	47.5 Hz Expt	47.5 Hz Predict	50 Hz Expt	50 Hz Predict	52.5 Hz Expt	52.5 Hz Predict
350	3.43	3.45	4.44	4.69	5.76	6.28	7.53	7.44
400	3.95	3.94	5.1	5.36	6.62	7.17	8.58	8.50
450	4.36	4.44	5.76	6.04	7.43	8.07	9.46	9.57
500	4.92	4.93	6.32	6.71	8.26	8.97	10.35	10.63
550	5.42	5.42	7	7.38	9.1	9.86	11.2	11.69
600	5.76	5.91	7.61	8.05	9.93	10.76	12.14	12.75
650	6.31	6.41	8.25	8.72	10.75	11.66	12.89	13.82

Table 7.1 Experimental and numerical results for the forced response of the feeder

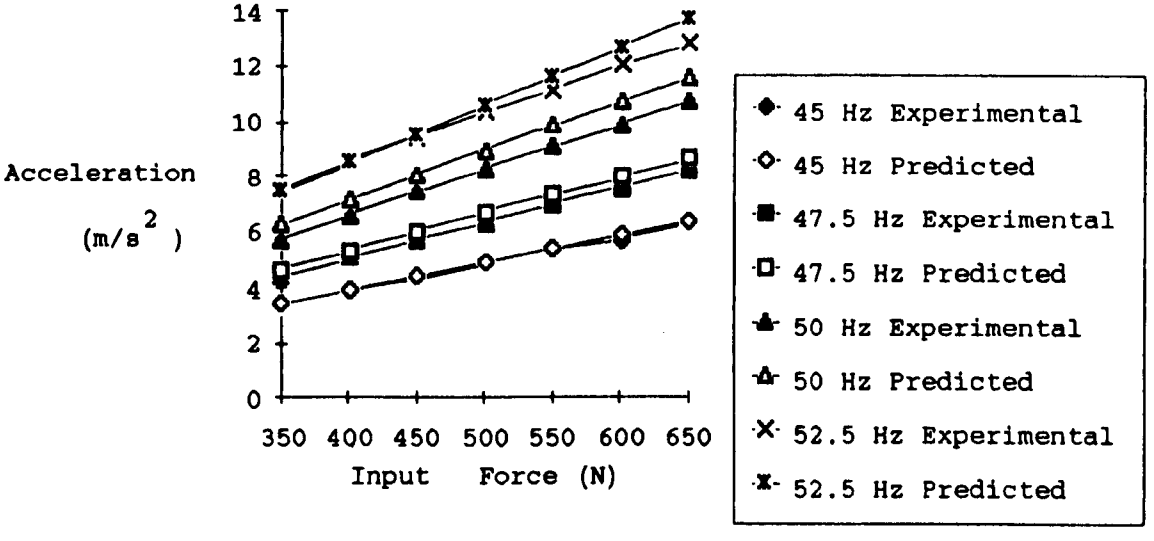

Fig.7.3 Graph of bowl acceleration against input force

7.5 Discussion of Results

The graphs of experimental results plotted in Fig.7.3 show good agreement between the predicted and experimental values of bowl acceleration within the selected ranges.

It is also interesting to note that the behaviour exhibited by the bowl appears to be linear within the region studied here. Since the bowl feeder was able to feed components successfully with the inputs at 50 Hz, it was felt that driving forces between 350 and 650 N corresponded quite closely to normal operation of the feeder.

8. VARIATION OF GEOMETRIC PARAMETERS OF THE BOWL FEEDER STRUCTURE

Having established a suitable numerical model which predicted acceleration values of the bowl, which from the earlier work of Redford and Boothroyd (2) was shown to be directly related to the mean conveying velocity of components, it was now possible to proceed to a consideration of how variations in the geometric parameters of the bowl would affect its performance.

Use was made of the 'table' facility of the spreadsheet package, which enabled a table to be drawn up by varying one input parameter over a specified range and recalculating the required output parameter at each value.

A programme of experimental work was undertaken to investigate the results obtained, varying the spring angle of a feeder in the range of 55 to 75 degrees in steps of 5 degrees.

8.1 Variation of geometric parameters using the spreadsheet model

One of the most flexible facilities offered by integrated spreadsheet packages is the ease with which recalculations can be carried out. This facilitates the quick and easy investigation of possible effects resulting from changes in a model's parameters. This is further enhanced with Microsoft Excel, which has a TABLE function. This allows a table to be drawn up by varying one of the input parameters of a model over a range of values. Up to two output parameters can then be recalculated for each value in the range. Alternatively, two input parameters can be varied simultaneously to investigate the effect on one output parameter.

The TABLE function was used in conjunction with the forced response model described in Chapter 7 to investigate changes in the spring angle of the bowl feeder whose input parameters are given in Chapter 7. The range of variation was from 55 degrees to 75 degrees in steps of 5 degrees, over a frequency range of 37.5 Hz to 60 Hz in steps of 2.5 Hz.

Tables of the resulting values of bowl accelerations from this analysis are given in Table 8.1.

Bowl Acceleration (m/s^2 N)		Forcing Frequency (Hz)				
		37.5	40	42.5	45	47.5
Spring Angle (deg.)	55	5.74E-03	7.07E-03	8.74E-03	1.09E-02	1.37E-02
	60	5.04E-03	6.32E-03	8.00E-03	1.03E-02	1.34E-02
	65	4.37E-03	5.63E-03	7.37E-03	9.86E-03	1.34E-02
	70	3.66E-03	4.89E-03	6.69E-03	9.30E-03	1.23E-02
	75	2.81E-03	3.91E-03	5.52E-03	7.18E-03	7.35E-03
Bowl Acceleration (m/s^2 N)		Forcing Frequency (Hz)				
		50	52.5	55	57.5	60
Spring Angle (deg.)	55	1.75E-02	2.28E-02	2.99E-02	3.84E-02	4.47E-02
	60	1.78E-02	2.37E-02	2.98E-02	3.20E-02	2.93E-02
	65	1.79E-02	2.13E-02	2.06E-02	1.78E-02	1.52E-02
	70	1.34E-02	1.20E-02	1.01E-02	8.69E-03	7.69E-03
	75	6.33E-03	5.34E-03	4.65E-03	4.19E-03	3.87E-03

Table 8.1 Predicted values of bowl acceleration in response to variations in spring angle and forcing frequency

8.2 Experimental Investigation

In order to verify the validity of the values of bowl acceleration predicted by the numerical model for a range of spring angles and frequencies, the same experimental apparatus and rig described in Chapter 7 were used again, keeping the force input fixed, and varying the spring angle and forcing frequency.

The bowl spring angle was varied by inserting inclined tubular spacers between the ends of the springs and the bowl and base as shown in Plate 8.1. The spacers themselves are shown in Plate 8.2. The length of the spacers was carefully chosen so that it was not necessary to adjust the length of the drive rod inserted in the force transducer below the bowl.

The spring angle was varied over the same range as that used with the numerical model, and for each angle acceleration measurements were taken for forcing frequencies of 45, 50 and 55 Hz. As with the previous experiment, after each change of spring angle, acceleration values were checked across the bowl to ensure uniformity, indicating that the bowl was correctly tuned, and that the central acceleration reading was a 'true' value for the bowl. The force input was held constant at 650 N throughout.

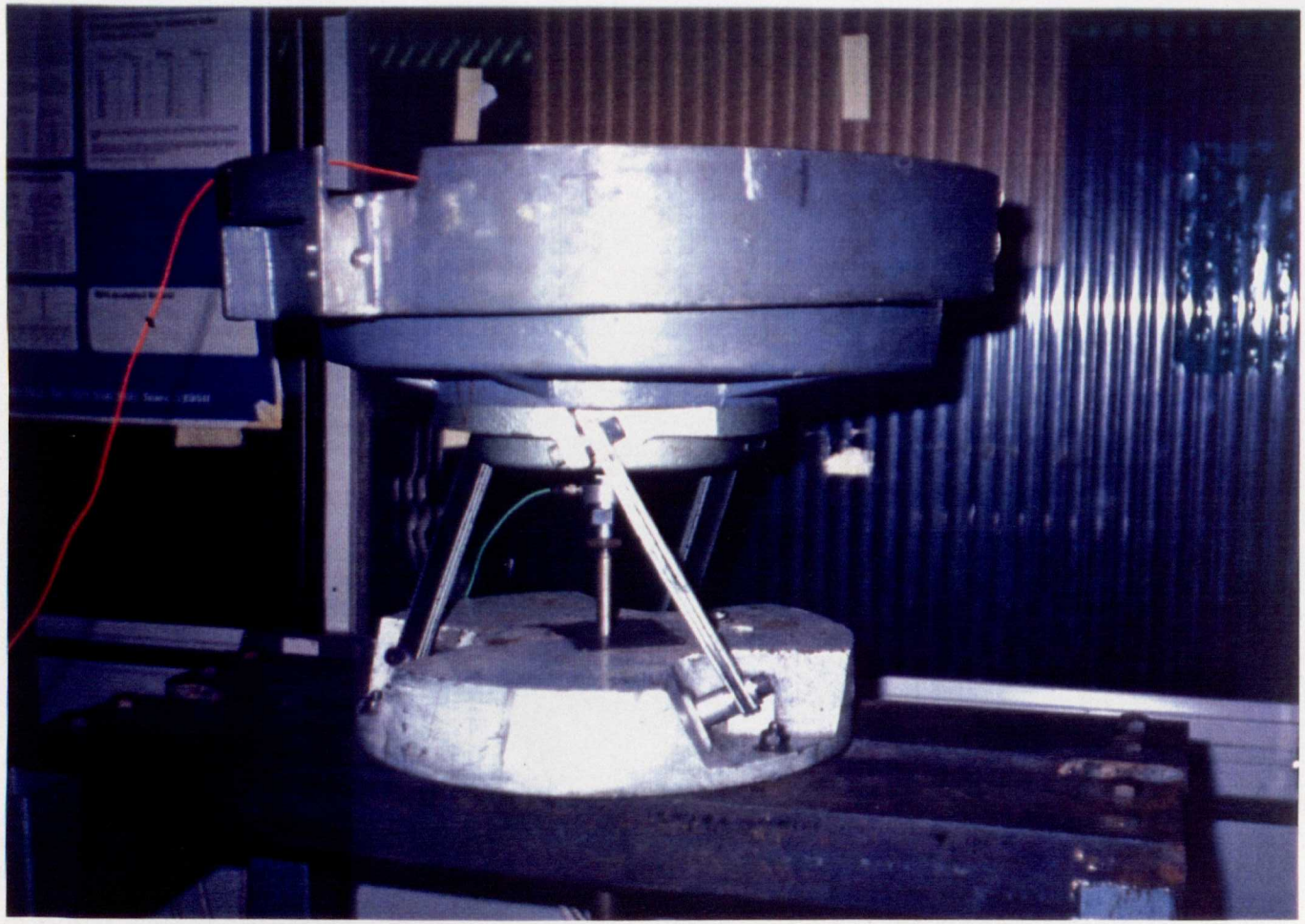

Plate 8.1 Photograph of bowl feeder showing tubular spacers inserted to vary the spring angle

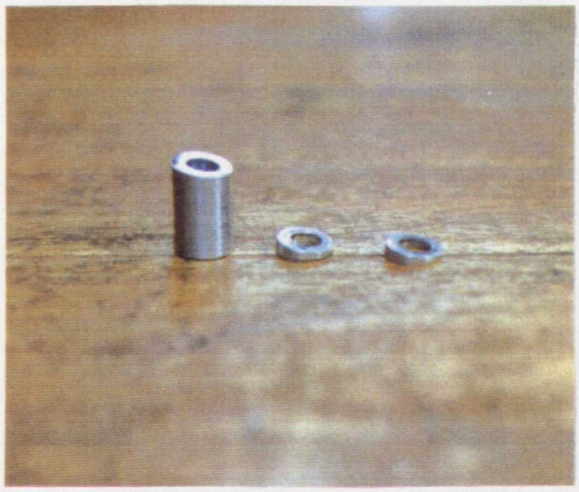

Plate 8.2 Inclined tubular spacers

The results obtained are given in Table 8.2.

8.3 Comparison of Experimental and Numerical Results

Graphs comparing experimental and numerical results at 45, 50 and 55 Hz are given as Fig.8.1, 8.2 and 8.3.

There is good correlation between the numerical and experimental results at 45 Hz, and for the three larger spring angles at 50 and 55 Hz. However, there is a significant discrepancy between predicted and experimental values for spring angles of 55 and 60 degrees at 50 and 55 Hz, the predicted values being greater. This variation is probably because the forcing frequencies of 50 and 55 Hz are very close to the first natural frequency of the system at 52.0 Hz. In this region the behaviour of the system is heavily dependent on its damping and, since this is difficult to model and predict this accurately, the response of the system is also dificult to predict. The effects of this are more pronounced for smaller spring angles, when the axial mode of vibration will involve more flexure of the springs. This contrasts with larger spring angles which will result in more axial deformation of the springs.

Bowl Acceleration (m/s^2 N)		Frequency Input (Hz) :		
		45	50	55
Spring Angle (deg.)	55	1.01E-02	1.24E-02	1.68E-02
	60	1.00E-02	1.41E-02	1.63E-02
	65	9.80E-03	1.65E-02	1.55E-02
	70	8.50E-03	1.03E-02	9.80E-03
	75	7.00E-03	6.00E-03	5.00E-03

Table 8.2 Experimental values of bowl acceleration in response to variations in spring angle and forcing frequency

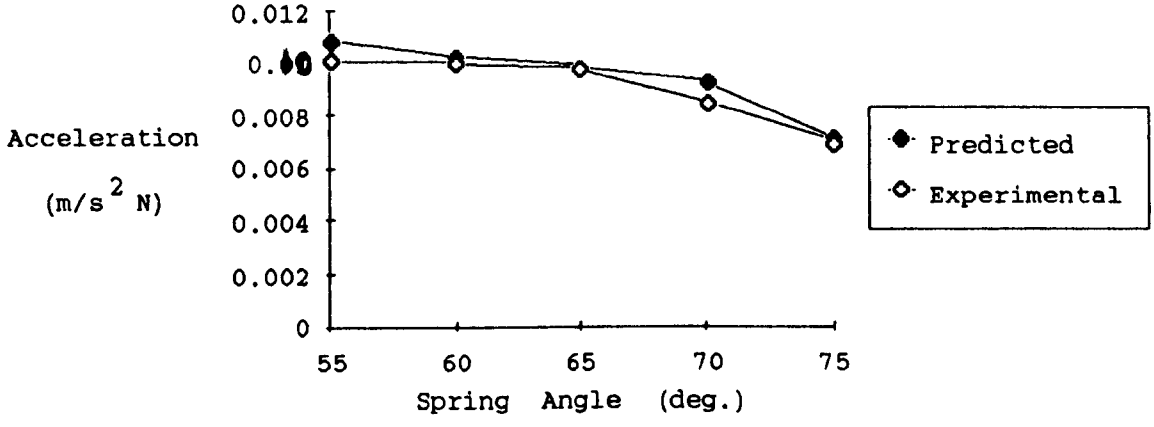

Fig.8.1 Graph of bowl acceleration against spring angle at 45 Hz

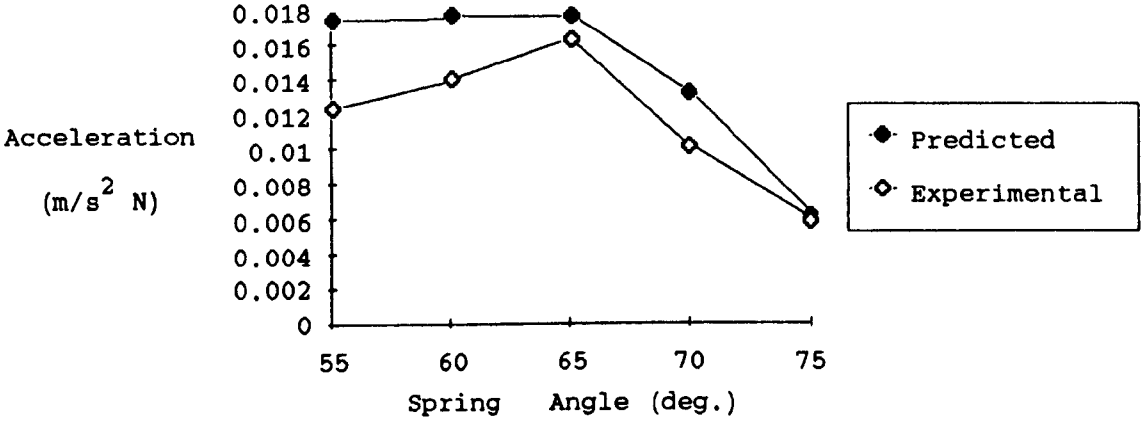

Fig.8.2 Graph of bowl acceleration against spring angle at 50 Hz

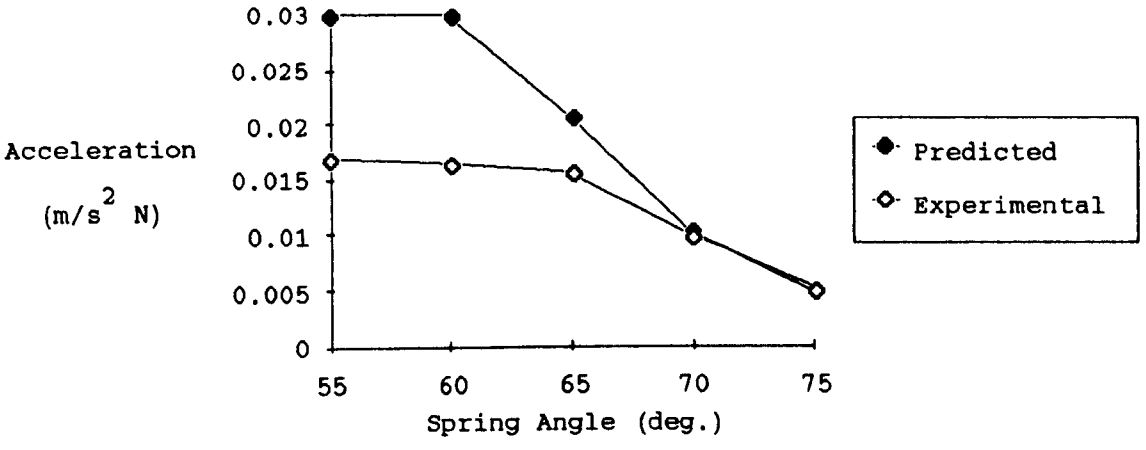

Fig.8.3 Graph of bowl acceleration against spring angle at 55 Hz

Because the flexural deformations tend to be larger than the axial deformations during the execution of the axial mode of vibration, this may result in the errors caused by the inaccurate modelling of the system damping being greater for spring angles of 55 and 60 degrees.

It is interesting to note that the graph at 50 Hz exhibits a peak for acceleration at 65 degrees, which has been chosen as the standard angle for a three spring-bank bowl feeder by the manufacturers of the feeder used in these investigations.

8.4 Variations in other geometric parameters

Having shown that the results predicted by the numerical model gave reasonably good agreement with experimental values, it was then decided to investigate how changes in other geometric parameters might affect the performance of the feeder. Again using the TABLE function, variations in the vertical acceleration of the bowl and the first natural frequency were investigated in response to the following:

i) spring length in the range from 0.17 m to 0.18 m (original value = 0.176 m);

ii) spring thickness in the range from 0.003 m to 0.0035 m (original value = 0.00323 m);

iii) spring spacing in the range from 0.001 m to 0.004 m (original value = 0.002 m); and

iv) bowl mass in the range from 9 kg to 12.5 kg (original value = 10.8 kg).

Plots of these variations are shown as Fig.8.4, 8.5, 8.6, and 8.7 respectively.

Fig.8.4 shows that as the spring length increases, the bowl acceleration increases. This is explained by observing the corresponding changes in natural frequency over this range, which actually decreases. As the first axial natural frequency approaches the forcing frequency of 50 Hz, the output acceleration will tend to rise. However, the potential improvements which may be accrued from a larger value of acceleration need to be balanced with the problems of running too close to resonance, namely: excessive noise, an increase in unpredictable behaviour, the loosening of fixings on the feeder itself, and an increase in failures due to fatigue.

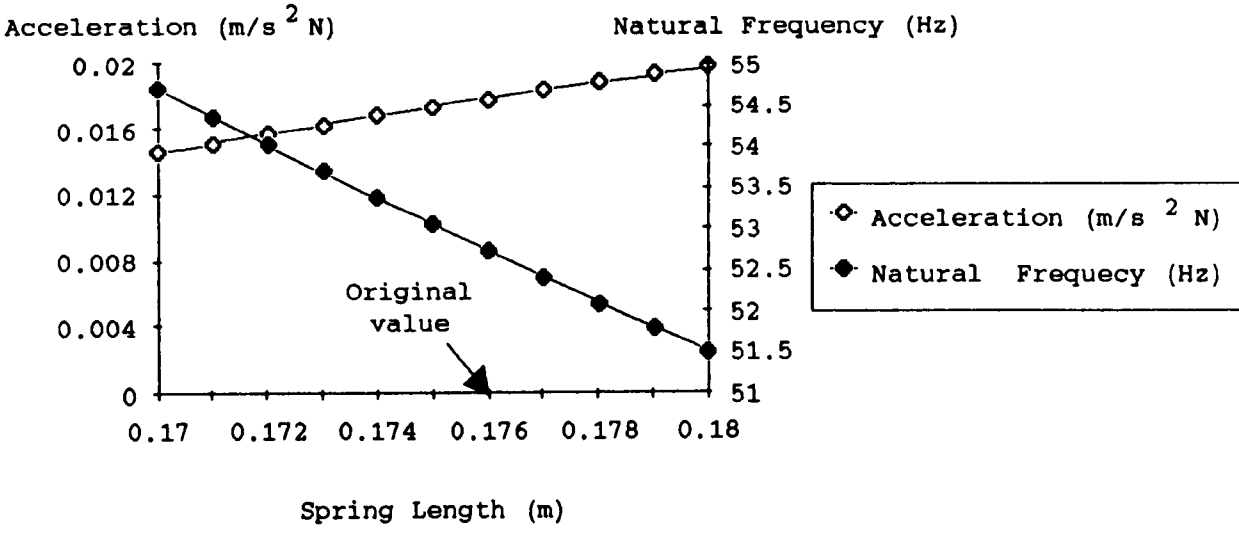

Fig.8.4 Predicted variations in acceleration and natural frequency in response to changes in spring length

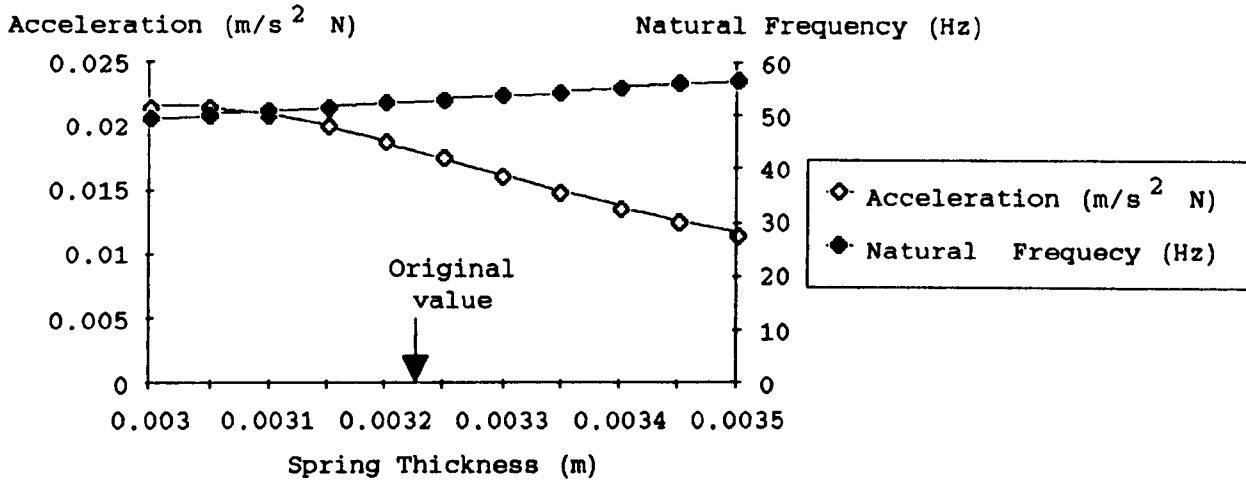

Fig.8.5 Predicted variations in acceleration and natural frequency in response to changes in spring thickness

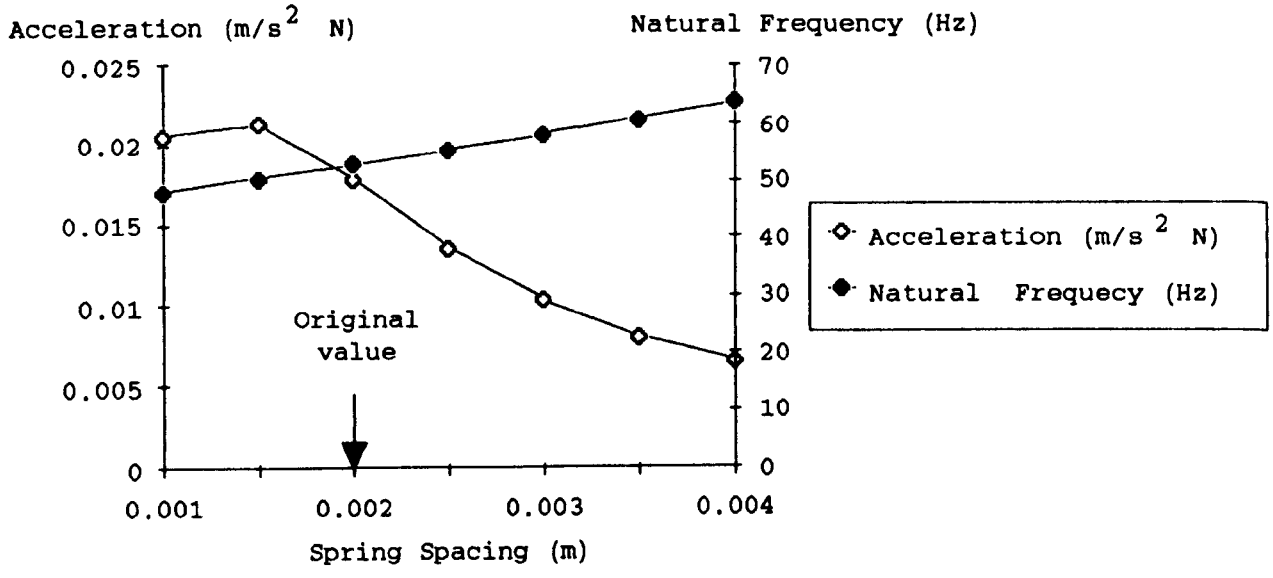

Fig.8.6 Predicted variations in acceleration and natural frequency in response to changes in spring spacing

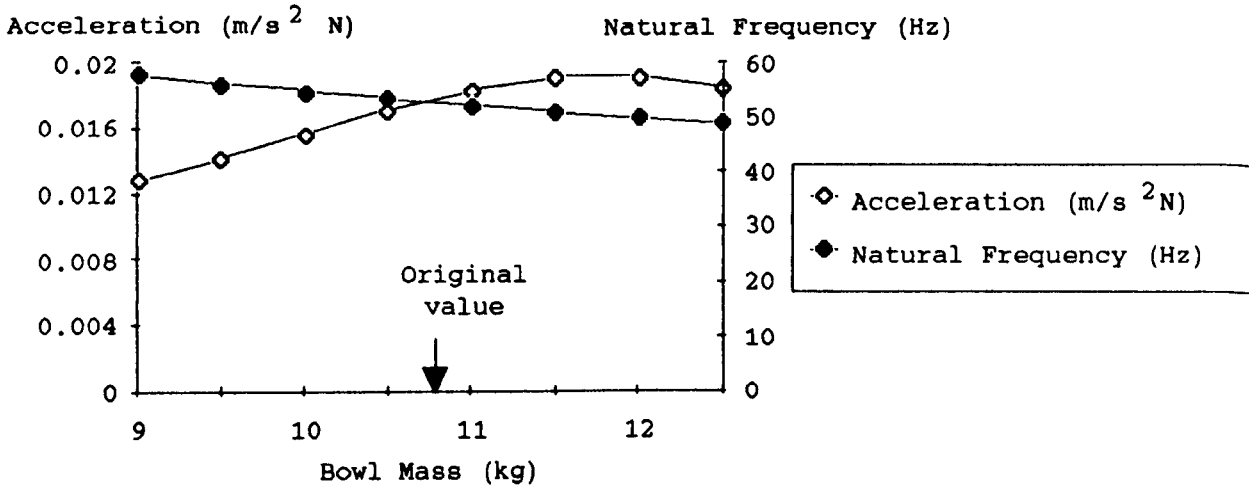

Fig.8.7 Predicted variations in acceleration and natural frequency in response to changes in bowl mass

Fig.8.5 shows that increases in spring thickness over this range cause a corresponding decrease in acceleration. This can be explained by the increase in stiffness which this gives, resulting in an increase in the natural frequency. As the natural frequency moves away from the forcing frequency, so the output drops. At the bottom end of the range, however, where the feeder has a natural frequency of 50 Hz, the variation in acceleration levels out, as would be expected.

Fig.8.6 shows that there is a peak in the response obtained by changing the spacing between springs at a value of 0.0015 m. This corresponds to the coincidence of the natural frequency with the forcing frequency.

Similarly, Fig.8.7 exhibits a fairly flat peak for the output at between 11.5 and 12 kg bowl mass. This also corresponds to the coincidence of the natural frequency with the forcing frequency.

9. DEVELOPMENT OF CUSTOMISED SOFTWARE FOR BOWL FEEEDER DESIGN

Having developed a numerical model of the feeder which predicts its dynamic characteristics, and therefore the resulting output in response to a forcing input, which can be used to investigate how changes in geometric parameters affect its performance, it is useful to reconsider the aims and objectives of this stage of the project as given at the start of Chapter 6. These were:

i) optimisation of the geometric parameters of the bowl feeder structure in order to achieve an increase in feed-rate; smoother, quieter running; and lower power consumption; and

ii) the production of a 'portable', user-friendly design tool which would enable development engineers to investigate the performance characteristics of alternative structures and arrangements.

The spreadsheet model had allowed an investigation of changes in geometric parameters to be carried out, and so it therefore only remained to adapt this model to produce a user-friendly design tool, and satisfy the second objective.

9.1 Description of the software used

The design tool developed was based on the spreadsheet model described in Chapter 6, written using the Microsoft Excel spreadsheet package. This consisted of a main worksheet where all the geometric and material input parameters to the bowl were entered and ,from this, the modal properties i.e. the eigenvalues and eigenvectors were calculated. The worksheet calls a macro which calculates the acceleration vector of the bowl in response to a harmonic input of 50 Hz.

Unlike the investigations carried out in Chapter 8, where input parameters were varied over a specified range and the resulting responses calculated using the TABLE fuction, the design tool described here only allows one set of input parameters to be tried at once.

9.2 Software tools used to create a 'customised' package

The Microsoft Excel(31) spreadsheet package has three main tools which can be used to customise an application which has been written by one user in order to make it easier for other users to run. These are:

i) Custom menus.

Custom menu-bars, menus and commands can be created using Macro Language functions and a menu definition table. They allow sequences of functions to be carried out automatically in response to the selection of a single command from those listed in the menu. This can save time in the execution of a program, but also makes the use of a program easier for someone wishing merely to use the program as a tool who is unfamiliar with the detail of its structure. Menus and commands can either be added to the Excel built-in menu-bars, or form part of a new menu-bar.

ii) Custom Dialog-Boxes.

Dialog-boxes are used to prompt the user for the input of information necessary to execute a program, or to inform the user of the results of a calculation. They allow a program to be used without a detailed knowledge of the location and type of input parameters on constituent worksheets. Custom dialog-boxes are created using the Macro language functions and a dialog-box definition table.

iii) Command Macros.

Function macros were used as part of the forced response model of the bowl feeder described in Chapter 6. Command macros are also programs written in the macro language to perform operations on the data stored on a spreadsheet. However, unlike function macros which are called by the spreadsheet in order to carry out a calculation and return a value to the calling spreadsheet, command macros carry out a sequence of actions automatically when they are run from the macro itself. They are therefore capable of carrying out tasks such as copying input values to a worksheet, or from one document to another; opening, closing and saving documents; calling other command macros, and returning calculated values to the user.

There is also a particularly useful type of command macro called an autoexec macro. This runs automatically whenever a document is opened and enables the macros controlling any custom built-in features of a program to be run automatically.

9.3 Description of the spreadsheet design tool

In order to make the forced response spreadsheet model described in Chapters 6 and 8 easy to use as a design tool, it was decided to add the following features:

i) a dialog-box which requests all the necessary input parameters for the model from the user before proceeding with the analysis. These are the geometric parameters of the springs and the bowl.

   A screen dump showing the dialog-box is given as Fig.9.1, and the dialog table used to define this using the macro language is given as Fig.9.2;

ii) a command-macro which inserts the specified values into the appropriate cells on the spreadsheet and then runs the forced response analysis;

iii) a dialog-box which returns the calculated values of the vertical bowl acceleration and the first natural frequency to the user. A copy of this is shown in Fig.9.3; and

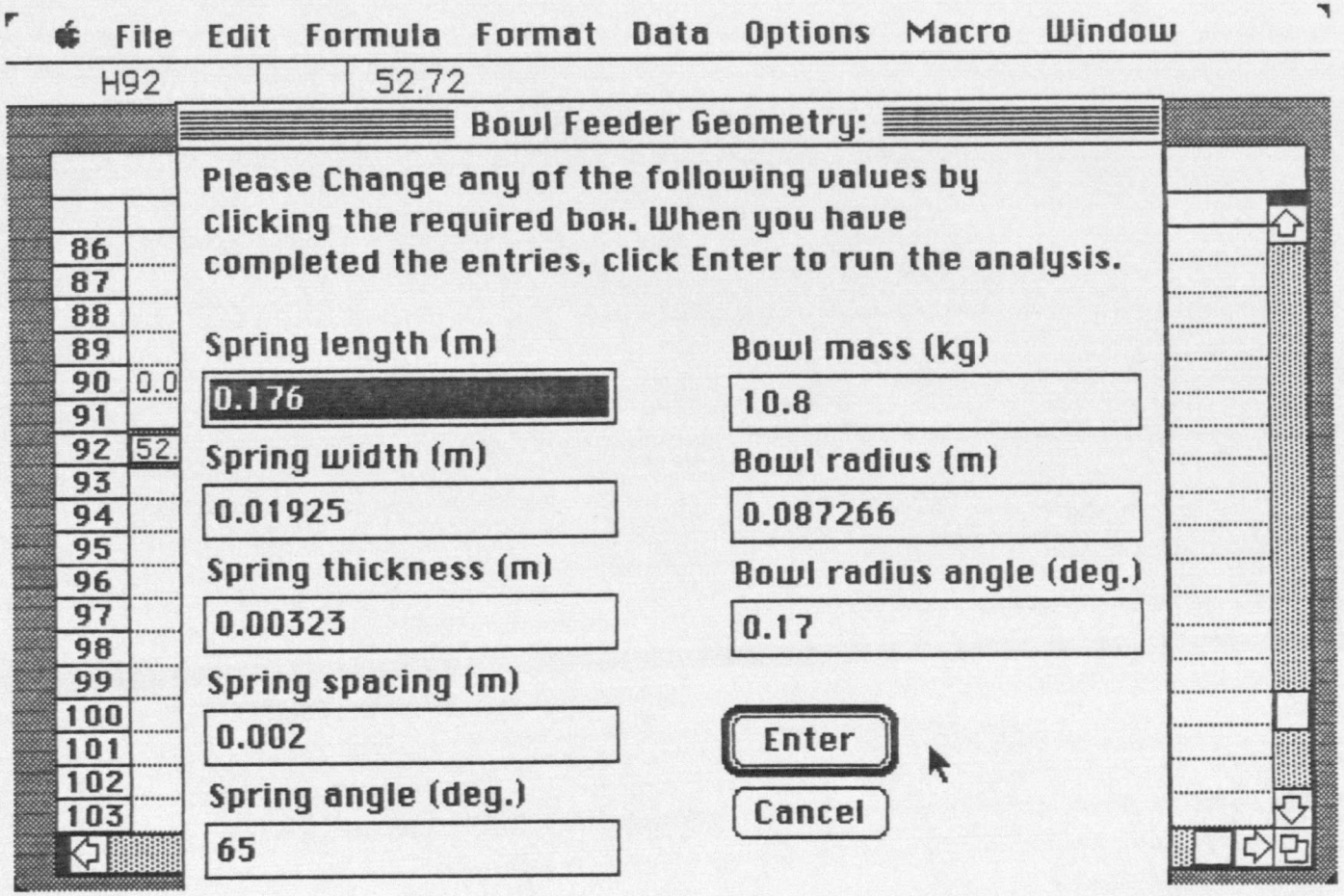

Fig.9.1 Dialog-box used for input of data

	Item Num	Horiz Pos	Vert Pos	Item Wdth	Item Hght	Text	Initial/Result
Static text	5					Bowl Feeder Geometry:	
Static text	5					Please Change any of the following values by	
Static text	5					clicking the required box. When you have	
Static text	5					completed the entries, click Enter to run the analysis	
Static text	5						
Static text	5					Spring length (m)	
Number edit box	8						0.176
Static text	5					Spring width (m)	
Number edit box	8						0.01925
Static text	5					Spring thickness (m)	
Number edit box	8						0.00323
Static text	5					Spring spacing (m)	
Number edit box	8						0.002
Static text	5					Spring angle (deg.)	
Number edit box	8						65
Static text	5	225	80			Bowl mass (kg)	
Number edit box	8						10.8
Static text	5					Bowl radius (m)	
Number edit box	8						0.087266
Static text	5					Bowl radius angle (deg.)	
Number edit box	8						0.17
OK button	1	225	250			Enter	
Cancel button	2					Cancel	

Fig.9.2 Table used to specify the dialog-box shown in Fig.9.1

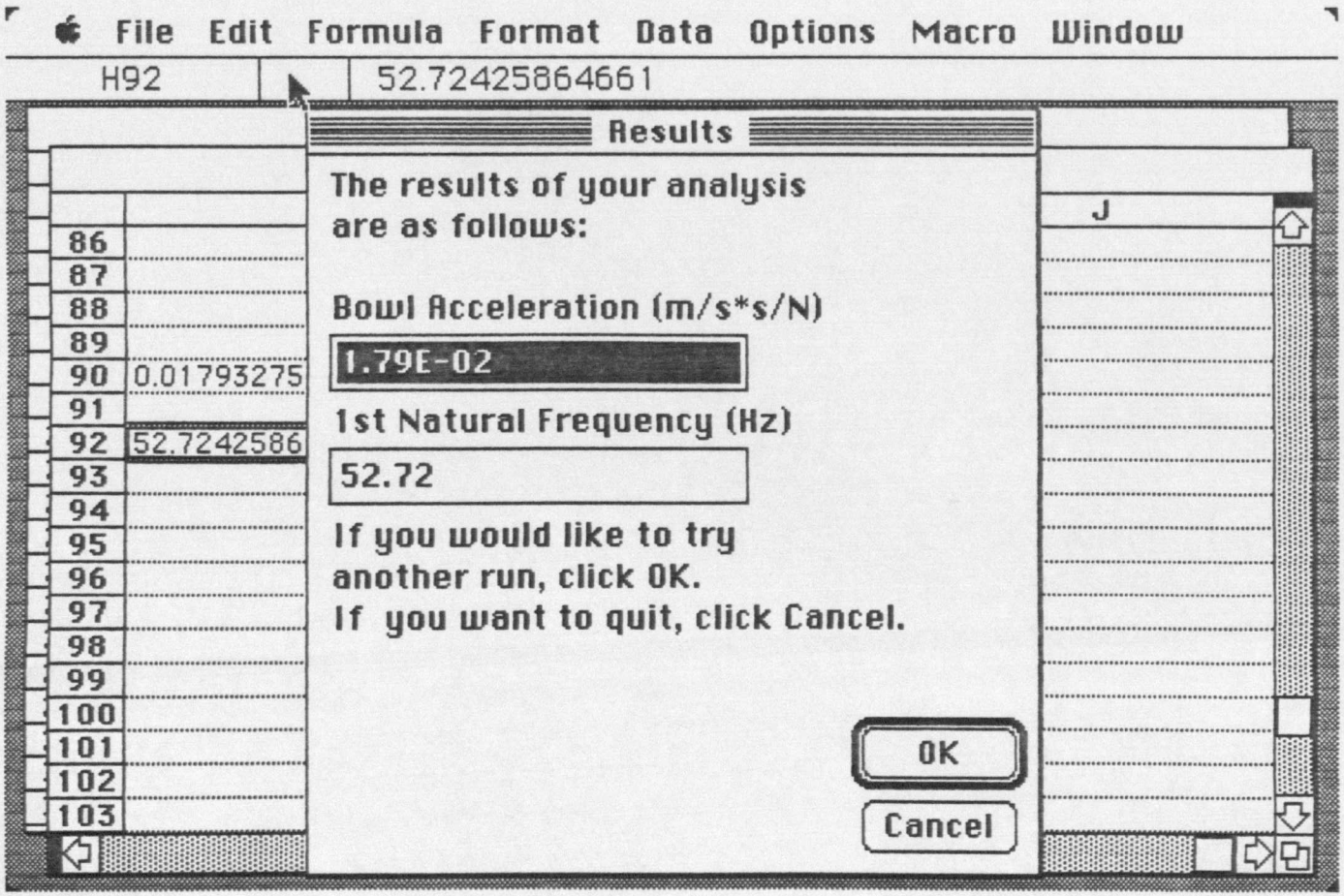

Fig.9.3 Dialog-box used for output of calculated values

iv) a command-macro which controls all of these stages, and is automatically run when the icon of the 'BowlFeeder' document is selected from the Macintosh desktop.

The constituent parts of the software are thus:

i) the autoexec command-macro, 'BowlFeeder', which runs when opened and controls the execution of the complete design package. A copy of this macro is given in Appendix 5;

ii) the spreadsheet, 'Worksheet', which calculates the modal properties of the model; and calls

iii) the function macro, 'Superposition', which calculates the output of the feeder in response to a harmonic forcing function of 50 Hz.

A flow chart showing the structure of the complete design package is given as Fig.9.4.

User documentation for running the software is given as Appendix 6.

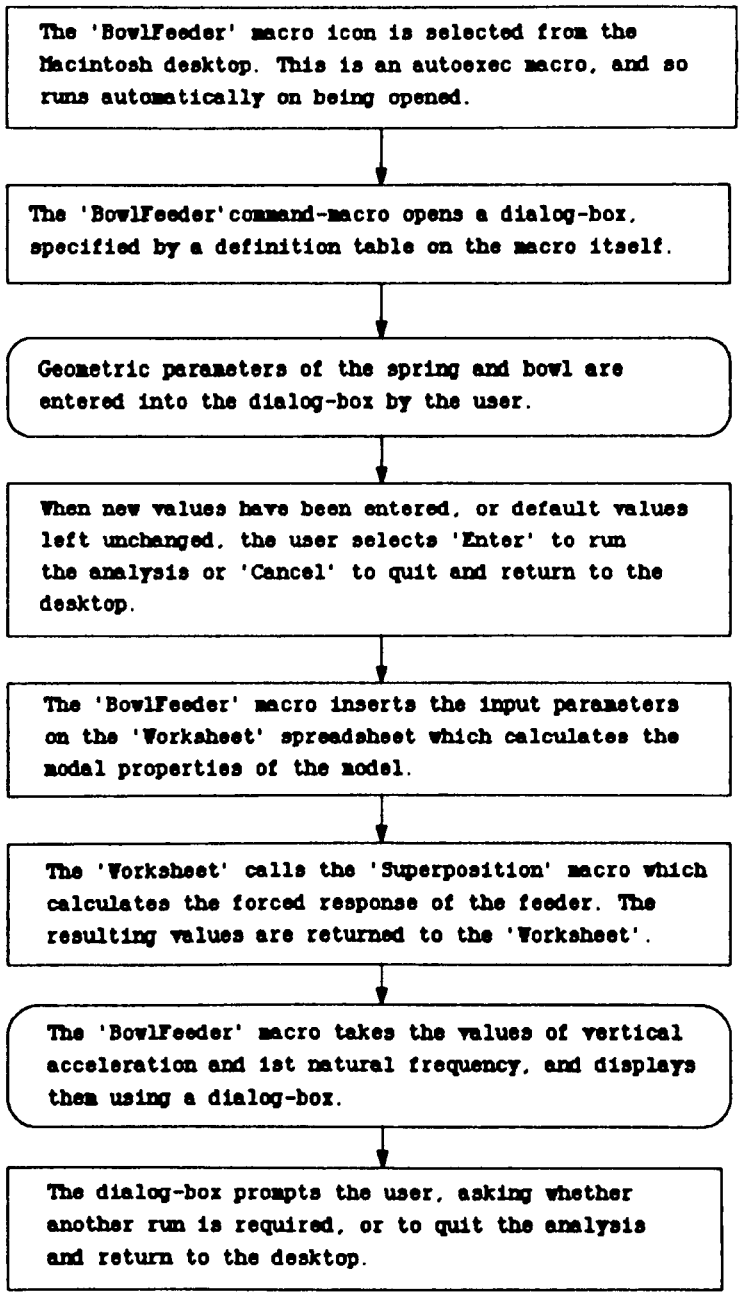

Fig. 9.4 Flow chart of the procedures used in the bowl feeder design tool package.

9.4 Testing of the design package

The spreadsheet design package was tested in its operation to ensure that selection of the appropriate box by the user resulted in the running of the analysis or quitting of the package as detailed in the User Manual. It was also necessary to check that the input parameters were stored correctly after each run.

The package was also tested by entering a range of input values which represented typical sizes and weights of components. These resulted in satisfactory operation of the package and are specified in the section on 'Entering Data' in the User Manual.

10. EXPERIMENTAL INVESTIGATION OF OPERATING PROBLEMS

The investigations carried out in this project have enabled the dynamic behaviour of the bowl feeder to be modelled so that the effect of changes in geometric and structural parameters can be investigated, and this has been incorporated into a spreadsheet package which can be used as a design tool. However, in addition to facilitating development work enabling the performance of prototypes to be investigated without the need to manufacture and modify feeders on a trial and error basis, the other reason for modelling the dynamic behaviour of a structure is to improve our understanding of this. This will aid the solution of problems which occur both during manufacture and operation, and may help to bring about fundamental changes in the design of the bowl feeder.

10.1 Dynamic Behaviour of the Bowl Feeder

The results of the numerical model for predicting the modal properties of the bowl feeder given in Chapter 5 suggest the following:

i) The natural frequency of the bowl closest to the driving frequency of 50 Hz is the axial mode with

vertical motion of the bowl. This would seem to concur with the findings of other authors(2), that the normal component of acceleration, which gives the more efficient 'hopping' motion, is one of the most important factors in improving the feed rate of components for in-phase feeding;

ii) The three spring-bank bowl feeder gives rise to tipping of the bowl at 118.0 Hz. This would imply a low stiffness associated with this particular mode which could result in its excitation by either asymmetric geometry or forces. Possible causes of this may be:

a) the fairly generous manufacturing tolerances allowed on the holes at the ends of the springs. This is done to ensure that the armature and coil of the electromagnet are parallel but, when combined with tolerances on other components, may result in asymmetry;

b) the asymmetry of the bowl because of its spiral track, the tooling used, or inaccuracies in the casting , fabrication or subsequent machining of the bowl;

c) differences in spring stiffness between the three banks; and

d) an asymmetric force being generated due to the cross-section of the armature and coil, their positioning relative to the spring banks, and relative to each other.

10.2 Experimental Investigation

In response to the points listed above, it was decided to undertake a further experimental investigation. The purpose of this was as follows:

i) to investigate the dynamic properties of the bowl feeder further; and

ii) to attempt to apply the knowledge gained to the solution of one of the most common problems which occurs in the manufacture and operation of bowl feeders, namely the incidence of dead-spots. These are regions on the spiral track where components either remain stationary or feed backwards.

A block diagram of the experimental apparatus used is shown in Fig.10.1.

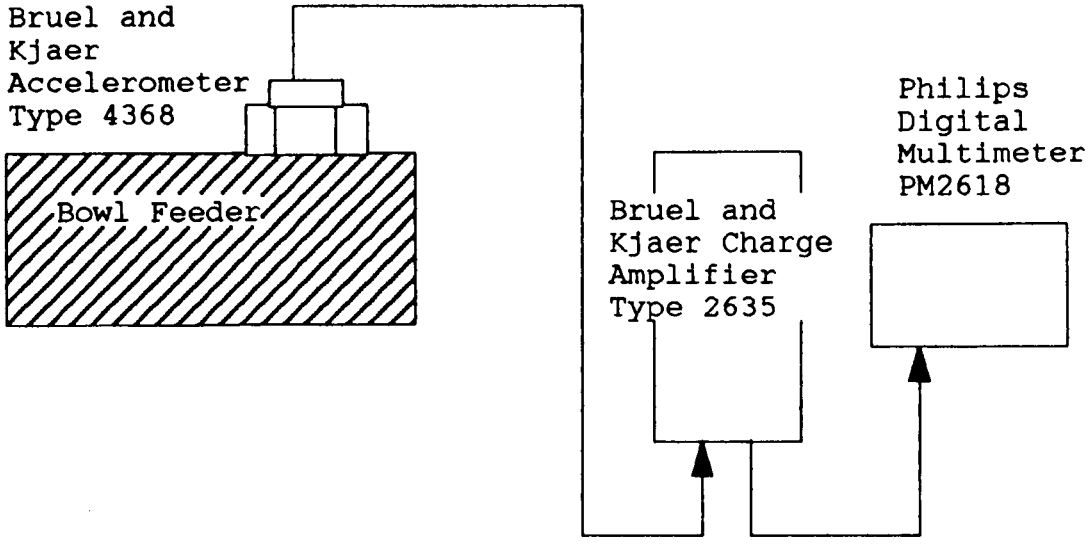

Fig.10.1 Block diagram of experimental apparatus and instrumentation used in the investigation of the cause of dead-spots

Measurements of acceleration were taken in the vertical, tangential and radial directions at the four points on the bowl's circumference shown in Fig.10.2 by clamping the mounting block described in Chapter 4 onto the bowl and using the magnetic base to attach the accelerometer. The Model 10 Aylesbury Automation feeder was used because it had been found to have a dead spot at point B on the bowl track. The digital multimeter gave r.m.s. values of acceleration (the waveforms were also viewed on an oscilloscope to check that they were sinusoidal in form).

The procedure used was as follows:

i) Readings of acceleration in the three directions were taken for settings of the controller from 0 to 100 in steps of 10. An increase in the controller setting corresponds to an increase in the power input to the feeder, but the scale provided is not necessarily linear, and has not been calibrated to any recognised unit of power. These results are given in Table 10.1.

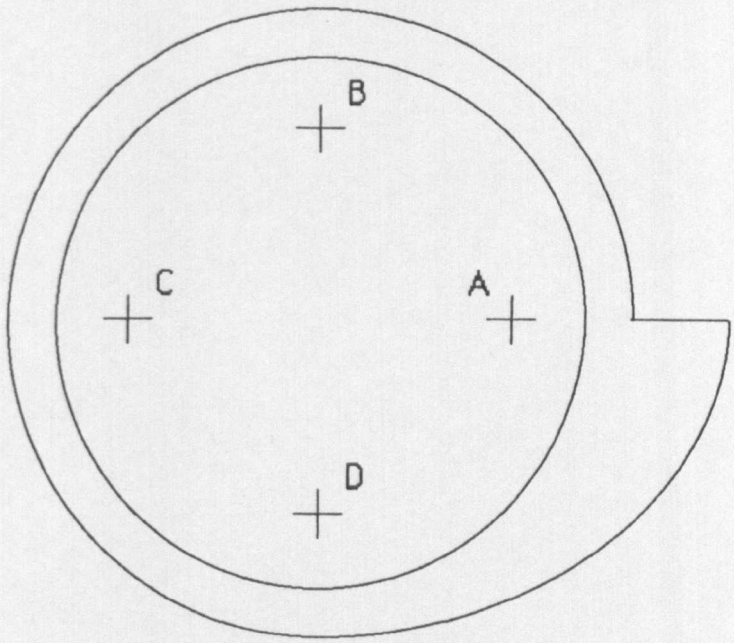

Fig.10.2 Plan view of the bowl feeder showing the four measurement points

	Point A			Point B		
Controller Setting	Vertical Accn./m/s^2	Radial Accn./m/s^2	Tangential Accn./m/s^2	Vertical Accn./m/s^2	Radial Accn./m/s^2	Tangential Accn./m/s^2
0	0.2	0.03	0.37	0.16	0.03	0.44
10	0.2	0.04	0.43	0.21	0.04	0.58
20	0.6	0.11	1.52	0.64	0.06	1.72
30	2.32	0.43	5.8	2.45	0.25	6.85
40	8.5	2.35	11.87	6.85	1.31	12.19
50	10.35	3.49	12.35	8.24	1.89	12.35
60	11	3.82	12.59	8.44	2.46	12.56
70	11.6	3.64	12.76	8.54	2.99	12.78
80	12	3.65	12.87	8.63	3.29	12.99
90	12.21	3.76	12.96	8.68	3.68	13.1
100	12.23	3.76	12.97	8.62	3.68	13.1
	Point C			Point D		
Controller Setting	Vertical Accn./m/s^2	Radial Accn./m/s^2	Tangential Accn./m/s^2	Vertical Accn./m/s^2	Radial Accn./m/s^2	Tangential Accn./m/s^2
0	0.19	0.02	0.36	0.19	0.02	0.39
10	0.25	0.02	0.45	0.25	0.03	0.49
20	0.74	0.06	1.5	0.68	0.05	1.62
30	2.15	0.18	5.9	2.68	0.16	6.41
40	7.39	2.09	11.9	8.68	0.93	11.81
50	8.9	3.49	12.35	9.92	1.42	12.4
60	9.35	3.86	12.54	10.56	2.16	12.66
70	9.69	3.78	12.65	10.84	2.27	12.76
80	10.68	4.03	12.7	11.3	2.37	12.79
90	11.17	4.4	12.91	11.7	2.51	12.81
100	11.12	4.43	12.91	11.7	2.5	12.81

Table 10.1 Acceleration readings at points A, B, C and D on the bowl for a range of power inputs

Table 10.1 shows that there is no change in the radial and tangential aceleration values between the four points; however, at point B where there is a dead-spot, the vertical acceleration is significantly lower and in fact reaches a plateau. It is also worth noting that the value of the vertical acceleration at this point gives an acceleration normal to the track less than the component of the acceleration due to gravity, which is given by

$$g \cos \theta = 9.81 \times \cos 0.79^{\circ}$$

$$= 9.809 \text{ m/s}^2$$

where θ is the track angle.

ii) To investigate whether the asymmetry of the bowl caused the dead-spot, the bowl was rotated by 120° to three different positions relative to the base, magnet and springs. Components were placed in the bottom of the bowl and their travel up the track observed in each case. The dead-spot remained in the same position and seemed unaffected by the rotation of the bowl.

iii) The next part of the experimental work was to investigate the relationship between the magnet and springs. The relative shape and position of the pole pieces of the magnet coil and the points of attachment of the springs to the bowl are shown in Fig.10.3. Spring bank no.2 is parallel with the longer side of the magnet.

Fig.10.3 shows that because of this arrangement the three spring banks are positioned at different distances from the outer pole pieces. This will mean that the forces transmitted to the three spring banks will differ. In order to investigate whether this asymmetrical relationship might be a cause of the dead-spot, it was decided to rotate the magnet relative to the springs about its vertical axis in steps of 30° to the three positions shown in Fig.10.4, position A representing the original position. This was done by drilling and tapping the base so that the coil could be securely repositioned in each orientation.

The position of the dead-spot was originally directly above the mounting point on the bowl of spring bank no.2.

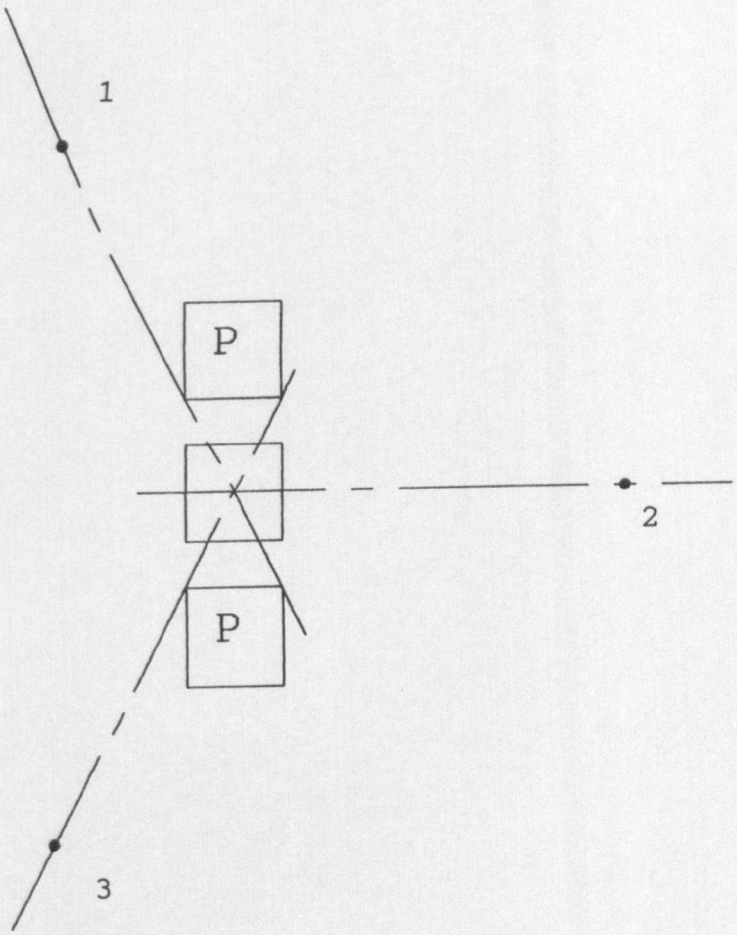

Fig.10.3 Plan view showing the attachment points of the spring banks on the bowl relative to the three pole pieces of the electromagnetic coil

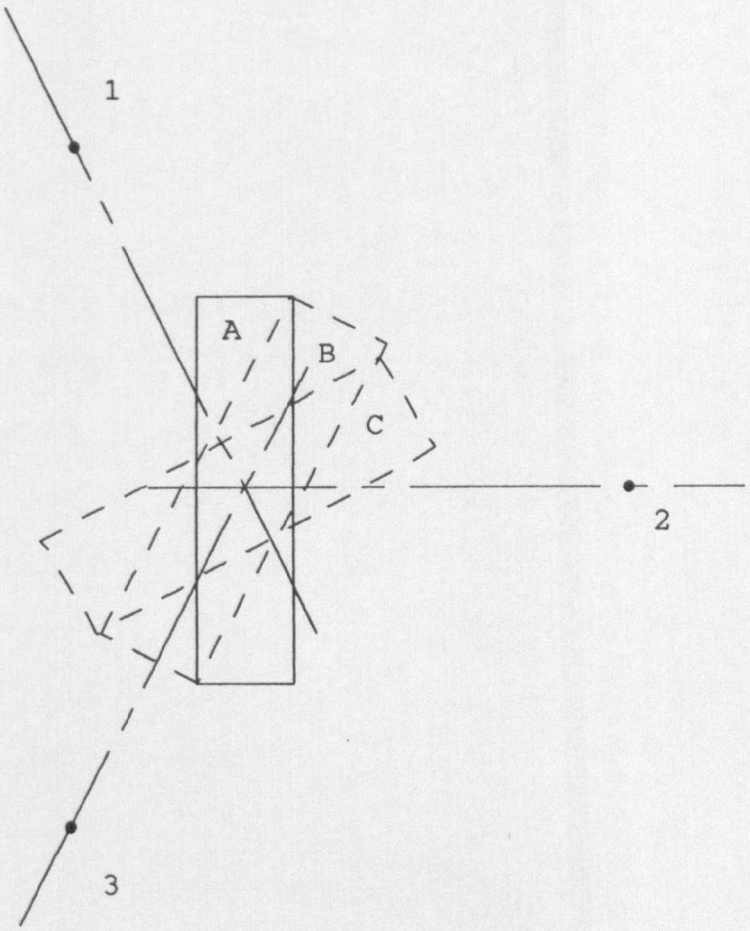

Fig.10.4 Plan view showing the three positions of the magnet, A, B and C, when rotated through 30 degrees

Consider rotation of the magnet through 30° clockwise to position B. This would result in the two outer pole pieces (labelled P in Fig.10.3) exerting equal forces on spring banks no.1 and 2, but exerting an even greater force on spring bank no.3. This would mean that the part of the bowl directly above bank no.3 would vibrate with greater vertical amplitude than elsewhere, and the part directly opposite bank no.3 would vibrate least. A further rotation through 30° clockwise would result in the magnet becoming parallel to spring bank no.1 in a similar position to the original configuration. It was therefore necessary to notice how both the magnitude and position of the dead-spot changed in these three positions.

With the magnet in position A, the dead-spot occured immediately above spring bank no.2. The control setting was increased to a value of 70, but components still remained stationary at this point. Above a setting of 70 the bowl began to strike the magnet, giving an unacceptable operating condition.

When the magnet was rotated through 30° to position B, the position of the dead-spot moved through 60° in the opposite direction to a point midway between

spring bank no.s 1 and 2. In this position, the dead-spot disappeared at a control setting of 50 when the components began to feed in a forward direction.

With the magnet rotated through a further 30° to position C, the dead-spot occurred directly above spring bank no.1, and did not disappear even with a control setting of 70 when the bowl and magnet started to strike one another.

10.3 Discussion

The results of part a) of the experimental work in 10.2 agree with the proposal that it is the vertical component of acceleration which has the most significant effect on component feed-rate. The fact that the value of vertical acceleration is less than the acceleration due to gravity would suggest that succesful forward motion is only achieved when the acceleration is large enough for the components to leave the track, resulting in 'hopping' motion.

Whilst the asymmetry of the bowl does not seem to give rise to the dead-spot encountered in this particular instance, the asymmetry of the drive and springs does.

This finding implies that, in order to minimise the chance of dead-spots occurring, any possible asymmetry of either the springs or drive should be removed at the design stage. There are two measures which could be taken here:

i) In order to increase the stiffness of the tipping mode, and do away with the asymmetrical arrangement of the springs relative to the drive, the number of spring banks should be increased to four instead of three. This has actually been adopted by Aylesbury Automation on their latest development, a high-speed feeder which offers higher feed-rates and more reliable component motion.

ii) The asymmetry of the drive could be overcome by replacing the three-pole electromagnet with an annular arrangement of coil and armature.

The benefits of these developments are:

i) Because these proposed modifications are less likely to excite the tipping mode of the bowl when executing its motion, this should also result in lower power consumption.

ii) The symmetrical arrangement of the springs relative to the drive in both cases will make tuning of the bowl easier; the spring stiffnesses of all banks should be very close in value.

iii) The occurrence of dead-spots caused by the asymmetrical arrangement of springs and drive will be reduced, resulting in more reliable feeding.

iv) The noise emitted from operating feeders is sometimes caused by the armature and coil striking each other. This is exacerbated by any tendency of the bowl to tip during its motion. Any reduction in the extent of tipping will therefore serve to reduce the noise generated.

It is possible that these developments would result in higher manufacturing costs. Any increase, however, would be outweighed by the benefits accruing from increased and more reliable feeding, lower power consumption, easier tuning, and less noise generation.

11. FURTHER WORK

The study described here has been successful in improving our understanding of the behaviour of vibratory bowl feeders with three banks of inclined springs. As a result, software has been produced to enable design engineers to investigate the performance of new machines with different geometric parameters. However, there are other areas of investigation which it would now be worthwhile pursuing:

i) The numerical model described here could be adapted to apply to alternative configuration feeders, such as those with four spring banks, for use as a design tool;

ii) Whilst an increase in the conveying velocity of components is desirable, it is essential that designers can predict whether changes in either parameters or operating conditions might result in unstable motion. This could manifest itself by excessively noisy feeding; an increase in power consumption; a drop in feeding velocity rather than an increase; the occurrence of dead spots; or fouling or jamming of tooling which may result in components not being successfully

oriented. None of the work undertaken previously attempts to predict the onset of instability. This would require the development of a full model which included both the feeder structure and the components, and the investigation of the possibility that different types of tooling might precipitate unstable behaviour.

Further consideration would need to be given to any possible non-linear behaviour, such as that of a loaded feeder given by Sakaguchi(10), and the work would also require the development of a more accurate model of the feeder structure as outlined in iii). The unstable motion of the components would probably best be treated by using a probabilistic approach;

iii) Results obtained from investigation of the variation of the spring angle given in Chapter 8 indicate that the simple assumption of a viscous damping model is not adequate in the region of resonance. Since bowl feeders are normally tuned to operate close to their resonant frequency, it is important that, prior to undertaking any further investigations which

will need to use a model of the feeder structure, the damping in this region is modelled accurately. Possible approaches are the use of a higher order damping model, the use of alternative methods for the estimation of damping, such as the work on multi degree-of-freedom systems by Ewins and Gleeson(37); and the use of modern system identification techniques such as the family of least-squares, frequency domain filters developed by Mottershead(38);

iv) For optimum performance of the feeder it is essential that the driving frequency is held close to the resonant frequency corresponding to the axial mode of vibration. It is often difficult to tune feeders to an exact resonant frequency during manufacture, and changes in operating parameters such as bowl loading can give rise to shifts in the natural frequencies. An alternative approach to this problem is the development of an active control system which monitors the output of the bowl and maintains this at the required level by changing the frequency of the force input.

12. CONCLUSION

The outcome of this numerical and experimental investigation of vibratory bowl feeders can be summarised as follows:

i) A numerical model of the dynamic characteristics of the bowl was developed, idealising the feeder as a lumped parameter eight degree-of-freedom system. This enabled the natural frequencies and mode shapes of the feeder to be predicted;

ii) The model was verified by testing the bowl feeder using experimental modal analysis. This showed good agreement with the numerical model at lower frequencies close to the operating range. The differences between predicted and measured values at higher frequencies could be accounted for by the flexural vibration of the bowl itself, which calculations indicate is likely to occur in this region;

iii) A numerical model of the forced response of a bowl feeder when driven by a harmonic excitation was developed using a spreadsheet package and verified experimentally;

iv) Geometric parameters of the bowl and springs were varied using the 'table' facility of the spreadsheet package, predicting both the vertical acceleration of the bowl and the first natural frequency. Earlier work by Redford and Boothroyd(2) had shown that there was a linear relationship between the vertical bowl acceleration and the mean conveying velocity of components;

v) In order to verify the predictions of the spreadsheet model in response to changes in geometric parameters, experimental work was undertaken varying the spring angle for three driving frequencies of 45, 50 and 55 Hz. These showed good agreement with the predicted results for the larger spring angles, but not at the smaller angles of 55° and 60°. This was thought to be due to the difficulties in modelling the damping of the structure accurately. The effects of this are more pronounced in close proximity to a resonant frequency;

vi) A customised design tool was developed using the spreadsheet package for the prediction of the forced response of the feeder. This allowed input

parameters to be entered using a custom dialog-box, the forced response analysis to be run, and the bowl acceleration and first natural frequency displayed in another dialog-box without any detailed knowledge of the spreadsheet or the model. This user-friendly package enables design engineers to investigate the behaviour of different arrangements of feeder structures before the prototype stage of development;

vii) An investigation of the causes of dead-spots was undertaken, to attempt to verify predictions of the dynamic behaviour of the bowl feeder. These had been made from the further understanding gained from the numerical modelling phase of the project. Dead-spots occur where the component of the acceleration of the bowl normal to the track drops to a value below the normal component of gravitational acceleration. This was shown to be due to the asymmetrical arrangement of the springs and electromagnetic coil relative to each other. Rotating the coil relative to the springs also rotated the position of the dead-spot;

viii) Solutions proposed to the problem of dead-spots were the use of four spring banks instead of three, and the specification of an annular shaped pole piece

for the electromagnetic coil; and

ix) Further work proposed is the adaption of the model to a four spring-bank feeder, an investigation of the combination of parameters and operating conditions which cause the unstable motion of components, the development of a more accurate model of the bowl feeder structure, with particular emphasis on its damping characteristics; and the development of a system of active control, keeping the driving frequency close to the resonant frequency.

Publications and Proceedings

1. Morrey, D. and Mottershead, J.E., 'Modelling of vibratory bowl feeders', Proc.I.Mech.E., 1986, Vol.200, No.C6, pp.431-437.

2. Morrey, D. and Mottershead, J.E., 'An Applications Exercise using Modal Analysis of a Vibratory Bowl Feeder', Fifth British Conference on the Teaching of Vibration and Noise, Sheffield City Polytechnic, 1985, pp.95-100.

3. Morrey, D. and Mottershead, J.E., 'Vibratory Bowl Feeder Design Using Numerical Modelling Techniques', Modern Practice in Stress and Vibration Analysis (Conference Proceedings), Stress Analysis Group IOP, Liverpool University, April 1989, pp.211-217.

References

1. Boothroyd, G., Poli, C. and Murch, L.E., 'Automatic Assembly', Marcel Dekker, 1982.

2. Redford, A.H. and Boothroyd, G., 'Vibratory Feeding', Proc.I.Mech.E., 1967-68, Vol.182, Pt.1, No.6, pp.135-146.

3. Winkler, G., 'Analysing the Hopping Conveyor', Int.J.Mech.Sci., 1979, Vol.21, pp.651-658.

4. Ng, K.L., Ang, L.A. and Chng, S.C., 'A computer model for vibrating conveyors', Proc.I.Mech.E., 1986, Vol.200, No.B2, pp.123-130.

5. Taniguchi, O., Sakata, M., Suzuki, Y. and Osanai, Y., 'Studies on Vibratory Feeder', Bulletin of JSME, 1963, Vol.6, No.21, pp.37-43.

6. Okabe, S. and Yokoyama, Y., 'Study on Vibratory Feeders: Calculation of Natural Frequency of Bowl-Type Vibratory Feeders', Journal of Mechanical Design, January 1981, Vol.103, pp.249-256.

7. Wiendahl, H.P. and Ahrens, H., 'Design of Vibratory Feeders', Assembly Automation, November 1984, pp.198-203.

8. Burgess, W.C., 'Third generation of resonant vibratory bowl feeders increase productivity', Society of Manufacturing Engineers Technical Paper, Assemblex Conference, Rosemont, Ill., October 1975, AD75-764.

9. Okabe, S., Kamiya, Y., Tsujikado, K. and Yokoyama, Y., 'Vibratory Feeding by Nonsinusoidal Vibration - Optimum Wave Form', Transactions of the ASME, April 1985, Vol.107, pp.188-195.

10. Sakaguchi, K., 'Vibration Characteristics of Loaded Vibratory Feeder', Bulletin of the JSME, September 1977, Vol.20, No.147, pp.1101-1106.

11. Paz, M. and Morris, J.M., 'The Use of Vibration for Material Handling', Journal of Engineering for Industry, Transactions of the ASME, August 1974, pp.735-740.

12. Parameswaran, M.A. and Ganapathy, S., 'Vibratory COnveying-Analysis and Design: A Review', Mechanism and Machine Theory, 1979, Vol.14, pp.89-97.

13. Ahrens, H., 'Fundamental investigations into parts feeding with vibratory bowl feeders and criteria for equipment design' Fortschr.-Ber.VDI-Z, Series 13, No.23, Dusseldorf: VDI-Verlag, 1983.

14. Sakaguchi, K. and Taniguchi, O., 'Studies on Vibratory Feeder (2nd Report)', Bulletin of the JSME, 1970, Vol.13, No.61, pp.881-887.

15. Roark, R.J. and Young, W.C., 'Formulas for Stress and Strain', McGraw-Hill, 1976 (5th Edition).

16. Numerical Algorithms Group, NAg Library Manual (Mark V), 1984.

17. UKAEA Culham Laboratory, GHOST-80 manual, March 1985.

18. Kennedy, C.C. and Pancu, C.D.P., 'Use of Vectors in Vibration Measurement and Analysis', J. Aero. Sci., 1947, 14(11).

19. Serridge, M. and Licht, T.R., 'Piezoelectric Accelerometers and Vibration Preamplifiers: Theory and Application Handbook', Brüel and Kjær, October 1986.

20. Entek Scientific Corporation, EMODAL V2.1 manual, 1983.

21. Ewins, D.J., 'Modal Testing: Theory and Practice', Research Studies Press Ltd., 1984.

22. Broch, J.T., 'Mechanical Vibration and Shock Measurements', Brüel and Kjær, October 1980.

23. Brüel and Kjær, 'Measuring Vibration', September 1982.

24. Brüel and Kjær, 'Structural Testing: Part 1 - Mechanical Mobility Measurements', April 1988.

25. Cooley, J.W. and Tukey, J.W., 'An algorithm for the Machine Calculation of Complex Fourier Series', Maths of Comput., 1965, 19(90), pp.297-301.

26. Lynn, P.A., 'An Introduction to the Analysis and Processing of Signals', Macmillan, 1986 (2nd Edition).

27. Open University, 'Electronic Signal Processing: Block I - IV', T326, Open University Press, 1984.

28. Newland, D.E., 'An Introduction to Random Vibrations and Spectral Analysis', Longman, 1984 (2nd Edition).

29. Microsoft Corporation, 'Microsoft Excel User's Guide', 1986.

30. Craig, R.R., 'Structural Dynamics: An Introduction to Computer Methods', Wiley.

31. Microsoft Corporation, 'Microsoft Excel: Arrays, Functions and Macros', 1987.

32. Thomson, W.T., 'Theory of Vibration with Applications', George Allen and Unwin, 1981 (2nd Edition).

33. Blevins, R.D., 'Formulas for Natural Frequency and Mode Shape', Van Nostrand Reinhold, 1979.

34. Kron, G., 'Diakoptics', MacDonald, 1963.

35. Wilkinson, J.H. and Reinsch, C., 'Handbook for Automatic Computation. Volume II, Linear Algebra', Springer-Verlag, 1971, pp.227-240.

36. Richards, T.H., 'Energy Methods in Stress Analysis', Ellis Horwood, 1977.

37. Ewins, D.J. and Gleeson, P.T., 'A method for the modal identification of lightly damped structures', Journal of Sound and Vibration, 1982, 84(1), pp.57-79.

38. Mottershead, J.E., 'A unified theory of recursive, frequency domain filters with application to system identification in structural dynamics', Trans. ASME, J. Vibrations, Acoustics, Stress and Reliability in Design, 1988, 110, 3, pp.360-365.

39. Tse, F.S., Morse, I.E. and Hinkle, R.T., 'Mechanical Vibrations: Theory and Applications', Allyn and Bacon, 1978.

APPENDICES

Appendix 1 - Constraint equations

a) Connection points on the bowl

Point a

(axial) $\Delta_{z1} + r_1\theta_{x1} = \Delta_v\cos\gamma + \Delta_w\sin\gamma$

(tangential) $r_1\theta_{z1} = (\Delta_v\sin\gamma - \Delta_w\cos\gamma)\cos\phi_1 - \Delta_u\sin\phi_1$

(radial) $0 = -\Delta_u\cos\phi_1 + (-\Delta_v\sin\gamma + \Delta_w\cos\gamma)\sin\phi_1$

(axial) $\theta_{z1} = \theta_v\cos\gamma + \theta_w\sin\gamma$

(tangential) $-\theta_{x1} = (\theta_v\sin\gamma - \theta_w\cos\gamma)\cos\phi_1 - \theta_u\sin\phi_1$

(radial) $-\theta_{y1} = -\theta_u\cos\phi_1 + (-\theta_v\sin\gamma + \theta_w\cos\gamma)\sin\phi_1$

Point b

(axial) $\Delta_{z1} - \frac{r_1}{2}\theta_{x1} - \frac{\sqrt{3}}{2}r_1\theta_{y1} = \Delta_v\cos\gamma + \Delta_w\sin\gamma$

(tangential) $r_1\theta_{z1} = (\Delta_v\sin\gamma - \Delta_w\cos\gamma)\cos\phi_1 - \Delta_u\sin\phi_1$

(radial) $0 = -\Delta_u\cos\phi_1 + (-\Delta_v\sin\gamma + \Delta_w\cos\gamma)\sin\phi_1$

(axial) $\theta_{z1} = \theta_v\cos\gamma + \theta_w\sin\gamma$

(tangential) $\frac{1}{2}\theta_{x1} + \frac{\sqrt{3}}{2}\theta_{y1} = (\theta_v\sin\gamma - \theta_w\cos\gamma)\cos\phi_1 - \theta_u\sin\phi_1$

(radial) $\frac{\sqrt{3}}{2}\theta_{x1} + \frac{1}{2}\theta_{y1} = -\theta_u\cos\phi_1 + (-\theta_v\sin\gamma + \theta_w\cos\gamma)\sin\phi_1$

Point c

$$(\text{axial})\Delta_{z1} - \frac{r_1}{2}\theta_{x1} + \frac{\sqrt{3}}{2}r_1\theta_{z1} = \Delta_v\cos\gamma + \Delta_w\sin\gamma$$

$$(\text{tangential}) \qquad r_1\theta_{z1} = (\Delta_v\sin\gamma - \Delta_w\cos\gamma)\cos\phi_1 - \Delta_u\sin\phi_1$$

$$(\text{radial}) \qquad 0 = -\Delta_u\cos\phi_1 + (-\Delta_v\sin\gamma + \Delta_w\cos\gamma)\sin\phi_1$$

$$(\text{axial}) \qquad \theta_{z1} = \theta_v\cos\gamma + \theta_w\sin\gamma$$

$$(\text{tangential}) \quad \frac{1}{2}\theta_{x1} - \frac{\sqrt{3}}{2}\theta_{y1} = (\theta_v\sin\gamma - \theta_w\cos\gamma)\cos\phi_1 - \theta_u\sin\phi_1$$

$$(\text{radial}) \quad \frac{\sqrt{3}}{2}\theta_{x1} + \frac{1}{2}\theta_{y1} = -\theta_u\cos\phi_1 + (-\theta_v\sin\gamma + \theta_w\cos\gamma)\sin\phi_1$$

b) Connection points on the base

Point d

$$(\text{axial})\Delta_{z2} + \{r_2\cos(\phi_1+\phi_2)\}\theta_{x2} + \{r_2\sin(\phi_1+\phi_2)\}\theta_{y2} = \Delta_v\cos\gamma + \Delta_w\sin\gamma$$

$$(\text{tangential}) \quad r_2\theta_{z2} = (\Delta_v\sin\gamma - \Delta_w\cos\gamma)\cos\phi_2 - \Delta_u\sin\phi_2$$

$$(\text{radial}) \qquad 0 = -\Delta_u\cos\phi_2 + (-\Delta_v\sin\gamma + \Delta_w\cos\gamma)\sin\phi_2$$

$$(\text{axial}) \qquad \theta_{z2} = \theta_v\cos\gamma + \theta_w\sin\gamma$$

$$(\text{tangential}) \; -\theta_{x2}\cos(\phi_1+\phi_2) - \theta_{y2}\sin(\phi_1+\phi_2) = (\theta_v\sin\gamma - \theta_w\cos\gamma)\cos\phi_2 - \theta_u\sin\phi_2$$

$$(\text{radial}) \; \theta_{x2}\sin(\phi_1+\phi_2) - \theta_{y2}\cos(\phi_1+\phi_2) = -\theta_u\cos\phi_2 + (-\theta_v\sin\gamma + \theta_w\cos\gamma)\sin\phi_2$$

Point e

$$(\text{axial})\Delta_{z2} - \{r_2\sin(\frac{\pi}{6} - \phi_1 - \phi_2)\}\theta_{x2} + \{r_2\cos(\frac{\pi}{6} - \phi_1 - \phi_2)\}\theta_{y2}$$

$$= \Delta_v\cos\gamma + \Delta_w\sin\gamma$$

$$(\text{tangential}) \quad r_2\theta_{z2} = (\Delta_v\sin\gamma - \Delta_w\cos\gamma)\cos\phi_2 - \Delta_u\sin\phi_2$$

$$(\text{radial}) \quad 0 = -\Delta_u\cos\phi_2 + (-\Delta_v\sin\gamma + \Delta_w\cos\gamma)\sin\phi_2$$

$$(\text{axial}) \quad \theta_{z2} = \theta_v\cos\gamma + \theta_w\sin\gamma$$

$$(\text{tangential}) \quad \theta_{x2}\sin(\frac{\pi}{6} - \phi_1 - \phi_2) + \theta_{y2}\cos(\frac{\pi}{6} - \phi_1 - \phi_2)$$

$$= (\theta_v\sin\gamma - \theta_w\cos\gamma)\cos\phi_2 - \theta_u\sin\phi_2$$

$$(\text{radial}) \quad -\theta_{x2}\cos(\frac{\pi}{6} - \phi_1 - \phi_2) + \theta_{y2}\sin(\frac{\pi}{6} - \phi_1 - \phi_2)$$

$$= -\theta_u\cos\phi_2 + (-\theta_v\sin\gamma + \theta_w\cos\gamma)\sin\phi_2$$

Point f

$$(\text{axial})\Delta_{z2} - \{r_2\sin(\frac{\pi}{6} + \phi_1 + \phi_2)\}\theta_{x2} + \{r_2\cos(\frac{\pi}{6} + \phi_1 + \phi_2)\}\theta_{y2}$$

$$= \Delta_v\cos\gamma + \Delta_w\sin\gamma$$

$$(\text{tangential}) \quad r_2\theta_{z2} = (\Delta_v\sin\gamma - \Delta_w\cos\gamma)\cos\phi_2 - \Delta_u\sin\phi_2$$

$$(\text{radial}) \quad 0 = -\Delta_u\cos\phi_2 + (-\Delta_v\sin\gamma + \Delta_w\cos\gamma)\sin\phi_2$$

$$(\text{axial}) \quad \theta_{z2} = \theta_v\cos\gamma + \theta_w\sin\gamma$$

$$(\text{tangential}) \quad \theta_{x2}\sin(\frac{\pi}{6} + \phi_1 + \phi_2) - \theta_{y2}\cos(\frac{\pi}{6} + \phi_1 + \phi_2)$$

$$= (\theta_v\sin\gamma - \theta_w\cos\gamma)\cos\phi_2 - \theta_u\sin\phi_2$$

$$(\text{radial}) \quad \theta_{x2}\cos(\frac{\pi}{6} + \phi_1 + \phi_2) + \theta_{y2}\sin(\frac{\pi}{6} + \phi_1 + \phi_2)$$

$$= -\theta_u\cos\phi_2 + (-\theta_v\sin\gamma + \theta_w\cos\gamma)\sin\phi_2$$

Appendix 2 - Coding for the solution of the eigenproblem based on the eight degree-of-freedom numerical model

```
C     * * * Vibration analysis of a vibratory bowl feeder * * * *


C     * * * Vibration analysis of a vibratory bowl feeder * * * *
C
C     * * * * * * * * * by D.Morrey * * * * * * * * * * * * * * *
C
C     This FORTRAN IV coded program calculates the natural
C
C     frequencies and mode shapes of 3-spring bank vibratory bowl
C
C     feeders. The necessary data is entered via the datafiles DIN
C
C     and MIN2. DIN contains : 1st line: Young's Modulus of the springs
C
C     (E), Shear Modulus of the springs (G),
C
C     2nd line: spring length  (L), spring width  (W), spring
C
C     thickness (T), spring spacing (TS), angle between spring
C
C     radius and perpendicular radius for the bowl (PH(1)),
C
C     spring angle (GA), perpendicular radius for the bowl (RA(1)).
C
C     MIN2 contains : 1st line : Bowl mass (M(1)), Base mass (M(2)),
C
C     2nd line: Bowl radius (R(1)), Base radius (R(2)), Bowl height (H(1)),
C
C     Base height (H(2)), Thicknesses of the bowl both vertically (T) and
C
C     horizontally (W),
C
C     3rd line: Perpendicular spring radius (RA), Bowl fixing plate
C
C     thickness (TH).
C
C     The program calculates mass and stiffness matrices for the feeder,
C
C     and then evaluates the eigenvalues and eigenvectors using NAg
C
C     Library subroutines.
C
C     The file unit numbers of the datafiles are:
C
C                              DIN    1
C
C                             OPUT    2
C
C                             MIN2    4
C
C                            DEIGN3   5
C
C                            DEIGN4   6
C
C      OPUT, DEIGN3, DEIGN4 are output files.
C     ******************************************************************
C
C     * * * * MAIN PROGRAM FOR VIBRATIONAL ANALYSIS 22.10.84 * * * *
C
C    ******************************************************************
```

```
C     * * * Vibration analysis of a vibratory bowl feeder * * * *


      REAL*8 ST(8,8),M(8,8)
      INTEGER I,J,DIN,OPUT,MIN2,DEIGN3,DEIGN4,INPT
      CALL STIFF(ST)
      CALL MASS(M)
      CALL EIGN(ST,M)
      STOP
      END
C     ***********************************************************************
C
C     SUBROUTINE FOR FORMULATION OF STIFFNESS MATRIX
C
C     ***********************************************************************
      SUBROUTINE STIFF(ST)
      REAL*8 E,IV,IU,IP,S(36,36),G,B(4,6),L,W,T,Q(6),H(6),PH(2),A
     *,GA,RA(2),C(36,8),Y(8,36),X(36,8),ST(8,8),BT(4,4)
      INTEGER I,J,N,IFAIL,K,R(9),V,CT
      DATA S,B,C,X/1296*0.0D0,24*0.0D0,288
     **0.0D0,288*0.0D0/
C     ***********************************************************************
C
C     READS IN DATA FROM DIN DATAFILE
C
C     ***********************************************************************
      READ (5,100) E,G
100   FORMAT (2E12.3)
      READ (5,101) L,W,T,TS,PH(1),GA,RA(1)
101   FORMAT (7F9.6)
C     ***********************************************************************
C
C     CALCULATES SECOND MOMENTS OF AREA IU & IV AND TORSIONAL CONSTANT
C     IP FOR A SPRING BANK COMPRISING THREE SPRINGS
C
C     ***********************************************************************
      IU=((3*W*T**3)/12)+(2*W*T*(T+TS)**2)
      IV=(3*T*W**3)/12
      BR=W/2
      AT=(3*T)/2
      IP=BR*AT**3*((16/3)-(3.36*AT/BR)*(1-(AT**4/(12*BR**4))))
C     ***********************************************************************
C
C     CALCULATES PERPENDICULAR RADIUS RA(2) AND ANGLE BETWEEN THIS AND
C     THE SPRING RADIUS PH(2) FOR THE BASE.
C
C     ***********************************************************************
      PH(2)=DATAN(((L*DCOS(GA))-(RA(1)*DSIN(PH(1))))/(RA(1)*DCOS(PH(1)))
     *)+PH(1)
      RA(2)=RA(1)*DCOS(PH(1))/COS(PH(2)-PH(1))
      WRITE (6,107) E,G
107   FORMAT (7HE/N/M*M,7X,7HG/N/M*M/(2E12.3))
      WRITE (6,108) L,W,T,(PH(I),I=1,2),GA,(RA(I),I=1,2)
108   FORMAT (3HL/M,6X,3HW/M,6X,3HT/M,6X,6HPH/RAD,12X,6HGA/RAD,3X,
     *4HRA/M/(8F9.6))
      WRITE (9,112) RA(1),GA,PH(1),L
      WRITE (10,112) RA(1),GA,PH(1),L
112   FORMAT (4F9.6)
      WRITE (6,996) IV,IU,IP
996   FORMAT (5HIV/M4,10X,5HIU/M4,10X,5HIP/M4/(3E12.3))
C     ***********************************************************************
```

```
C     * * * Vibration analysis of a vibratory bowl feeder * * * *


C
C     CALCULATES ELEMENTS OF BASIC 12*12 STIFFNESS MATRIX FOR ONE SPRING
C     BANK
C
C     ************************************************************************
      S(1,1)=12.0D0/(L**3)
      S(1,2)=6.0D0/(L*L)
      S(1,3)=-S(1,1)
      S(1,4)=S(1,2)
      S(2,2)=4.0D0/L
      S(2,3)=-6.0D0/(L*L)
      S(2,4)=2.0D0/L
      S(3,3)=S(1,1)
      S(3,4)=-6.0D0/(L*L)
      S(4,4)=4.0D0/L
      DO 120 I=2,4
      KL=0
      KL=I-1
      DO 121 J=1,KL
121   S(I,J)=S(J,I)
120   CONTINUE
      S(5,5)=S(1,1)
      S(5,6)=-S(1,2)
      S(5,7)=S(1,3)
      S(5,8)=-S(1,4)
      S(6,6)=S(2,2)
      S(6,7)=-S(2,3)
      S(6,8)=S(2,4)
      S(7,7)=S(3,3)
      S(7,8)=-S(3,4)
      S(8,8)=S(4,4)
      DO 124 I=6,8
      KM=0
      KM=I-1
      DO 125 J=5,KM
125   S(I,J)=S(J,I)
124   CONTINUE
      DO 672 I=1,4
      DO 673 J=1,4
673   S(I,J)=S(I,J)*E*IV
672   CONTINUE
      DO 674 I=5,8
      DO 675 J=5,8
675   S(I,J)=S(I,J)*E*IU
674   CONTINUE
      A=W*T
      DO 581 I=9,10
      DO 582 J=9,10
      S(I,J)=(E*A)/L
      IF ((I-J).EQ.0) GO TO 582
      S(I,J)=-S(I,J)
582   CONTINUE
581   CONTINUE
      DO 676 I=11,12
      DO 677 J=11,12
      S(I,J)=(G*IP)/L
      IF ((I-J).EQ.0) GO TO 677
      S(I,J)=-S(I,J)
```

```
677   CONTINUE
676   CONTINUE
      DO 740 I=1,12
      DO 741 J=1,12
741   S(I+12,J+12)=S(I,J)
740   CONTINUE
C     ***************************************************************
C
C     CALCULATES THE OTHER ELEMENTS OF THE 36*36 STIFFNESS MATRIX
C
C     ***************************************************************
      DO 742 I=13,24
      DO 743 J=13,24
743   S(I+12,J+12)=S(I,J)
742   CONTINUE
      WRITE (6,114) ((S(I,J),J=1,36),I=1,36)
114   FORMAT (18HSTIFFNESS MATRIX K/(12E8.1/12E8.1/12E8.1/))
C     ***************************************************************
C
C     FORMULATION OF CONNECTION MATRIX USING SUBROUTINE CNECT3
C
C    ***************************************************************
      CALL CNECT3(C,GA,PH,RA)
      WRITE (6,116) ((C(I,J),J=1,8),I=1,36)
116   FORMAT (17HCONNECTION MATRIX/(8F9.4))
C     ***************************************************************
C
C     TRANSPOSE OF CONNECTION MATRIX
C
C     ***************************************************************
      DO 681 I=1,8
      DO 682 J=1,36
682   Y(I,J)=C(J,I)
681   CONTINUE
      WRITE (6,180) ((Y(I,J),J=1,36),I=1,8)
180   FORMAT (1HY/(12E8.1/12E8.1/12E8.1/))
C    ***************************************************************
C
C     MULTIPLICATION OF STIFFNESS MATRIX AND CONNECTION MATRIX
C
C    ***************************************************************
      CALL MULT(X,S,C,36,8,36)
      WRITE (6,150) ((X(I,J),J=1,8),I=1,36)
150   FORMAT (16HPRODUCT OF S & C/(8E12.3))
C     ***************************************************************
C
C     MULTIPLICATION OF CTRANSPOSE AND X
C
C     ***************************************************************
      CALL MULT(ST,Y,X,8,8,36)
      WRITE (6,118) ((ST(I,J),J=1,8),I=1,8)
118   FORMAT (16HSTIFFNESS MATRIX/(8E12.3))
      RETURN
      END
C     ***************************************************************
C
C     SUBROUTINE TO CALCULATE CONNECTION MATRIX MK.2 22.10.84
C     USING MATRIX INVERSION
```

```
C     * * * Vibration analysis of a vibratory bowl feeder * * * *


C
C     ************************************************************
      SUBROUTINE CNECT3(C,G,P,R)
      REAL*8 C(36,8),G,P(2),R(2),MG(36,8),ML(36,36),AA(36,36)
     *,WKSPCE(100),BB(36,8),X02AAF,PI
      DATA MG,ML/288*0.0D0,1296*0.0D0/
      PI=4.0D0*DATAN(1.0D0)
      MG(1,1)=1.0D0
      MG(1,2)=R(1)
      MG(2,4)=R(1)
      MG(4,4)=1.0D0
      MG(5,2)=-1.0D0
      MG(6,3)=-1.0D0
      MG(7,1)=1.0D0
      MG(7,2)=-R(1)/2.0D0
      MG(7,3)=-R(1)*DSQRT(3.0D0)/2.0D0
      MG(8,4)=R(1)
      MG(10,4)=1.0D0
      MG(11,2)=1.0D0/2.0D0
      MG(11,3)=DSQRT(3.0D0)/2.0D0
      MG(12,2)=-DSQRT(3.0D0)/2.0D0
      MG(12,3)=1.0D0/2.0D0
      MG(13,1)=1.0D0
      MG(13,2)=-R(1)/2.0D0
      MG(13,3)=R(1)*DSQRT(3.0D0)/2.0D0
      MG(14,4)=R(1)
      MG(16,4)=1.0D0
      MG(17,2)=1.0D0/2.0D0
      MG(17,3)=-DSQRT(3.0D0)/2.0D0
      MG(18,2)=DSQRT(3.0D0)/2.0D0
      MG(18,3)=1.0D0/2.0D0
      MG(19,5)=1.0D0
      MG(19,6)=R(2)*DCOS(P(2))
      MG(19,7)=R(2)*DSIN(P(2))
      MG(20,8)=R(2)
      MG(22,8)=1.0D0
      MG(23,6)=-DCOS(P(2))
      MG(23,7)=-DSIN(P(2))
      MG(24,6)=DSIN(P(2))
      MG(24,7)=-DCOS(P(2))
      MG(25,5)=1.0D0
      MG(25,6)=-R(2)*DSIN((PI/6.0D0)-P(2))
      MG(25,7)=-R(2)*DCOS((PI/6.0D0)-P(2))
      MG(26,8)=R(2)
      MG(28,8)=1.0D0
      MG(29,6)=DSIN((PI/6.0D0)-P(2))
      MG(29,7)=DCOS((PI/6.0D0)-P(2))
      MG(30,6)=-DCOS((PI/6.0D0)-P(2))
      MG(30,7)=DSIN((PI/6.0D0)-P(2))
      MG(31,5)=1.0D0
      MG(31,6)=-R(2)*DSIN((PI/6.0D0)+P(2))
      MG(31,7)=R(2)*DCOS((PI/6.0D0)+P(2))
      MG(32,8)=R(2)
      MG(34,8)=1.0D0
      MG(35,6)=DSIN((PI/6.0D0)+P(2))
      MG(35,7)=-DCOS((PI/6.0D0)+P(2))
      MG(36,6)=DCOS((PI/6.0D0)+P(2))
      MG(36,7)=DSIN((PI/6.0D0)+P(2))
```

```
C     * * * Vibration analysis of a vibratory bowl feeder * * * *


      WRITE (6,559) ((MG(I,J),J=1,8),I=1,36)
559   FORMAT (2HMG/(8E8.1))
      ML(1,5)=DCOS(G)
      ML(1,9)=DSIN(G)
      ML(2,5)=DSIN(G)*DCOS(P(1))
      ML(2,9)=-DCOS(G)*DCOS(P(1))
      ML(2,1)=-DSIN(P(1))
      ML(3,1)=-DCOS(P(1))
      ML(3,5)=-DSIN(G)*DSIN(P(1))
      ML(3,9)=DCOS(G)*DSIN(P(1))
      ML(4,2)=DCOS(G)
      ML(4,11)=DSIN(G)
      ML(5,2)=DSIN(G)*DCOS(P(1))
      ML(5,11)=-DCOS(G)*DCOS(P(1))
      ML(5,6)=-DSIN(P(1))
      ML(6,6)=-DCOS(P(1))
      ML(6,2)=-DSIN(G)*DSIN(P(1))
      ML(6,11)=DCOS(G)*DSIN(P(1))
      ML(7,17)=DCOS(G)
      ML(7,21)=DSIN(G)
      ML(8,17)=DSIN(G)*DCOS(P(1))
      ML(8,21)=-DCOS(G)*DCOS(P(1))
      ML(8,13)=-DSIN(P(1))
      ML(9,13)=-DCOS(P(1))
      ML(9,17)=-DSIN(G)*DSIN(P(1))
      ML(9,21)=DCOS(G)*DSIN(P(1))
      ML(10,14)=DCOS(G)
      ML(10,23)=DSIN(G)
      ML(11,14)=DSIN(G)*DCOS(P(1))
      ML(11,23)=-DCOS(G)*DCOS(P(1))
      ML(11,18)=-DSIN(P(1))
      ML(12,18)=-DCOS(P(1))
      ML(12,14)=-DSIN(G)*DSIN(P(1))
      ML(12,23)=DCOS(G)*DSIN(P(1))
      ML(13,29)=DCOS(G)
      ML(13,33)=DSIN(G)
      ML(14,29)=DSIN(G)*DCOS(P(1))
      ML(14,33)=-DCOS(G)*DCOS(P(1))
      ML(14,25)=-DSIN(P(1))
      ML(15,25)=-DCOS(P(1))
      ML(15,29)=-DSIN(G)*DSIN(P(1))
      ML(15,33)=DCOS(G)*DSIN(P(1))
      ML(16,26)=DCOS(G)
      ML(16,35)=DSIN(G)
      ML(17,26)=DSIN(G)*DCOS(P(1))
      ML(17,35)=-DCOS(G)*DCOS(P(1))
      ML(17,30)=-DSIN(P(1))
      ML(18,30)=-DCOS(P(1))
      ML(18,26)=-DSIN(G)*DSIN(P(1))
      ML(18,35)=DCOS(G)*DSIN(P(1))
      ML(19,7)=DCOS(G)
      ML(19,10)=DSIN(G)
      ML(20,7)=DSIN(G)*DCOS(P(2)-P(1))
      ML(20,10)=-DCOS(G)*DCOS(P(2)-P(1))
      ML(20,3)=-DSIN(P(2)-P(1))
      ML(21,3)=-DCOS(P(2)-P(1))
      ML(21,7)=-DSIN(G)*DSIN(P(2)-P(1))
      ML(21,10)=DCOS(G)*DSIN(P(2)-P(1))
```

```
      ML(22,4)=DCOS(G)
      ML(22,12)=DSIN(G)
      ML(23,4)=DSIN(G)*DCOS(P(2)-P(1))
      ML(23,12)=-DCOS(G)*DCOS(P(2)-P(1))
      ML(23,8)=-DSIN(P(2)-P(1))
      ML(24,8)=-DCOS(P(2)-P(1))
      ML(24,4)=-DSIN(G)*DSIN(P(2)-P(1))
      ML(24,12)=DCOS(G)*DSIN(P(2)-P(1))
      ML(25,19)=DCOS(G)
      ML(25,22)=DSIN(G)
      ML(26,19)=DSIN(G)*DCOS(P(2)-P(1))
      ML(26,22)=-DCOS(G)*DCOS(P(2)-P(1))
      ML(26,15)=-DSIN(P(2)-P(1))
      ML(27,15)=-DCOS(P(2)-P(1))
      ML(27,19)=-DSIN(G)*DSIN(P(2)-P(1))
      ML(27,22)=DCOS(G)*DSIN(P(2)-P(1))
      ML(28,16)=DCOS(G)
      ML(28,24)=DSIN(G)
      ML(29,16)=DSIN(G)*DCOS(P(2)-P(1))
      ML(29,24)=-DCOS(G)*DCOS(P(2)-P(1))
      ML(29,20)=-DSIN(P(2)-P(1))
      ML(30,20)=-DCOS(P(2)-P(1))
      ML(30,16)=-DSIN(G)*DSIN(P(2)-P(1))
      ML(30,24)=DCOS(G)*DSIN(P(2)-P(1))
      ML(31,31)=DCOS(G)
      ML(31,34)=DSIN(G)
      ML(32,31)=DSIN(G)*DCOS(P(2)-P(1))
      ML(32,34)=-DCOS(G)*DCOS(P(2)-P(1))
      ML(32,27)=-DSIN(P(2)-P(1))
      ML(33,27)=-DCOS(P(2)-P(1))
      ML(33,31)=-DSIN(G)*DSIN(P(2)-P(1))
      ML(33,34)=DCOS(G)*DSIN(P(2)-P(1))
      ML(34,28)=DCOS(G)
      ML(34,36)=DSIN(G)
      ML(35,28)=DSIN(G)*DCOS(P(2)-P(1))
      ML(35,36)=-DCOS(G)*DCOS(P(2)-P(1))
      ML(35,32)=-DSIN(P(2)-P(1))
      ML(36,32)=-DCOS(P(2)-P(1))
      ML(36,28)=-DSIN(G)*DSIN(P(2)-P(1))
      ML(36,36)=DCOS(G)*DSIN(P(2)-P(1))
      WRITE (6,558) ((ML(I,J),J=1,36),I=1,36)
558   FORMAT (2HML/(12E8.1/12E8.1/12E8.1))
      IFAIL=0
      CALL F04AEF (ML,36,MG,36,36,8,C,36,WKSPCE,AA,36,BB,
     *36,IFAIL)
      IF (IFAIL.EQ.0) GO TO 600
      WRITE (6,601) IFAIL
601   FORMAT (22HERROR IN F04AEF IFAIL=,I2)
600   RETURN
      END
C     ************************************************************
C
C     SUBROUTINE FOR MULTIPLICATION OF MATRICES
C
C     This subroutine multiplies B(N*M) and C(M*P) and gives a
C     product A(N*P).
C
C     ************************************************************
```

```
C     * * * Vibration analysis of a vibratory bowl feeder * * * *


      SUBROUTINE MULT(A,B,C,N,P,M)
      INTEGER N,P,M,I,J,K
      REAL*8 A,B,C
      DIMENSION A(N,P),B(N,M),C(M,P)
      DO 663 I=1,N
      DO 662 K=1,P
      DO 661 J=1,M
661   A(I,K)=A(I,K)+(B(I,J)*C(J,K))
662   CONTINUE
663   CONTINUE
      RETURN
      END
C     ************************************************************
C
C     SUBROUTINE FOR FORMULATION OF MASS MATRIX
C
C     ************************************************************
      SUBROUTINE MASS(S)
      REAL*8 R(2),T,M(2),P(2),H(2),W,S(8,8),MIX,PI
      PI=4.0D0*DATAN(1.0D0)
C     ************************************************************
C
C     READS IN DATA FROM MIN2 DATAFILE
C
C     ************************************************************
      READ (8,101) (M(I),I=1,2)
101   FORMAT (2F9.4)
      READ (8,102) (R(I),I=1,2),(H(I),I=1,2),T,W
102   FORMAT (6F9.4)
      READ (8,105) RA,TH
105   FORMAT (3F9.4)
C     ************************************************************
C
C     CALCULATES THE DENSITIES OF THE BOWL P(1) AND THE BASE P(2)
C
C     ************************************************************
      P(1)=M(1)/((PI*R(1)*R(1)*T)+(2*PI*W*R(1)*H(1))+(PI*TH*RA**2))
      P(2)=M(2)/(PI*R(2)*R(2)*H(2))
      WRITE (6,100) (P(I),I=1,2)
100   FORMAT (3HRO1,6X,3HRO2/(2E12.3))
C     ************************************************************
C
C     CALCULATES THE ELEMENTS OF THE 8*8 MASS MATRIX, IDEALISING THE
C     BOWL AS TWO SOLID DISCS AND A HOLLOW CYLINDER ARRANGED CONCENTRICALLY
C
C     ************************************************************
      DO 439 I=1,8
      DO 438 J=1,8
      S(I,J)=0.0D0
438   CONTINUE
439   CONTINUE
      S(1,1)=M(1)
      S(2,2)=(3.0D0*R(1)**2+T**2)*P(1)*PI*T*R(1)**2/12.0D0+(R(1)*
     **2/2.0D0+H(1)**2/12.0D0+H(1)**2/4.0D0)*P(1)*PI*2.0D0*R(1)*W
     **H(1)+P(1)*RA**2*TH*PI*(RA**2/4.0D0+TH**2/3.0D0)
     *+P(1)*PI*T*((R(1))**2-R(1)**2)*(((R(1))**2-R(1)**2)/
     *4+H(1)**2)
      S(3,3)=S(2,2)
```

```
C     * * * Vibration analysis of a vibratory bowl feeder * * * *


      S(4,4)=(((PI*T*(R(1)**4))/2.0D0)+(H(1)*W*PI*(R(1)**3)*2.0D0)+(PI
     **RA**4*TH/2))*P(1)
     *+(H(1)*T*PI*((R(1))**3-R(1)**3)*2)*P(1)
      S(5,5)=M(2)
      S(6,6)=P(2)*PI*R(2)*R(2)*H(2)*(((R(2)*R(2))/4.0D0)+((H(2)*H(2
     *))/12.0D0))
      S(7,7)=S(6,6)
      S(8,8)=(P(2)*PI*(R(2)**4)*H(2))/2.0D0
      WRITE (6,103) ((S(I,J),J=1,8),I=1,8)
103   FORMAT (11HMASS MATRIX/(8E12.3))
      WRITE (11,104) ((S(I,J),J=1,4),I=1,4)
104   FORMAT (4E12.3)
      RETURN
      END
C     ***********************************************************************
C
C     SUBROUTINE FOR CALCULATION OF EIGENVALUES
C
C     ***********************************************************************
      SUBROUTINE EIGN(ST,M)
      REAL*8 ST(8,8),M(8,8),DL(8),E(8),D(8),Z(8,8),X02ADF,XO
     *2AAF,RS(4,4),RM(4,4),DUM1(8,4),DUM2(8,4),DUM3(8)
      DATA DL,E,D,Z/8*0.0D0,8*0.0D0,8*0.0D0,64*0.0D0/
      N=8
      IFAIL=0
      PI=4*ATAN(1.0)
      DO 887 I=1,4
      DO 888 J=1,4
      RS(I,J)=ST(I,J)
      RM(I,J)=M(I,J)
888   CONTINUE
887   CONTINUE
C     ***********************************************************************
C
C     FORMULATION OF GENERAL SYSTEM MATRIX
C
C     ***********************************************************************
      CALL F01AEF(N,ST,N,M,N,DL,IFAIL)
      IF (IFAIL.EQ.0) GO TO 20
      WRITE (6,104) IFAIL
104   FORMAT (22HERROR IN F01AEF IFAIL=,I2)
      STOP
20    WRITE (6,105)
105   FORMAT (19HLOWER TRIANGLE OF P)
      DO 40 I=1,N
      WRITE (6,106) (ST(I,J),J=1,I)
106   FORMAT (7E12.3)
40    CONTINUE
      WRITE (6,107)
107   FORMAT (26HSTRICT LOWER TRIANGLE OF L)
      DO 60 I=2,N
      WRITE (6,106) (M(I,J-1),J=2,I)
60    CONTINUE
      WRITE (6,108)
108   FORMAT (13HDIAGONAL OF L)
      WRITE (6,106) (DL(I),I=1,N)
C     ***********************************************************
C
```

```
C     * * * Vibration analysis of a vibratory bowl feeder * * * *


C     TRIDIAGONALISATION OF SYSTEM MATRIX
C
C     ************************************************************
      CALL F01AJF(N,X02ADF(IT),ST,N,D,E,Z,N)
      WRITE (6,109) (D(I),E(I),(Z(I,J),J=1,N),I=1,N)
109   FORMAT (3X,1HD,11X,1HE,11X,7HARRAY Z/(10E12.3))
C     ************************************************************
C
C     EIGENVALUES AND EIGENVECTORS
C
C     ************************************************************
      CALL F02AMF(N,X02AAF(IT),D,E,Z,N,IFAIL)
      IF (IFAIL.EQ.0) GO TO 80
      WRITE (6,110) IFAIL
110   FORMAT (22HERROR IN F02AMF IFAIL=,I2)
      STOP
80    M1=1
      M2=N
C     ************************************************************
C
C     EIGENVECTORS OF ORIGINAL MATRIX
C
C     ************************************************************
      CALL F01AFF(N,M1,M2,M,N,DL,Z,N)
      WRITE (6,111) (D(I),I=1,N)
111   FORMAT (11HEIGENVALUES/(1H ,8E12.3))
      DO 124 I=1,N
      IF (D(I).LT.0.0) GO TO 124
      DUM3(I)=SQRT(D(I))/(2*PI)
124   CONTINUE
      WRITE (6,115) (DUM3(I),I=1,N)
115   FORMAT (19HNATURAL FREQUENCIES,8F9.2)
      WRITE (6,112) ((Z(I,J),J=1,N),I=1,N)
112   FORMAT (12HEIGENVECTORS/(1H ,8E12.3))
      DO 1032 I=1,8
      DO 1033 J=1,4
      DUM1(I,J)=Z(I,J)
1033  CONTINUE
1032  CONTINUE
      DO 1034 I=1,8
      DO 1035 J=1,4
1035  DUM2(I,J)=Z(I,J 4)
1034  CONTINUE
      WRITE (9,113) ((DUM1(I,J),J=1,4),I=1,8)
      WRITE (10,113) ((DUM2(I,J),J=1,4),I=1,8)
113   FORMAT (4E12.3)
      WRITE (9,113)(D(I),I=1,4)
      WRITE (10,113) (D(I),I=5,8)
      CALL RESTR2(RS,RM)
      RETURN
      END
```

Appendix 3 - Coding for the graphical display of mode shapes

```
C
C
C
C     GHOST PROGRAM FOR PLOTTING MODE SHAPES GENERATED BY
C     VIB.FTN AND VIB2.FTN   MK.1   02.05.1984
C
      DIMENSION X(40),Y(40),D(4),HB(3),RB(2),CT(4),ROT(4),CTB(4),ROTB(4)
      INTEGER MODAT,MODES2(32)
      DATA MODAT/6/
      CALL PAPER(1)
      CALL PSPACE(0.0,1.31,0.0,1.0)
      CALL MAP(-0.55,0.50,-0.30,0.50)
      CALL RADIAN
      CALL THICK(3)
      CALL SUBVB(X,Y,S,B,R,C,D,CT,ROT,CTB,ROTB)
      CALL BROKEN (10,10,10,10)
      CALL POSITN (X(12),Y(12))
      CALL LOCATE (X(12)+0.025,Y(12)+0.22)
      CALL ROTATE (ROT(1))
      CALL ELLPSE (R,CT(1))
      CALL POSITN (X(16),Y(16))
      CALL LOCATE (X(16)+0.325,Y(16)+0.22)
      CALL WINDOW (0.175,0.50,0.22,0.50)
      CALL ROTATE (ROT(2))
      CALL ELLPSE (R,CT(2))
      CALL WINFOL
      CALL POSITN (X(20),Y(20))
      CALL LOCATE (X(20)+0.025,Y(20)-0.12)
      CALL WINDOW (-0.55,0.175,-0.30,0.22)
      CALL ROTATE (ROT(3))
      CALL ELLPSE (R,CT(3))
      CALL WINFOL
      CALL POSITN (X(24),Y(24))
      CALL LOCATE (X(24)+0.325,Y(24)-0.12)
      CALL WINDOW (0.175,0.50,-0.30,0.22)
      CALL ROTATE (ROT(4))
      CALL ELLPSE (R,CT(4))
      CALL WINFOL
      CALL POSITN (X(28),Y(28))
      CALL LOCATE (X(28)+0.025,Y(28)+0.22)
      CALL WINDOW (-0.55,0.175,0.0,0.35)
      CALL ROTATE (ROTB(1))
      CALL ELLPSE (S,CTB(1))
      CALL WINFOL
      CALL POSITN (X(32),Y(32))
      CALL LOCATE (X(32)+0.325,Y(32)+0.22)
      CALL WINDOW (0.175,0.50,0.0,0.35)
      CALL ROTATE (ROTB(2))
      CALL ELLPSE (S,CTB(2))
      CALL WINFOL
      CALL POSITN (X(36),Y(36))
      CALL LOCATE (X(36)+0.025,Y(36)-0.12)
      CALL WINDOW (-0.55,0.175,-0.30,0.0)
      CALL ROTATE (ROTB(3))
      CALL ELLPSE (S,CTB(3))
      CALL WINFOL
      CALL POSITN (X(40),Y(40))
      CALL LOCATE (X(40)+0.325,Y(40)-0.12)
      CALL WINDOW (0.175,0.50,-0.3,0.0)
      CALL ROTATE (ROTB(4))
```

```
C
      CALL ELLPSE (S,CTB(4))
      CALL WINFOL
      CALL FULL
      CALL ROTATE (0.0)
      CALL POSITN(X(7),Y(7))
      CALL LOCATE(-0.33,0.0)
      READ (MODAT,100) BA,BH
100   FORMAT (2F9.6)
      READ (MODAT,101) (HB(I),I=1,3)
      READ (MODAT,100) (RB(I),I=1,2)
101   FORMAT (3F9.6)
      CALL ELLPSE (BA,(BA/3.0))
      CALL POSITN (-BA,0.0)
      CALL LINE (0.0,-BH)
      CALL POSITN (BA,0.0)
      CALL LINE (0.0,-BH)
      CALL POSITN (0.0,-BH)
      CALL ELLPSE (BA,(BA/3.0))
      DO 35 I=1,3
      CALL POSITN (X(I),Y(I))
      CALL JOIN (X(I+3),Y(I+3))
35    CONTINUE
      CALL POSITN (X(8),Y(8))
      CALL ELLPSE (R,C)
      CALL MOVE (0.0,HB(1))
      CALL ELLPSE (RB(1),(RB(1)/3.0))
      CALL MOVE (0.0,HB(2))
      CALL ELLPSE (RB(2),(RB(2)/3.0))
      CALL MOVE (RB(2),0.0)
      CALL LINE (0.0,HB(3))
      CALL MOVE ((-2*RB(2)),-HB(3))
      CALL LINE (0.0,HB(3))
      CALL MOVE (RB(2),0.0)
      CALL ELLPSE (RB(2),(RB(2)/3.0))
      CALL UNLOC
      CALL POSITN (X(7),Y(7))
      CALL LOCATE (0.025,0.22)
      DO 10 I=1,3
      CALL POSITN (X(I),Y(I))
      CALL JOIN (X(I+3),Y(I+3))
10    CONTINUE
      CALL POSITN (X(7),Y(7))
      CALL ELLPSE (S,B)
      CALL POSITN (X(8),Y(8))
      CALL ELLPSE (R,C)
      CALL PTPLOT(X,Y,7,8,232)
      CALL BROKEN (10,10,10,10)
      DO 50 I=9,11
      CALL POSITN (X(I),Y(I))
      CALL JOIN (X(I+16),Y(I+16))
50    CONTINUE
      CALL FULL
      CALL POSITN (X(7),Y(7))
      CALL LOCATE (0.325,0.22)
      DO 20 I=1,3
      CALL POSITN (X(I),Y(I))
      CALL JOIN (X(I+3),Y(I+3))
20    CONTINUE
```

```
C
      CALL POSITN (X(7),Y(7))
      CALL ELLPSE (S,B)
      CALL POSITN (X(8),Y(8))
      CALL ELLPSE (R,C)
      CALL PTPLOT(X,Y,7,8,232)
      CALL BROKEN (10,10,10,10)
      DO 60 I=13,15
      CALL POSITN (X(I),Y(I))
      CALL JOIN (X(I+16),Y(I+16))
60    CONTINUE
      CALL FULL
      CALL POSITN (X(7),Y(7))
      CALL LOCATE (0.025,-0.12)
      DO 30 I=1,3
      CALL POSITN (X(I),Y(I))
      CALL JOIN (X(I+3),Y(I+3))
30    CONTINUE
      CALL POSITN (X(7),Y(7))
      CALL ELLPSE (S,B)
      CALL POSITN (X(8),Y(8))
      CALL ELLPSE (R,C)
      CALL PTPLOT (X,Y,7,8,232)
      CALL BROKEN (10,10,10,10)
      DO 70 I=17,19
      CALL POSITN (X(I),Y(I))
      CALL JOIN (X(I+16),Y(I+16))
70    CONTINUE
      CALL FULL
      CALL POSITN (X(7),Y(7))
      CALL LOCATE (0.325,-0.12)
      DO 40 I=1,3
      CALL POSITN (X(I),Y(I))
      CALL JOIN (X(I+3),Y(I+3))
40    CONTINUE
      CALL POSITN (X(7),Y(7))
      CALL ELLPSE (S,B)
      CALL POSITN (X(8),Y(8))
      CALL ELLPSE (R,C)
      CALL PTPLOT (X,Y,7,8,232)
      CALL BROKEN (10,10,10,10)
      DO 80 I=21,23
      CALL POSITN (X(I),Y(I))
      CALL JOIN (X(I+16),Y(I+16))
80    CONTINUE
      CALL FULL
      CALL BORDER
      CALL CTRMAG(18)
      CALL UNLOC
      CALL PLOTCS (-0.35,0.43,'VIBRATION ANALYSIS OF VIBRATORY BOWL FEED
     *ER.',44)
      CALL PLOTCS (-0.075,0.14,'1st MODE: NATURAL',17)
      CALL PLOTCS (-0.075,0.10,'FREQUENCY = ',12)
      CALL TYPENF (D(1),1)
      CALL TYPECS ('HZ',2)
      CALL PLOTCS (0.225,0.14,'2nd MODE: NATURAL',17)
      CALL PLOTCS (0.225,0.10,'FREQUENCY = ',12)
      CALL TYPENF (D(2),1)
      CALL TYPECS ('HZ',2)
```

```
C
      .


      CALL PLOTCS (-0.075,-0.20,'3rd MODE: NATURAL',17)
      CALL PLOTCS (-0.075,-0.24,'FREQUENCY = ',12)
      CALL TYPENF (D(3),1)
      CALL TYPECS ('HZ',2)
      CALL PLOTCS (0.225,-0.20,'4th MODE: NATURAL',17)
      CALL PLOTCS (0.225,-0.24,'FREQUENCY = ',12)
      CALL TYPENF (D(4),1)
      CALL TYPECS ('HZ',2)
      DO 998 I=1,24
999   FORMAT(2F6.2)
998   CONTINUE
      CALL GREND
      STOP
      END
C
C     SUBROUTINE FOR CALCULATION OF PLOTTING POINTS FOR
C     STATIC CONFIGURATION  MK.1  02.05.1984
C
      SUBROUTINE SUBVB(X,Y,S,B,R,C,D,CT,ROT,CTB,ROTB)
      REAL X(40),Y(40),L,TH(4),DEL(4),ZE(8,4),D(4),SUM(4),THX(4),THY(4),
     *CT(4),ROT(4),THB(4),DELB(4),SUMB(4),THXB(4),THYB(4),CTB(4),ROTB(4)
      INTEGER DEIGN3
      DATA DEIGN3/5/
      READ (DEIGN3,100) RA,GA,PH,L
100   FORMAT (4F9.6)
      PI=ATAN(1.0)*4.0
      R=RA/COS(PH)
      H=L*SIN(GA)
      Z=L*COS(GA)
      C=R/3.0
      S=SQRT((R*R)+(Z*Z)-(2.0*R*Z*COS((PI/2.0)-PH)))
      B=S/3.0
      AP=ATAN(SQRT((1/(((S*S)+(R*R)-(Z*Z))/(2.0*S*R))**2)-1))
      X(1)=R
      Y(1)=H
      X(2)=-R*COS(PI/3.0)
      Y(2)=H+(SIN(PI/3.0)*C)
      X(3)=-R*COS(PI/3.0)
      Y(3)=H-(C*SIN(PI/3.0))
      X(4)=S*COS(AP)
      Y(4)=B*SIN(AP)
      X(5)=S*COS(AP+((2.0*PI)/3.0))
      Y(5)=B*SIN(AP+((2.0*PI)/3.0))
      X(6)=S*COS(AP+((4.0*PI)/3.0))
      Y(6)=B*SIN(AP+((4.0*PI)/3.0))
      X(7)=0.0
      Y(7)=0.0
      X(8)=0.0
      Y(8)=H
      READ (DEIGN3,101) ((ZE(I,J),J=1,4),I=1,8)
101   FORMAT (4E12.3)
      READ (DEIGN3,101) (D(I),I=1,4)
      DO 50 J=1,4
      SUM(J)=SQRT(ZE(1,J)**2+(R*ZE(2,J))**2+(R*ZE(3,J))**2+(R*ZE(4,J))**
     *2)
      DEL(J)=(ZE(1,J)*0.01)/SUM(J)*3.0
      THX(J)=(ZE(2,J)*0.01)/(R*SUM(J)*3.0)
      THY(J)=(ZE(3,J)*0.01)/(R*SUM(J)*3.0)
```

```
C
      TH(J)=(ZE(4,J)*0.01)/(R*SUM(J)*3.0)
      SUMB(J)=SQRT(ZE(5,J)**2+(S*ZE(6,J))**2+(S*ZE(7,J))**2+(S*ZE(8,J))*
     **2)
      DELB(J)=(ZE(5,J)*0.01)/SUMB(J)*3.0
      THXB(J)=(ZE(6,J)*0.01)/(S*SUMB(J)*3.0)
      THYB(J)=(ZE(7,J)*0.01)/(S*SUMB(J)*3.0)
      THB(J)=(ZE(8,J)*0.01)/(S*SUMB(J)*3.0)
997   FORMAT (5E14.4)
50    CONTINUE
      I=0
      DO 51 J=1,4
      X(9+I)=R*(COS(TH(J))-1.0+COS(THX(J)))
      Y(9+I)=H+DEL(J)+(R*THX(J))+(C*SIN(TH(J)))
      X(10+I)=-(R*COS((PI/3.0)-TH(J)))-(R*COS(PI/3.0)*(1.0-COS(THX(J))))
      Y(10+I)=H+DEL(J)-(R*THX(J)*COS(PI/3.0))+(C*SIN((PI/3.0)-TH(J)))
     *-(C*THY(J))
      X(11+I)=-(R*COS((PI/3.0)+TH(J)))-(R*COS(PI/3.0)*(1.0-COS(THX(J))))
      Y(11+I)=H+DEL(J)-(R*THX(J)*COS(PI/3.0))-(C*SIN((PI/3.0)+TH(J))*
     *(1.0-THY(J)))
      X(12+I)=0.0
      Y(12+I)=H+DEL(J)
      CT(J)=C*(1.0-SIN(THY(J)))
      ROT(J)=THX(J)
      X(25+I)=S*(COS(THB(J)+AP)-1.0+COS(THXB(J)))
      Y(25+I)=DELB(J)+(S*THXB(J)*COS(AP))+(B*SIN(THB(J)+AP))-(B*THYB(J
     *))
      X(26+I)=(S*COS(AP+(2.0*PI/3.0)+THB(J)))
      Y(26+I)=DELB(J)-(S*THXB(J)*COS(AP+(2.0*PI/3.0)))+
     *(B*SIN(AP+(2.0*PI/3.0)+THB(J)))-(B*THYB(J))
      X(27+I)=S*COS(AP+(4.0*PI/3.0)+THB(J))
      Y(27+I)=DELB(J)-(S*COS(AP+PI/3.0)*THXB(J))-(B*SIN(AP+(PI/3.0)+THB(
     *J)))+(B*THY(J))
      X(28+I)=0.0
      Y(28+I)=DELB(J)
      CTB(J)=B*(1.0-SIN(THYB(J)))
      ROTB(J)=THXB(J)
996   FORMAT (2E14.4)
      I=I+4
51    CONTINUE
      DO 52 I=1,4
      IF (D(I).LE.0.0) D(I)=0.0
      D(I)=(SQRT(D(I)))/(2.0*PI)
52    CONTINUE
      RETURN
      END
```

Appendix 4 - Macro used to predict the forced response of a bowl feeder

	A	B
1	Superposition	
2	=RESULT(64)	
3	=ARGUMENT("modal",64)	
4	=ARGUMENT("eigen1",64)	
5	=ARGUMENT("eigen2",64)	
6	=ARGUMENT("mass",64)	
7	=ARGUMENT("fns",64,A13:A14)	
8	=ARGUMENT("forcevectr",64)	
9	=ARGUMENT("dampingconst",1)	
10	=ARGUMENT("forcefn",1)	
11	=SET.NAME("fone",A13)	
12	=SET.NAME("ftwo",A14)	
13	52.723215635055	
14	670.79503048243	
15	=fone*2*PI()	
16	=ftwo*2*PI()	
17	=forcefn*2*PI()	
18	=SET.VALUE(A19:B20,{0,0;0,0})	
19	=1/(SQRT((A15^2-A17^2)^2+4*dampingconst^2*A15^2*A17^2)*MMULT(TRANSPOSE(eigen1),MMULT(mass,eigen1)))	=0
20	=0	=1/(SQRT((A16^2-A17^2)^2+4*dampingconst^2*A16^2
21	=GOTO(B19)	=GOTO(A22)
22	=SET.NAME("super",A19:B20)	
23	=SET.VALUE(A24:B25,A19:B20)	
24	1.7670939916641E-07	0
25	0	5.0052466922721E-09
26	=SET.NAME("output",A28:A29)	
27	=SET.VALUE(A28:A29,{0;0})	
28	=A17^2*MMULT(modal,MMULT(super,MMULT(TRANSPOSE(modal),forcevectr)))	
29	=A17^2*MMULT(modal,MMULT(super,MMULT(TRANSPOSE(modal),forcevectr)))	
30	=SET.VALUE(A32:A33,{0;0})	
31	=SET.VALUE(A32:A33,output)	
32	0.017934516685092	
33	0.43133187044798	
34	=RETURN(A32:A33)	

Appendix 5 - Auto-exec macro, 'Bowl Feeder', for the control of the execution of the customised design software

	A
30	=DIALOG.BOX(B5:H27)
31	=IF(A30,GOTO(A32),GOTO(A67))
32	=OPEN("SuperpositionMacro")
33	=OPEN("WORKSHEET")
34	=CALCULATION(3)
35	=SELECT(!B5)
36	=FORMULA(H11)
37	=SELECT(!B6)
38	=FORMULA(H13)
39	=SELECT(!B7)
40	=FORMULA(H15)
41	=SELECT(!B8)
42	=FORMULA(H17)
43	=SELECT(!B10)
44	=FORMULA(H19*PI()/180)
45	=SELECT(!B27)
46	=FORMULA(H21)
47	=SELECT(!B28)
48	=FORMULA(H23)
49	=SELECT(!B29)
50	=FORMULA(H25*PI()/180)
51	=CALCULATION(1)
52	=!C118
53	=!J117
54	=ACTIVATE("BOWLFEEDER")
55	=SELECT(H90)
56	=FORMAT.NUMBER("0.00E+00")
57	=FORMULA(A52)
58	=SELECT(H92)
59	=FORMAT.NUMBER("0.00")
60	=FORMULA(A53)
61	=DIALOG.BOX(B85:H97)
62	=ACTIVATE("WORKSHEET")
63	=CLOSE(FALSE)
64	=ACTIVATE("SUPERPOSITIONMACRO")
65	=CLOSE(FALSE)
66	=IF(A61,GOTO(A30),GOTO(A67))
67	=SAVE()
68	=QUIT()
69	=RETURN()

Appendix 6 - User manual for operation of the design software

VIBRATORY BOWL FEEDER

DESIGN SOFTWARE

- USER MANUAL

1. Introduction

The BOWL FEEDER software package has been developed to assist engineers in the prediction of the performance of vibratory bowl feeders. A diagram of the type of machine covered is shown in Fig.1. This has a fixed frequency electromagnetic drive with three spring banks of inclined leaf springs.

Earlier work by Redford and Boothroyd (1) has shown that the mean conveying velocity of components is directly related to the vertical acceleration of the bowl; in addition, minimising power consumption depends on maintaining the first natural frequency close to the operating frequency of 50 Hz. The BOWL FEEDER design package allows an alternative set of geometric parameters of the bowl and springs to be entered, and an analysis to be run giving the vertical acceleration of the bowl and the first natural frequency of the feeder as output data. This enables the performance of different configurations to be easily compared.

BOWL FEEDER runs on the Apple Macintosh Plus, and was written using the Microsoft EXCEL (2) spreadsheet package. It is not necessary to know how to use EXCEL, but a limited knowledge of the Macintosh Plus tools used for file handling has been assumed in this manual.

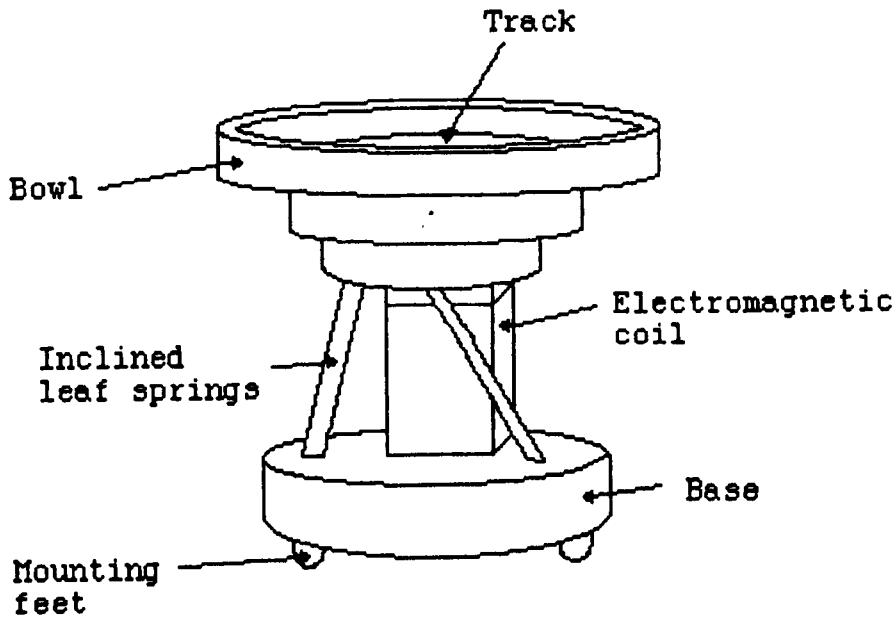
Track
Bowl
Electromagnetic coil
Inclined leaf springs
Base
Mounting feet

Fig.1

It is recommended that you run the package either on a machine with two 800K disk-drives, or a machine with a hard disk. Although it is possible to run the package on a machine with a single 800K disk-drive, this would involve a large number of disk swaps, which is very tedious and time consuming.

2. Loading BOWL FEEDER

You are supplied with two 800K double sided 3 1/4" floppy disks. Insert the disk labelled SYSTEM DISK in the internal drive of your Macintosh Plus and switch on the computer. Insert the disk labelled EXCEL in the external drive (it is possible to run the software with a single drive, but this would involve a lot of disk swaps, and is not recommended). A view of the main desktop now appears on the screen, as shown in Fig.2. This gives a list of the files stored on the EXCEL and SYSTEM disks. Select and open the file called 'Bowl Feeder' by double-clicking its icon to the left of its name in the list of files stored on the disk. This will now become darkened as shown in Fig.2. This automatically runs the 'Bowl Feeder' spreadsheet.

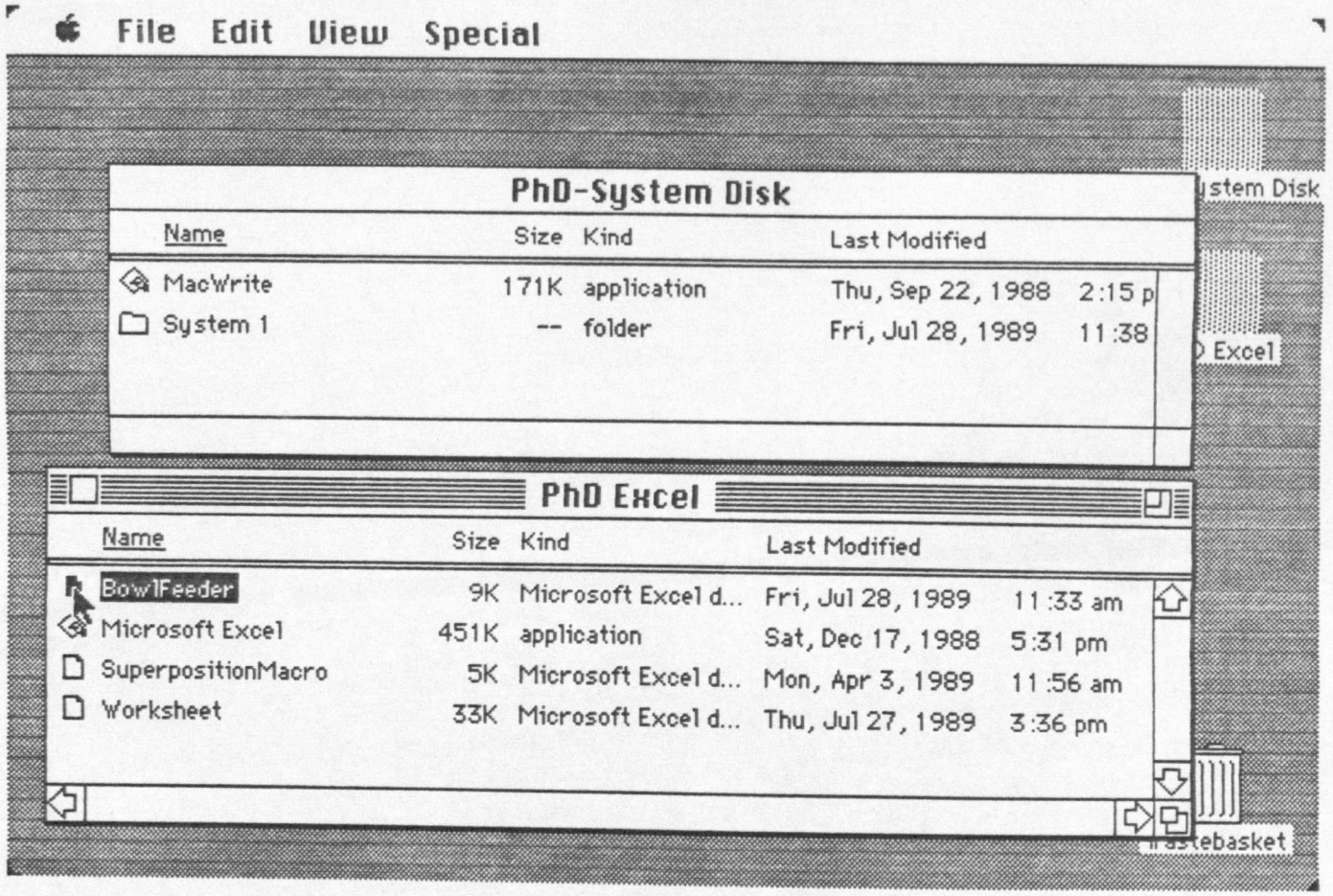
File Edit View Special
PhD-System Disk
Name Size Kind Last Modified
MacWrite 171K application Thu, Sep 22, 1988 2:15 p
System 1 -- folder Fri, Jul 28, 1989 11:38
PhD Excel
Name Size Kind Last Modified
BowlFeeder 9K Microsoft Excel d... Fri, Jul 28, 1989 11:33 am
Microsoft Excel 451K application Sat, Dec 17, 1988 5:31 pm
SuperpositionMacro 5K Microsoft Excel d... Mon, Apr 3, 1989 11:56 am
Worksheet 33K Microsoft Excel d... Thu, Jul 27, 1989 3:36 pm

Fig.2

3. Entering Data

After a short while, a dialog-box appears asking you for geometric input parameters. This is shown in Fig.3. The parameters which can be changed and the recommended ranges for their values are:

Spring length	0.16 - 0.19 m
Spring width	0.015 - 0.025 m
Spring thickness	0.001 - 0.005 m
Spring spacing	0.0005 - 0.003 m
Spring angle	40 - 80 degrees
Bowl mass	8 - 25 kg
Bowl radius	0.05 - 0.3 m
Bowl radius angle	0 - 90 degrees

Spring length is the distance between the centres of the fixing bolts at the ends of the springs. Spring thickness is the thickness of a single leaf spring, and spring spacing is the gap between the adjacent leaf springs in a spring bank. The spring angle is the angle of inclination of a spring bank to rhe horizontal. This is labelled γ in Fig.4. The bowl radius and radius angle are labelled r and ϕ in Fig.4.

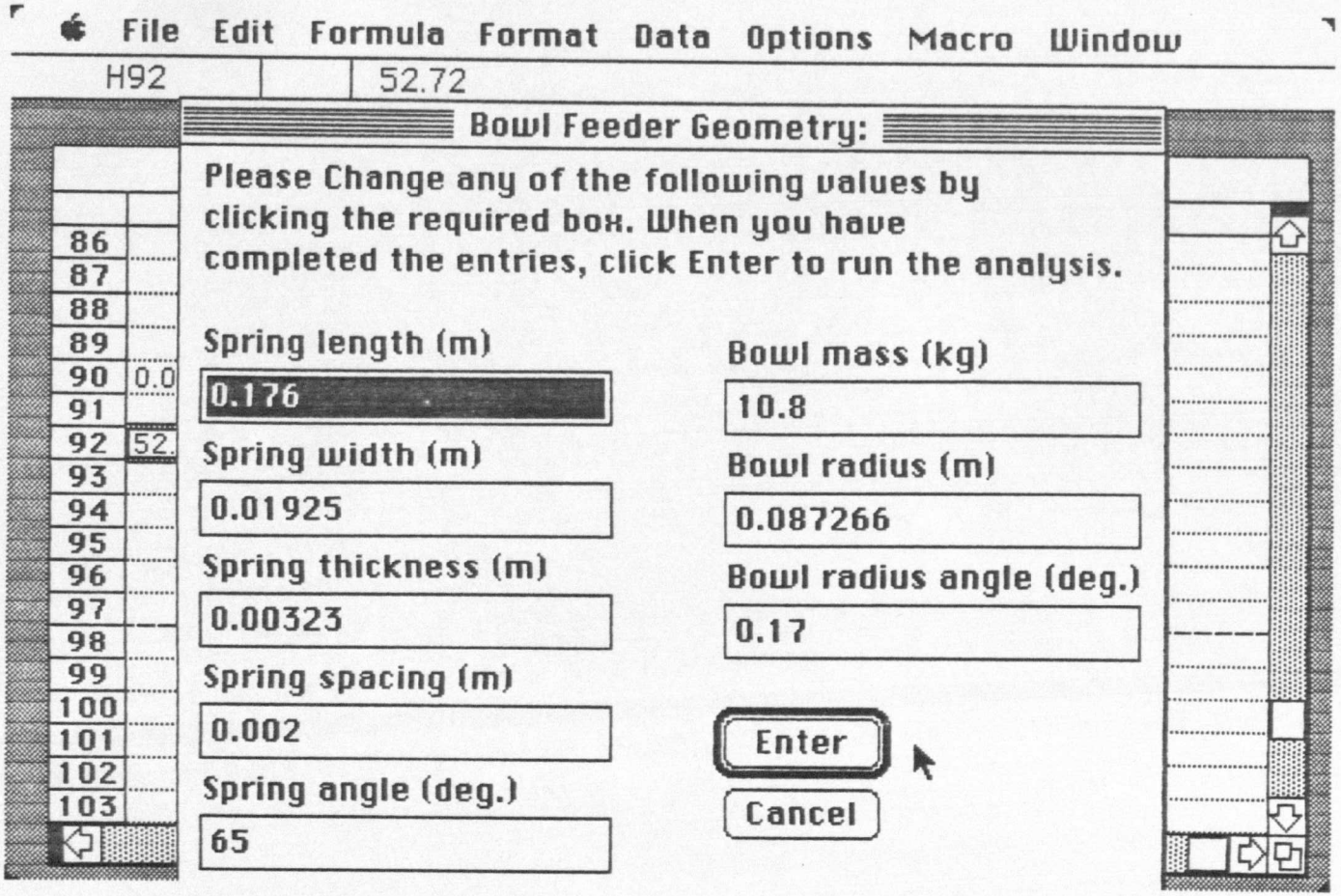
File Edit Formula Format Data Options Macro Window
H92
52.72
Bowl Feeder Geometry:
Please Change any of the following values by clicking the required box. When you have completed the entries, click Enter to run the analysis.
Spring length (m)
0.176
Spring width (m)
0.01925
Spring thickness (m)
0.00323
Spring spacing (m)
0.002
Spring angle (deg.)
65
Bowl mass (kg)
10.8
Bowl radius (m)
0.087266
Bowl radius angle (deg.)
0.17
Enter
Cancel
86
87
88
89
90
91
92
93
94
95
96
97
98
99
100
101
102
103
0.0
52.

Fig.3

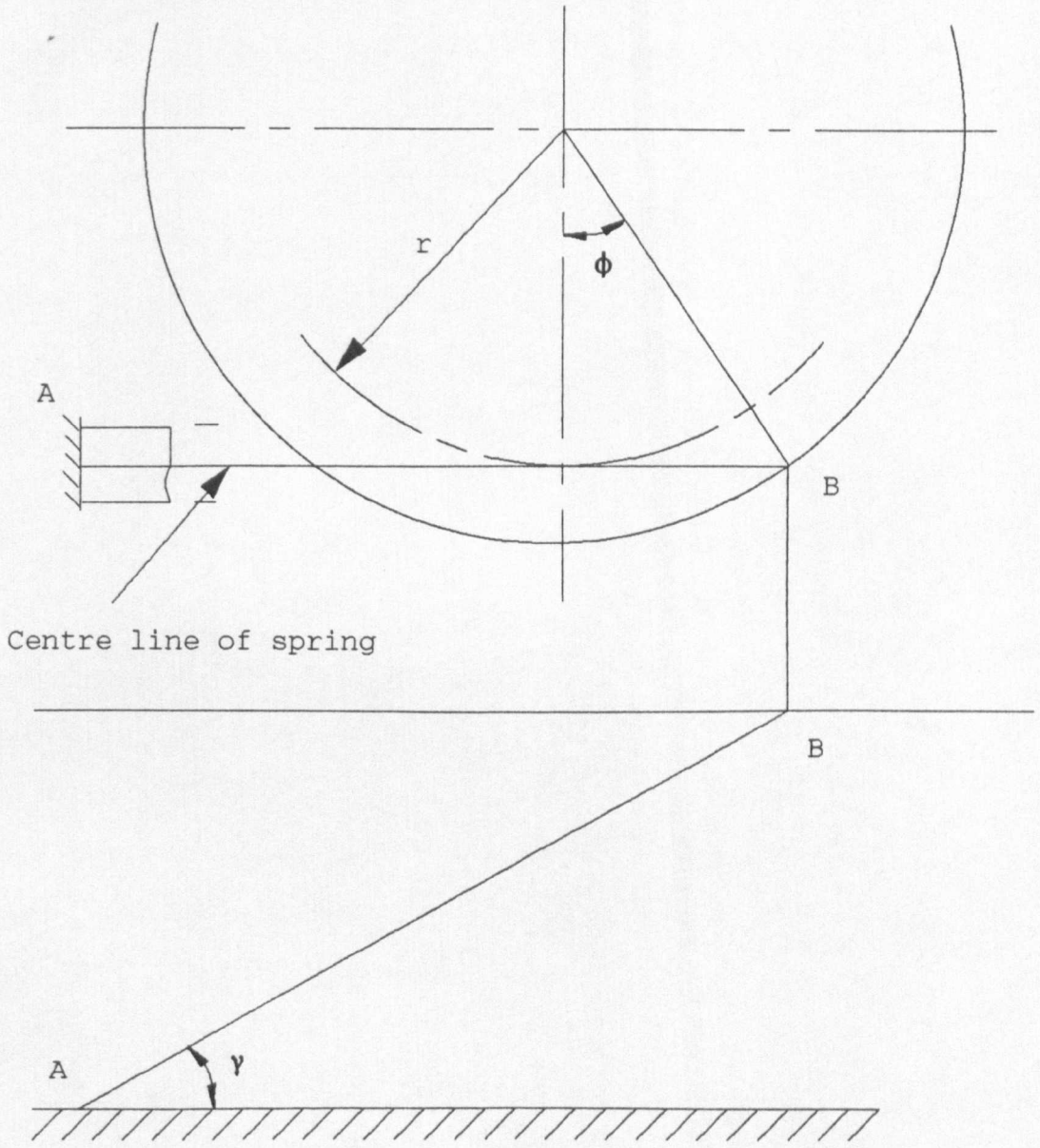

Fig.4

The units for each parameter are given as part of the dialog-box; take care to enter values with the correct units. The values which are held in the dialog-box when it first appears are either those shown in Fig.3 (if this is the first time you have used the package), or those values which you entered the last time you ran an analysis with the package.

To change an input parameter, select the appropriate input-box by clicking it; a cursor then appears in the box, and the value can then be changed by using text editor keys. If you then wish to change another value, DO NOT press ENTER or RETURN (this will run the analysis), just select a new input-box and change this value. It is possible to change any or all of the input parameters.

It is not possible to change parameters such as the material properties of the bowl and springs, the number of springs and spring banks, and the frequency of the driving input to the feeder.

Having changed the input parameters, if you are satisfied with these and would like to run the analysis, proceed to section 5. If you wish to quit at this stage, proceed to section 4.

4. Quitting

To quit at this stage, select the Cancel box. The input values which you have entered will not be stored.

5. Running the Analysis

When you are satisfied with your selection of input parameters, you can run the analysis by clicking the 'Enter' box or by either pressing the ENTER or the RETURN key.

6. Display of Results

After a while, another dialog-box appears, displaying the results of your analysis. This is shown in Fig.5. The bowl acceleration is given as m/s^2 per N of input force. This value will therefore need to be multiplied by the amplitude of the force of the driving coil to be used. A medium size feeder normally requires a driving force of around 650 N.

At this stage you can either repeat the analysis by clicking the OK box, or quit by selecting the Cancel box. The values which you entered in your most recent analysis will appear in the next input dialog-box.

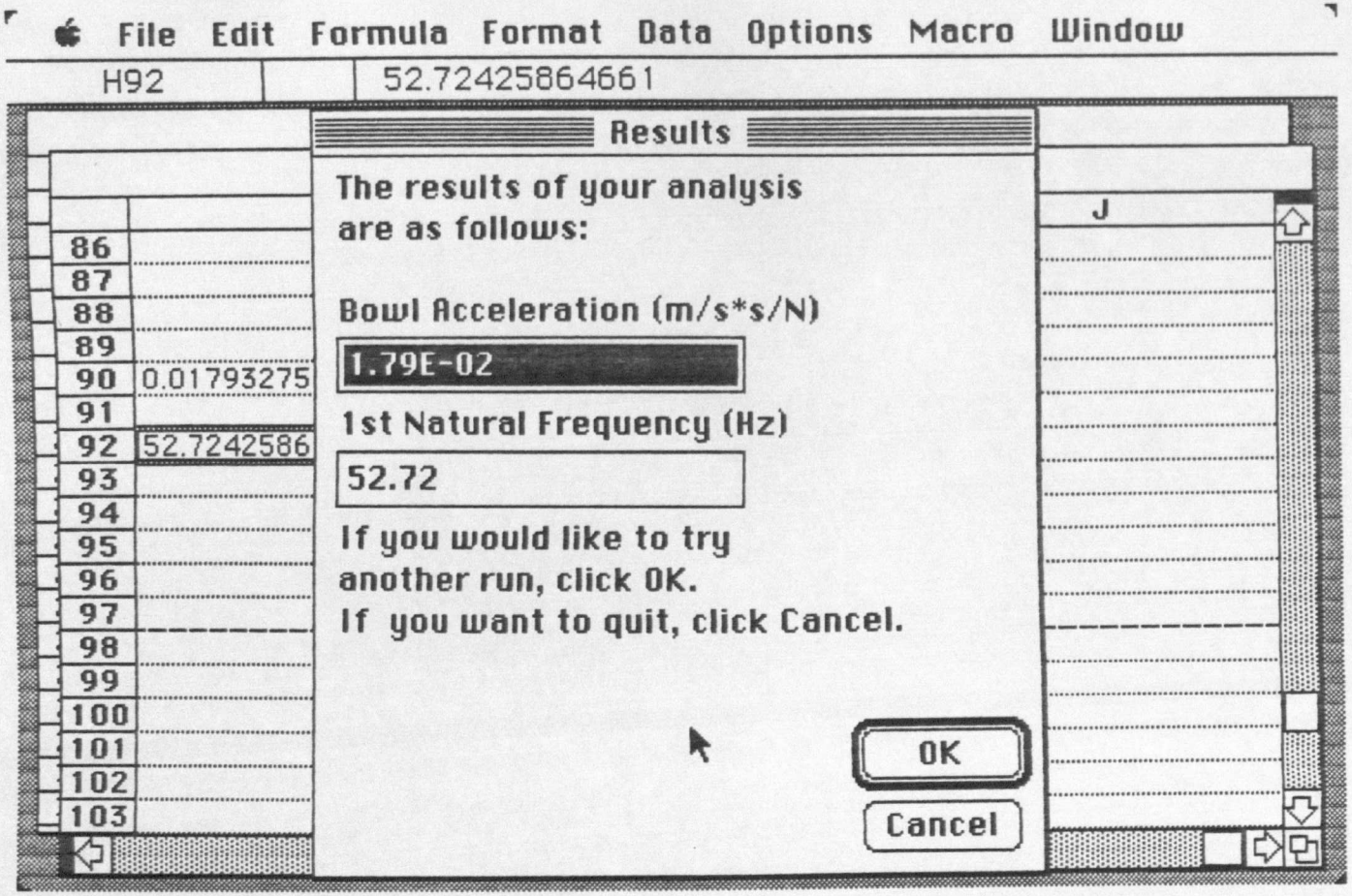
File Edit Formula Format Data Options Macro Window
H92
52.72425864661
Results
The results of your analysis
are as follows:
Bowl Acceleration (m/s*s/N)
1.79E-02
1st Natural Frequency (Hz)
52.72
If you would like to try
another run, click OK.
If you want to quit, click Cancel.
OK
Cancel
J
86
87
88
89
90
0.01793275
91
92
52.7242586
93
94
95
96
97
98
99
100
101
102
103

Fig.5

7. Printing

If you have an Apple printer, it is possible to dump either the input or output dialog-boxes to the printer. With the Caps-Lock down, hold down both the Command and Shift keys while you type the number 4.

References

1. Redford, A.H. and Boothroyd, G.: 'Vibratory Feeding', Proc.I.Mech.E., 1967-68, Vol.182, Pt.1, No.6, p.135-146.

2. Microsoft Corporation, Microsoft Excel User's Guide, 1986.

PAGE/PAGES
EXCLUDED
UNDER
INSTRUCTION
FROM
UNIVERSITY